Department of Precision and Microsystems Engineering

Design of a robot mounted X-type projection welding machine

M. Gritter

Report no : 2021.076
Coach : M.Sc. A. Amoozandeh Novabeh
Professor : prof.dr.ir. J.L. Herder
Specialisation : Mechatronic System Design
Type of report : M.Sc. Thesis Report
Date : 11 October 2021

TU Delft Delft University of Technology

Challenge the future

Design of a robot mounted X-type projection welding machine

By

M. Gritter

to obtain the degree of Master of Science
at the Delft University of Technology,
to be defended publicly on Wednesday October 15, 2021 at 10:30.

Student number	4300181	
Project duration	August 14, 2019 – October 15,2021	
Thesis committee	Prof. dr. ir. J. L. Herder	TU Delft, supervisor, chair
	Ir. A. Amoozandeh Nobaveh	TU Delft, daily supervisor

This thesis is confidential and cannot be made public until October 15, 2024.

An electronic version of this thesis is available at http://repository.tudelft.nl/.

Preface

On my last day before handing in this report, I am finally allowed to write this section. I can happily look back at my time at the TU Delft. I have gained a lot of knowledge throughout the years and was part of some amazing projects, starting in my first year by building a walking beer crate, later a 2D positioning system and now finishing it off with a projection welding machine.

I gained lots of great friends in and outside of the university with whom I could study together or go to the bar or party with. This made my time in Delft very enjoyable and never boring. Saying goodbye to the life of a student will be hard, but hey, soon I can call myself a M.Sc. graduate!

Not long after I started this graduation project, the COVID-19 epidemic started and everyone was forced to work from home. During this time, I found out the hard way that working from home all day every week was not cut out for me, especially with such a highly individual project. The motivation and concentration was hard to find sometimes. I would like to thank everyone who supported me in a time where I needed it, with a special thanks to my parents, roommates and supervisors form both the company and university who stayed supportive throughout the whole process.

M. Gritter
Delft, October 2021

Table of Contents

Preface iii
1 Summary 1
2 Introduction 3
2.1 Electric resistance welding 4
2.2 Physical aspects 6
2.3 Welding machines and equipment 7
2.3.1 Mechanical system 8
2.3.2 Electrical system 8
2.3.3 Hydraulic system 9
2.4 Arplas welding 9
2.4.1 Arplas C-type welding gun 11

Part I: Literature

3 Literature survey: Decision tree for a resistance welding method and machine based on part geometry and application 17
4 Modelling and testing of welding machines 31
4.1 Modeling of welding machines 31
4.2 Testing 32
5 Factors influencing weld quality 35
5.1 Physical influences 36
5.1.1 Thermal expansion 36
5.1.2 Lorentz forces 36
5.1.3 Shunt effect 37
5.2 Weld tests 37
6 Machine design research 39
6.1 Weld equipment 39
6.2 Mechanical characteristics 40
6.2.1 Quality 41
6.2.2 Electrode life 41
6.2.3 Touching 41

6.2.4 Follow-up ... 42

Part II: Testing the current C-type

7 Introduction ... 45
7.1 Goal ... 45
7.2 Analysis of Arplas system ... 45
7.2.1 Welding procedure ... 46
7.2.2 Model of welding gun ... 47
7.2.3 Frequency analysis of the model ... 49
8 Method ... 52
8.1 Experiment setup ... 52
8.2 Experiment 1: Touching behavior ... 53
8.2.1 Lower arm stiffness ... 53
8.2.2 Sheet stiffness ... 54
8.2.3 Total stiffness acting on workpiece ... 55
8.2.4 Damping of the system ... 55
8.2.5 Model B validation ... 56
8.3 Experiment 2: Welding behavior ... 56
8.3.1 Continuous measurement of mechanical characteristics ... 57
8.3.2 Machine characteristics Rymenant method ... 57
8.3.3 Stiffness during welding ... 58
8.3.4 Follow-up acceleration ... 58
8.3.5 Model C validation ... 58
9 Results ... 59
9.1 Experiment 1: Touching ... 59
9.1.1 Lower arm stiffness ... 61
9.1.2 Sheet stiffness ... 62
9.1.3 Total stiffness acting on workpiece ... 63
9.1.4 Damping of the system ... 63
9.2 Experiment 2: Welding behavior ... 65
9.2.1 Continuous measurement of machine characteristics ... 65
9.2.2 Machine characteristics Rymenant method ... 66

9.2.3 Stiffness during welding 67
9.2.4 Follow-up acceleration 69
10 Discussion 70
10.1 Experiment 1 70
10.2 Results. Analysis and Evaluation Experiment 2 71
11 Conclusion 73
11.1 Mechanical characteristics 73
11.2 Requirement distillation 74

Part III: Designing the X-type

12 Introduction 77
12.1 Design problem 78
12.2 Functions and requirements 79
12.3 MosCoW requirements 82
13 Concept generation 83
13.1 Possible solutions for each function 83
14 Concept selection 87
14.1 Design criteria 87
14.2 Multi Criteria Analysis 90
14.3 Final concept 92
15 Detailed design 94
15.1 Components 95
15.2 Working principle 96
15.3 Model of the X-type 99
15.4 Design choices/considerations 102
15.5 Configuration tool 108
16 Experimental validation 111
16.1 Method 111
16.1.1 Equipment 111
16.1.2 Experiments 112
16.1.3 Experiment setup 114
16.2 Results 116

16.2.1 Experiment 1: Max force and total stiffness check 116
16.2.2 Experiment 2: Horizontal bending 117
16.2.3 Experiment 3: Electrode rotation 118
16.2.4 Experiment 4: Follow-up characteristics 119
16.3 Discussion 125
17 Design conclusion 128
18 Overall conclusion and recommendations 129
19 References 131
Appendix A. Literature resistance welding 135
A.1 Physical aspects 135
Joule Heating 135
Dynamic resistance 137
Peltier effect 138
A.2 Welding equipment 139
Welding gun 139
Electrode 140
A.3 Weld quality and inspection 141
All weld inspection techniques 142
A.4 Factors influencing weld quality 144
A.5 Modelling of welding machines 147
A.6 Machine characteristic test methods 149
Appendix B. Concept phase 151
B.1 Concept generation 151
B.2 Concept selection 153
Strength potential calculations 153
Appendix C. Detailed design 154
C.1 Motor selection 154
C.2 Power source 155
C.3 Spring selection 156
C.4 Material selection 157
C.5 Positioning system 158
C.6 Frequency analysis 159

Appendix D. Testing the X-type 160
D.1 Horizontal displacement 160
D.2 Rotation measurements 161
D.3 Follow-up characteristics 164
Appendix E. Full part list 165

1 Summary

Resistance welding is a joining technique that makes use of the electrical resistance between two metal sheets. Heat is generated by sending current through the metal sheets, forming a weld in the process. There are different types of resistance welding, one of them resistance being projection welding (RPW). Projection welding uses, as the name suggests, a projection to focus the current into a small area, therefore requiring less force and current as its main competitor, resistance spot welding.

The company Arplas Systems has a unique way of using projection welding. By making a projection with a specific geometry, metal sheets can be welded together leaving almost no mark on one welded sheet. Especially in the car industry this is useful since the ugly spots usually left with spot welding do not need to be covered with plastic sheets anymore.

The company wants to extend their product portfolio with a far-reaching, or X-type, welding machine. X-type projection welding machines do not exist on the market yet, and they would like one that will weld similar to as they have now with the C-type welding machine. This will therefore be the goal of this thesis:

"Design a robot mounted far-reaching projection welding machine, using the technology of Arplas Systems, with at least similar mechanical characteristics as the current welding machine."

First, a literature survey is performed to gain knowledge about resistance welding, factors influencing weld quality, modeling and testing of resistance welding machines, and the factors to take into account when designing a projection weld machine. Secondly, to be able to design a machine with similar mechanical characteristics, the current machine is tested for its mechanical characteristics. Finally, the requirement for the X-type can be set and a design is made. A prototype is produced and tested to verify the calculations and simulations.

The first literature survey is focused on resistance welding and their corresponding machines. Decision trees were made for future engineers to quickly find the correct resistance welding method and the corresponding resistance welding machine for their application.

The second literature study focused on modeling, testing, and designing resistance welding machines. Many researches have been done on spot welding machines, while some papers are specifically for projection welding. The main difference between spot welding machines and projection welding machines is that for projection welding it is important to keep contact with the metal sheets while the projection collapses, which is called follow-up. The collapse happens a very short timespan, typically a few milliseconds, therefore projection welding machines need a fast follow-up system to account for that.

What became clear was that the machine characteristics are hard to predict and measure. Tradeoffs need to be made and sometimes the results are contradictory. It could be concluded that electrode alignment, fast follow-up and low friction are the most crucial factors for projection welding machines.

Using the gained knowledge, models of the different stages during a welding process were made of Arplas's current C-type machine. By adding a displacement sensor to the dynamic electrode and using the already integrated force sensor, everything was set for the tests.

Tests were performed to find the machine characteristics and to validate the model. Analyzing the touching behavior of the electrodes resulted in finding the lower arm stiffness, the damping coefficient and the moving mass. Analysis of the experiments with welding lead to the total machine stiffness, and the acceleration of the moving electrode during follow-up. With these results, requirements were set for the to be designed X-type.

The design of the X-type starts off with an analysis of the functions and necessary requirements. In the concept phase many different concepts were made and a pattern became visible. The placement of the actuator, the location of the follow-up spring, and the addition of an alignment tool were the three main categories the concepts had in common. Setting up criteria and a multi criteria analysis for each of those categories resulted in a final concept: an actuator above the pivot point, a follow-up spring at the base and no misalignment tool.

During the detailed design phase, choices were made to be able to reach the set requirements. Two dynamic arms are used so the electrodes center on the workpiece like scissor. A passive positioning system keeps the arms in initial position while minimizing its influence during welding. The static and dynamic models are used for the calculation of the follow-up characteristics.

The final stage of the X-type design is building the prototype and testing it. The prototype passed with flying colors, welding both steel and aluminum samples. The electrode alignment is excellent and the total machine stiffness is very close to the calculated values. The machine was mounted on a robot as well and was able to make consecutive welds using one of Arplas's welding programs.

However, improvements should be made to the bearings, which generate too much friction for the correct follow-up stiffness during welding. Measurements for the follow-up acceleration should be done again since the measurements taken in the tests did not correspond with the data acquired with the slowmotion camera and force sensor.

For future research, the model could be further investigated to predict the machine behavior and fine-tune the machine characteristics. Furthermore, a follow-up spring with an increasing stiffness ratio could be researched to better manipulate the drop force.

2 Introduction

In your house, car or at work you will daily use products made of metal sheets joined together. Many welding and joining techniques exist to produce these goods. One of these joining techniques is resistance welding. Resistance welding makes use of the electrical resistance between the metal sheets. Heat is generated by sending current through the metal sheets, forming a weld where the sheets make contact.

There are several different forms of resistance welding, with the most commonly known method being resistance spot welding (RSW). Resistance spot welding has been an important manufacturing process for especially the car industry, but other typical applications are electronics and other general sheetwork such as cabinets or metal buckets. Even the dentist uses spot welding for the metal braces. The key advantage is that no other materials are needed for the bond, making this process extremely cost effective.

There is a downside to spot welding though. High pressure and high currents need to be applied to the metal sheets and after welding is done, a small indent is left. Resistance projection welding (RPW) is a derived and similar process as spot welding, but with one key difference: a projection in one (or both) of the sheets. This projection focusses the current to a small area, making it more efficient than spot welding.

As environmental concern is growing, there is more demand for sustainable welding machines. The company Arplas Systems has filled this gap with projection welding guns requiring less energy than conventional spot welding guns. Furthermore, they patented a technique to make an almost invisible weld on one of the surfaces, making plastic covers for ugly weld spots unnecessary. Especially in the car industry, this is a great financial, sustainable and aesthetic improvement.

Their product portfolio consists of manual, stationary and robotic C-type welding guns, as well as the tools required for maintenance. Adding a far-reaching, or X-type, welding gun to their portfolio would significantly increase their applications and create more opportunities for otherwise difficult welding locations. Because X-type guns usually have a large throat length and are indirectly actuated (far away from weld location), they are especially useful in tight spaces and hard to reach spots.

The mechanics and dynamics of an X-type welding machines are different from the C-type machines and although X-type machines already exist for spot welding, there are no X-type *projection* welding machines on the market yet. This will therefore be the goal of this thesis:

"The design of a far-reaching projection welding machine, using the technology of Arplas Systems, with at least similar mechanical characteristics as the current welding machine."

Important to note is that the main goal is to design the mechanism of a far-reaching welding gun. The secondary goal is to make welds in both steel and aluminum sheets. The mechanical characteristics of the welding gun should have priority over the electrical system and weld strength.

During the process the question that will need to be answered are:

- What types of resistance welding are currently possible and what machine designs are used for which applications?
- What factors influence the weld quality during projection welding?
- What machine characteristics influence the weld quality, and what are the optimal machine characteristics?
- How are projection welding machines modeled and tested?
- What are the machine characteristics of Arplas's current C-type machine?
- How can the machine characteristics of the current machine be converted to an X-type design?
- How can an X-type projection welding machine be designed to meet all the requirements?
- Do the experimental results show that the X-type is working properly?

The subjects in this thesis can be split into three main categories: the literature studies, the testing of the current C-type machine, and the designing of an X-type machine. Therefore, the report is divided into three parts.

First, in Part I, a literature survey is done about the different types of resistance welding and their corresponding machines. More literature research is done for the factors influencing weld quality, the modelling and testing of projection welding machines, and finally, factors to take into account when designing a resistance welding machine.

Before diving into the concept generation of the X-type machine, the mechanical characteristics of the current C-type system need to be known. In part II, Arplas's C-type machine is analyzed to find the mechanical and follow-up characteristics. These are then, together with the literature results, converted to requirements for the X-type machine.

Part III contains the actual design process, from functions and requirements, to concept generation and selection, to detailed design. Part III is concluded with the experimental validation of the prototype.

2.1 Electric resistance welding

Resistance spot welding is part of the family of electric resistance welding (ERW) techniques. ERW is a thermo-electric process based on the principle that electrical resistance generates heat. ERW uses the contact resistance between two conducting metal parts to join them together. Besides spot welding there are other types of ERW techniques. These are classified considering the geometry of the weld and the way of applying pressure, these are:

- Spot Welding
- Projection welding
- Seam welding
- Flash welding
- Upset welding
- Special case ERW methods

Spot welding is the most common ERW method and uses two flat metal sheets with electrodes clamped on both sides. A high-density current is sent through the electrodes, which have a small surface area to concentrate the generated heat in a spot. The heat melts the sheets locally and forms a weld called a "nugget". The weld is completed after a cooling time, or forging time, to harden the nugget. Figure 2.1 graphically illustrates the spot welding process.

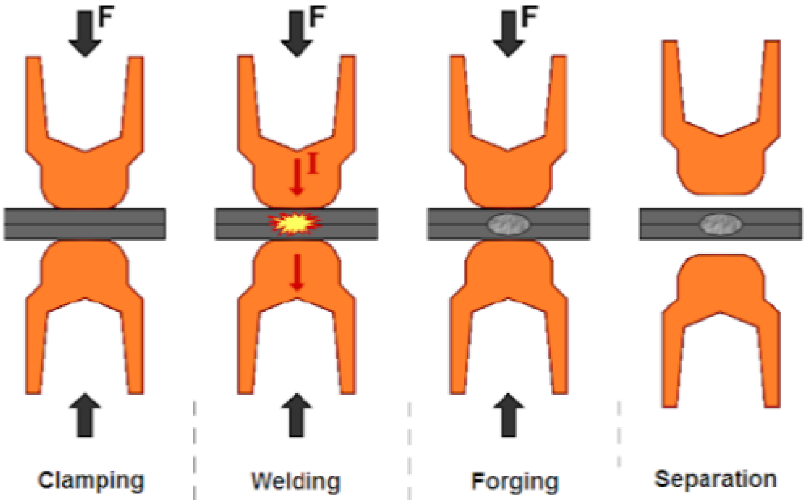

Figure 2.1: Steps in a RSW process [1].

The three most important welding parameters are weld current, weld time, and electrode force. The electrode force changes the contact area on a micro scale due to the surface roughness, changing the current density. Weld current and time are the amount and time the current is applied. These parameters form the basis for almost every ERW weld and changing them significantly influences the weld performance.

Other commonly used terminologies are squeeze time, hold time and off time. Squeeze time is the time it takes to apply and stabilize the electrode force. Hold time is the time it takes to solidify the nugget while the electrode force is still present. The off time is the time it takes to move to the next welding spot. A simple welding profile is depicted in figure 2.2.

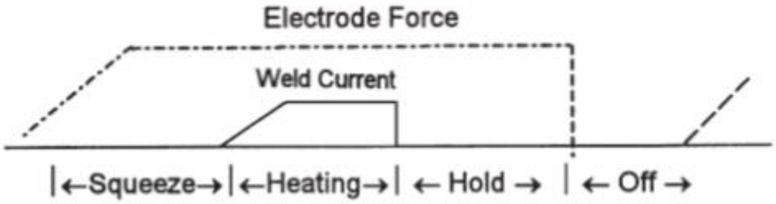

Figure 2.2: Example of a welding profile [2].

2.2 Physical aspects

Joule heating is the main physical phenomenon electrical resistance welding is based upon. This is the generation of heat due to current flowing through an electrical resistance. The total heat delivered depends on the current and the resistance of the product and can be expressed with the formula:

$$Q(t) = \int_0^t I(t)R(t)dt \tag{2.1}$$

Where Q(t) is the total heat energy delivered, I(t) is the current sent through the electrodes, and R(t) is the total resistance. The amount of energy needed for a weld depends on the material properties, sheet thickness, and type of electrodes. Too much energy can result in a hole instead of a weld and too little energy will not produce enough heat to liquefy the metal.

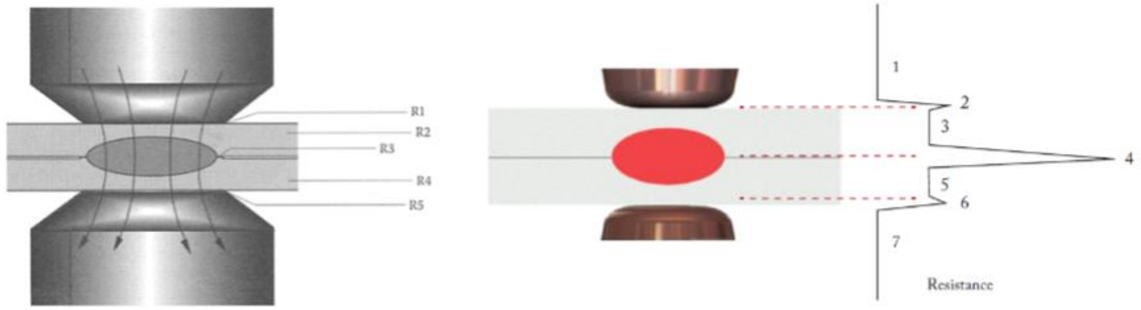

(a) (b)

Figure 2.3: (a) Different resistances when current flows through the electrodes. (b) The relative resistances in resistance welding for a 2-sheet stack showing that the contact resistance between the metal sheets is relatively the highest and thus heat generation will focus there. [3]

The total resistance of a stack of sheets can be found by summing up five resistances as shown in figure 2.3a. R_1 and R_5 are the contact resistances between the electrode and the sheet, R_2 and R_4 are the bulk resistances of the sheets and R_3 is the contact resistance between the two metal sheets.

The contact resistance is different for different materials contacting each other. Copper on steel has a much lower contact resistance than steel on steel, meaning that most of the heat will be generated at the contact between the steel sheets. Figure 2.3b shows the relative resistances to each other. It can be seen that the contact resistances are higher than the bulk resistances and the contact resistance between the steel sheets is dominant.

The bulk resistance of a material is determined by its electrical resistivity. This means that R_2 and R_4 depend on the resistivity with the following relation:

$$R = \frac{\rho L}{A} \tag{2.2}$$

With ρ the resistivity of the material, L the thickness of a sheet and A the area the current goes through. High resistivity results in large bulk resistances.

For the contact resistances R_1, R_3 and R_5 high resistances will be found because of irregularities on the surfaces. These irregularities, or surface roughness, result in a smaller and discrete contact area. As current flows through a smaller area due to the discrete contact points, the resistance will increase which will generate more heat. To increase the contact area, a higher electrode force can be used although it lowers the contact resistance. This is shown in figure 2.4. [3]

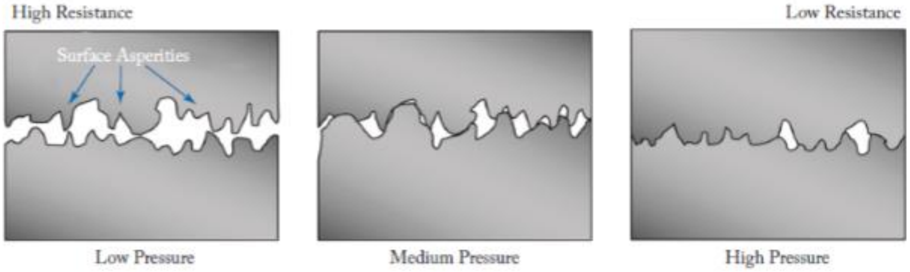

Figure 2.4: The relation between electrode force and contact resistance [3].

2.3 Welding machines and equipment

There are many different welding guns available on the market for all different kinds of materials, thicknesses, shapes, etc. Choosing the right welding equipment for your application is very important. First, there is the difference between manual and automatic operated. Manual operation needs skilled personnel to do the welding. The machine is fixed and the quality of the weld relies upon the welder.

Automatic operation uses a robot to move to the desired locations and automatically do the welding. Robot mounted welding equipment is therefore faster and more precise as manual welding. Furthermore, the shape of the workpiece and welding gun become more important for automatic operation as the robot will not always be able to reach the weld due to its kinematics.

For welding machines, a difference can be made between the mechanical, electrical system and hydraulic system. The mechanical system provides the electrode force, while the electrical system provides the welding current. The hydraulic system is necessary for the cooling of electrodes and other hot components.

2.3.1 Mechanical system

The mechanical system depends mostly on the type of actuator and the shape of the arms. The actuator, usually pneumatic or electric, provides the electrode force. The shape of the arms is mainly determined by the geometry of the workpiece, the necessary electrode force and the accuracy of the electrode alignment.

Two types of welding gun shapes dominate the market nowadays: the C-type and the X-type. Figure 2.5 shows both designs. With a C-type gun, the motor is usually placed in-line with the electrodes and can therefore be seen as a direct drive application. X-type guns usually rotate around a pivot point or use some other mechanism to place the motor far from the tips, making X-types an indirect drive application and perfect for far-reaching objectives.

The C-type is generally smaller and stiffer than an X-type but has trouble reaching some workpiece geometries. An X-type is more versatile but lacks rigidity as the arms become longer. If high forces are necessary, the C-type is generally the best choice. For more reachability, the X-type is preferred.

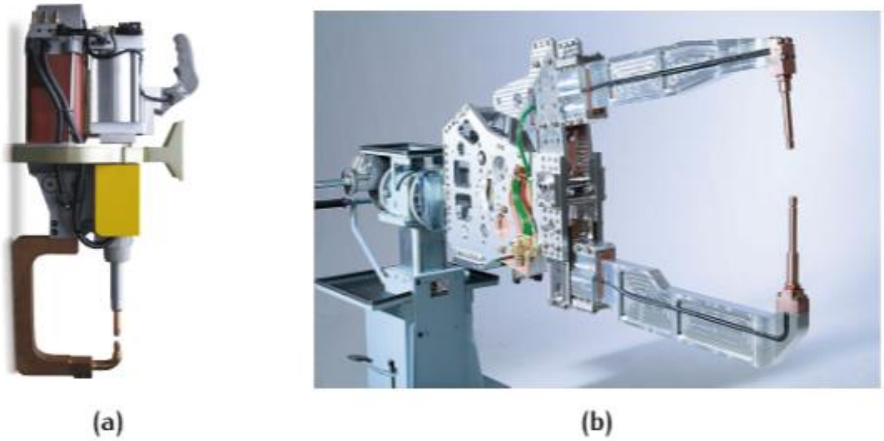

Figure 2.5: Different shapes of a welding gun. (a) C-type [4]*. (b) X-type* [5].

2.3.2 Electrical system

The electrical system provides the welding current. The power source, electrical connections and the electrodes are the main components. The power source provides AC or DC current, the connections conduct the current to the electrodes and the electrodes are in contact with the workpiece.

The shape and material of the electrodes are critical for high weld quality. Especially the electrode material should be carefully selected based on workpiece material and thickness ratio.

2.3.3 Hydraulic system

Every component conducting current generates heat when welding current is applied. When welding consecutively, the heat generated in the conducting components cannot be dissipated fast enough. High temperatures negatively influence not only the lifetime of the components, but also the weld quality. Cooling of the sensitive components such as the electrodes are essential for welding with high frequency. Usually water is used as cooling fluid.

2.4 Arplas welding

The company Arplas Systems uses resistance projection welding instead of spot welding. Projection welding also uses electrical resistance to generate heat and has almost the same setup. The difference in this process is that the weld is localized by means of raised sections, or projections, on one or both of the workpieces to be joined. The generated heat will concentrate in this projection, melting only the area where the projection of one sheet touches the other sheet. Therefore, less energy is required to make a weld. Some examples of projections are shown figure 2.6.

Other advantages and limitations for RPW are [6]–[9]:

- The possible thickness ratio (typical 6:1 and more) is quite larger than for regular spot welding (3:1 max.)
- Currents and forces involved are much smaller than for conventional spot welding
- Welds can be spaced closer than RSW
- Deformation and wear is limited due to larger surface area of electrode
- Uniformity of projections permits accurate and consistent location and the final products results more satisfactory
- The equipment needs some form of rapid response of the loading system, because the projection collapse brings a loss of force
- Weld size is limited by projection size

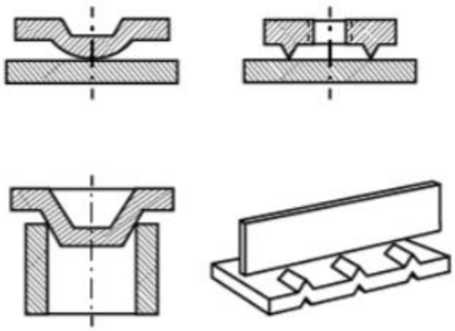

Figure 2.6: Examples of projection. In the top left a protrusion. In the top right an extrusion on one sheet. In the bottom left a complex projection on both sides. In the bottom right another example of protrusions [10].

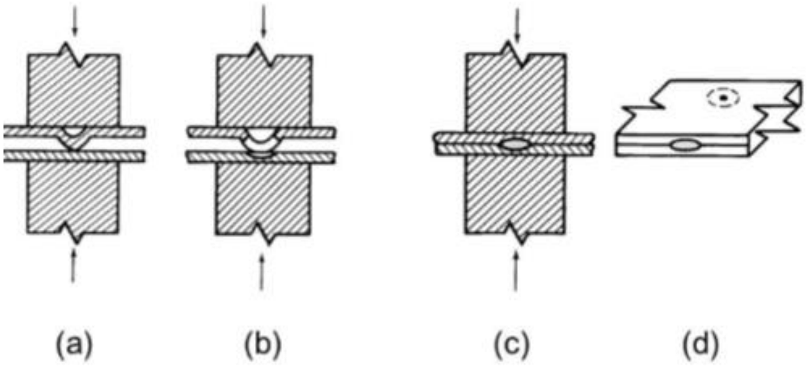

Figure 2.7: The process of PSW [10].

As said before, the welding process is very similar to spot welding. Welding force is applied to the metal sheets and current is applied to generate heat. But here is where projection welding changes with respect to spot welding. when current is applied, the projection heats up, softens, collapses and forms a nugget. This process is depicted in figure 2.7.

The collapse of the weld happens in a very short time span. In a few milliseconds most of the projection has already collapsed. It is crucial to keep the electrodes in contact with the metal sheets so the formation of the weld is not disrupted. This is why most projection welding machines have a follow-up system integrated.

Arplas has invented and patented the shape and dimensions of the protrusion to make a weld where only one side of the workpiece show signs of welding in terms of surface roughness [11], [12]. The triangular shaped protrusion for steel and a convex shape for aluminum result in a nugget formation in such a way that the sheet without the protrusion is almost unblemished. Table 2.1 shows some standard projection dimensions and welding settings for steel and aluminum with the machines of Arplas.

Table 2.1: Standards for welding steel or aluminum samples. The electrode force and current parameters differ with a changing sheet thickness.

	Steel	**Aluminum**
Dimple form	Triangular	Convex
Dimple height	0.7 mm	0.45 mm
Electrode force	1200 N	2500 N
Weld current	20 kA	38 kA
Weld time	6 ms	25 ms + 15ms downslope

2.4.1 Arplas C-type welding gun

The present welding gun Arplas uses is a C-type gun (figure 2.8). This gun comprises of a servo or pneumatic motor, a mass-spring follow-up system, flat electrodes, a transformer, copper armature, laminated shunts, water-cooling, sensors, and a housing.

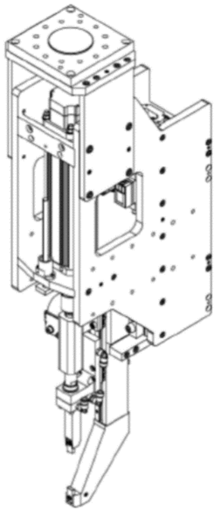

Figure 2.8: Arplas servo actuated C-type robotic welding gun.

The servomotor can move the upper electrode up and down. When the welding machine has moved to its welding location, the upper electrode is moved downwards and as soon as the electrodes touch the workpiece, the servomotor starts adding the electrode force. The electrode force is not directly applied to the electrodes though.

A follow-up spring is located between the motor and the upper electrode, so the motor will push against the spring, compressing it. The compression spring provides the necessary follow-up to keep contact with the metal sheets when the current is applied and the projection, or dimple, collapses. After the weld is done, the arms are opened again

More about the welding gun of Arplas will be discussed in chapter 7.

Part I: Literature

At the start of the graduation, I did not possess much knowledge about resistance welding and the resistance weld machines. A literature survey was performed to gain information and confirm the research gap provided by the company. A paper was written to summarize the discovered information and to help future engineers choose the correct resistance welding process and machine. The paper can be found in chapter 3.

After being introduced resistance welding, a more thorough investigation was performed to gain knowledge about the factors influencing the weld process, and the modelling and testing of spot and projection welding machines.

Literature about designing spot welding guns was easier to find than literature about designing projection welding guns. Since the welding process are quite similar, literature of both was used. However, conclusions made in literature for spot welding guns may not always be the same for projection welding machines.

More detailed information can be found in Appendix A.

3 Literature survey: Decision tree for a resistance welding method and machine based on part geometry and application

Decision tree for a resistance welding method and machine based on part geometry and application

HTE 2020

M. Gritter
Supervisors: *J.L. Herder, A. Amoozandeh Nobaveh*

January 29, 2020

Abstract

Resistance welding has been used for a long time. A lot of information can be found about different welding methods using resistance welding and their machines . But when a costumer or engineer would like a welding machine, the process of finding the right machine can become very complicated. Some studies were done for selecting a welding process, but these selection processes did not identify differences between the resistance welding processes. Here the resistance welding methods and the machines were investigated and decision trees were created using the advantages and limitations of the welding methods and machines. One general decision tree was successfully made for finding the right welding method. For some welding methods a second decision tree was made to find the right machine for that welding method.

Keywords: Resistance welding, decision tree, process selection.

1 Introduction

Electric resistance welding (ERW) is a very common process for joining metals. This type of welding can be used for a lot of different applications, from welding enormous steel structures in the maritime industry, to welding aluminium car frames in the automotive industries or even welding extremely small gold wires for circuit boards and microchips.

In previous studies, the resistance welding methods have been explained in detail [1–9] and the processes have been modeled more accurately which resulted in a better understanding of the fundamentals involved [10–12]. Different machine designs have been made to be able to use these methods in places that are difficult to reach or to be able to automate the process efficiently.

When choosing or designing a welding method and welding machine, a lot of different options are available. Finding the right machine for a particular application can quickly become confusing. There have been studies about a selection process for welding processes, but these are too general. For example spot welding and seam welding are different welding methods, but in the selection process in previous studies, one could use these interchangeable as the characteristics discussed there are all similar [13, 14].

The goal of this paper is therefore to find the differences between the resistance welding methods, and create one or more decision trees which points to a suitable ERW solution, if available.

In section 2, the fundamentals of ERW are explained and the different possible methods. In section 3 the methods and corresponding machines are investigated to produce the decision trees. Section 4 discusses the decision trees and section 5 contains the conclusion.

2 Method

Electric Resistance Welding

Resistance welding is a thermo-electric process where the necessary heat is generated by applying current. Key advantages include [15]:

- Short weld cycles
- No consumables, such as brazing materials, solder, or welding rods
- A safe working environment because of low voltages
- A reliable electro-mechanical joint is formed

ERW processes are based on the phenomenon Joule heating. Joule heating is the heating of a material by sending electrical current through. This current together with the electrical resistance of the material or interface determines the heat generated. The equation for Joule heating is

$$Q = \int_0^t I(t)^2 R(t) \mathrm{d}t \qquad (1)$$

With Q being the generated heat, $I(t)$ the welding current and $R(t)$ the electrical resistance [8].

This formula indicates that higher weld currents, weld times and resistances generate more heat. The formula for the electrical resistance is

$$R = \frac{\rho L}{A} \tag{2}$$

With ρ the resistivity of the material, L the thickness of a sheet and A the area the current goes through. By choosing the right electrodes, the highest resistance will be located at the interface between the metals as shown in Figure 1 [16]. Most of the heat will be generated at this interface, locally melting the metals and creating a nugget.

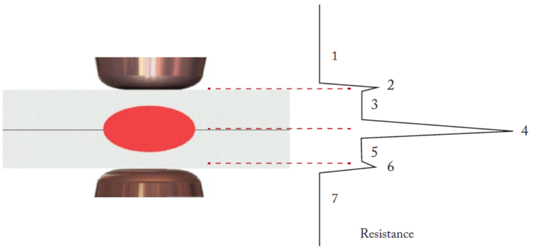

Figure 1: *The relative resistances in resistance welding for a 2-sheet stack up showing that the contact resistances are relatively higher than bulk resistances.*

When force is applied on the electrodes, the contact resistance can be influenced. This is because of irregularities on the surfaces. These irregularities, or surface roughness, result in a smaller and discrete contact area depicted in Figure 2. In Equation 2 it can be seen that increasing the contact area will decrease the contact resistance [16].

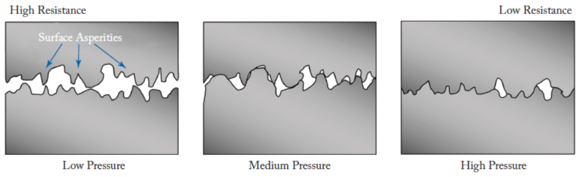

Figure 2: *The relation between electrode force and contact resistance.*

Summarizing the most important parameters in ERW: Weld current, weld time, and electrode force. These parameters are important in every welding method discussed here [7]:

- Resistance Spot Welding
- Resistance Projection Welding
- Resistance Seam Welding
- Upset Welding
- Flash Welding
- Special ERW methods

Using Google Scholar, Scopus and the TU Delft repository, these methods were investigated and the advantages and limitations are listed to be able to combine these in a resistance welding method decision tree. Advantages and limitations that distinguishes one method from another are especially important.

In order to find the corresponding welding machine, different types of machines for each method are investigated. For each method with multiple options for machine design, a separate decision tree will be made.

3 Results

3.1 Welding methods

Resistance spot welding

Resistance spot welding (RSW) is the most common method of resistance welding. This method uses two electrodes and a stack-up of metal sheets, depicted in Figure 1. When the sheets are pressed together, a high current is sent through the electrodes initiating the Joule heating. After the welding current has heated the metals and formed the nugget, the electrode force remains on the material to forge the weld for a short time, ensuring a high strength weld. A small indentation on both sides of the metal sheets will be present.

If the welds are spaced too close together, shunting could decrease the welding current with almost 32% [17]. The main advantages and limitations are [7, 8, 14]:

- The ratio of the two elements thicknesses should be less than 3:1.
- Generally for sheet thicknesses smaller than 1/8 inch (3.2 mm).
- Minimum distance between welds is 10 times the thickness.
- Clean surfaces, especially for metals like aluminum and stainless steel
- The size and shapes of the electrodes determine the size and strength of the weld.
- The weld forms only at the spot where the electrodes are in contact with the metal.
- If the current is not strong enough, hot enough or the metal is not held together with enough force, the spot weld may be small or weak.
- Warping and a loss of fatigue strength can occur around the point where metal has been spot welded.
- The metal may become less resistant to corrosion.

Resistance projection welding

Resistance projection welding (RPW) is a variation of spot welding. Projection welding uses, as the name suggests, a projection to focus the current to a small area. The projection could be an extrusion, a dimple or a natural projection like a bolt. The small contact area increases the contact resistance significantly, focusing the heat generation to the interface between the metals as shown in Figure 3. When the projection collapses, the electrodes need to stay in contact with the metal sheets. Hence fast follow-up behaviour is essential with RPW.

The increase in efficiency lowers the required amount of electrode force and welding current needed to make the same weld as with spot welding. This also allows welding multiple projections with one electrode and welding thicker sheets. Therefore RPW is preferred over RSW if the application allows it and the projection can be made without significantly increasing the cost per part.

The advantages and limitations for RPW are [2, 6, 7, 18]:

- Up to 6 welds per cycle (at the same time)
- Welds can be spaced closer than RSW
- Different electrode shapes can be used as long as the surfaces of the electrodes touch the parts to be joined
- Larger electrode means less wear
- Deformation is limited due to larger surface of electrode
- Proper heat balance can be obtained easily.
- Projection welding is capable of accepting mating elements of widely different thicknesses.
- The possible thickness ratio (typical 6:1 and more) is quite larger than for regular spot welding (3:1 max.).
- Can also be used for welding very large parts
- Currents and forces involved are much smaller than for conventional spot welding.
- Projection welds are smaller than spot welds. Uniformity of projections permits accurate and consistent location and the final products results more satisfactory.
- Occasional surface presence of light rust is less critical, because current breaks through at the protrusions.
- Generally used for products with a thickness larger than 0.3mm [14], as the higher temperatures of projection welding would result in the workpiece collapsing.
- Prior process of making the projection is needed, which can make the low quantity production expensive.
- Projection should be strong enough to withstand electrode force before passing current
- The equipment needs some form of rapid response of the loading system, because the projection collapse brings a loss of force.
- Weld size is limited by projection size.

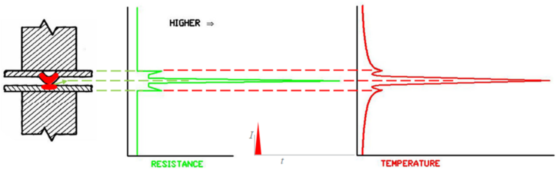

Figure 3: *RPW layout with the bulk and contact resistances, and corresponding temperature graph.*

Resistance seam welding

Resistance seam welding (RSEW) is a welding process with the same working method as spot welding, but the electrodes are motor driven circular disks, making it possible to weld continuously, with overlapping welds or with roll stop welds at high speed (Figure 4). This method makes it possible to produce air- or watertight tanks.

Seam welding shares a lot of advantages and disadvantages with spot welding. Although shunting is more common with seam welding, resulting in higher welding currents.

Advantages and limitations of RSEW are [7, 19]:

- Capable of producing continuous, leak tight welds.
- Overlap can be less than spot or projection welding, and seam width can be less than the diameter of spot welds.
- Generally practical for metal thicknesses ranging from 0.03 to 4.75 mm
- Straight or uniform curved line with no obstructions or sharp corners.
- Length of longitudinal seam joint are limited by throat depth
- Metal thicknesses larger than 3.2mm are more difficult to weld than with RSW or RPW.
- Seam welding can be done at very high speeds (up to 100 m/min [20]).

- Coated steels are generally more weldable using seam welding than spot welding, because coating residue can be continuously removed from the electrode wheels if special provisions are made.

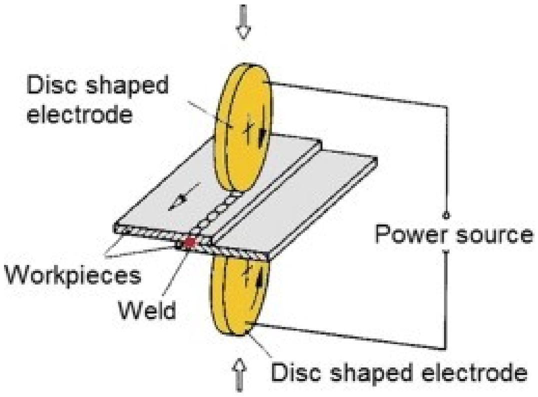

Figure 4: *Working principle of a seam welding machine*

Upset welding

Upset welding is a bit different as the previous methods, however it still uses the same principle. Both upset welding and flash welding are end-to-end welding methods. With upset welding, the ends are positioned face to face and some pressure is applied bringing them tightly together. The welding current is then sent through the electrodes attached on both sides. First the material is heated at the interface between both ends because of the high contact resistance. Secondly, when the required forging heat is generated, an upset force is applied. The current is stopped and the abundant material of pressing the ends together forms an upset as shown in Figure 5.

Advantages and limitations of UW are [7, 8]:

- High quality, absence of typical fusion defects
- Metallurgical properties comparable to those of hot worked material.
- Simple, sturdy and reliable equipment operated by unskilled workers
- Tolerance for minor alloy deviations
- Large selection of materials, including difficult to weld ones.
- Preferred over flash welding for many small components
- Equipment generally suitable to one type of applications only
- Creates an upset that maybe has to be removed
- The parts to be joined need an almost identical cross section
- Mainly pipes, tubes, bars and wires
- Wires from 1.3 to 31.8 mm diameter

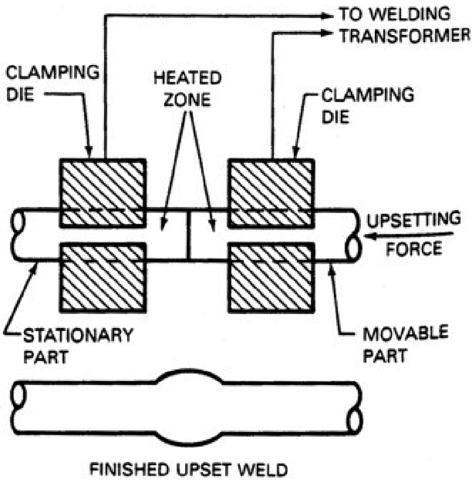

Figure 5: *Upset welding machine and process.*

Flash welding

Flash welding is quite similar to upset welding except for the separation of current and upset force, and the predetermined distance between the ends before sending the current. This predetermined distance causes arcs between the faces as a result of the current. When melting temperature is acquired due to the arcs, the current is stopped and then the upset force is applied. This type of welding is especially useful for welding ends that are corroded as the temperature rise is mainly caused by the arcs instead of pure contact resistance. Figure 6 shows a typical setup for flash welding.

- Flash welding can be applied to any metal that can be forged.
- Cross-sectional shapes other than circular can be flash welded; for example, angles, H-sections, and rectangles.
- Parts of similar cross section can be welded with their axes aligned or at an angle to each other, within limits.
- Sizes range from 0.2-mm-thick sheet to sections up to 0.1 m2 in area.
- The molten metal film on the faying surfaces and its ejection during upsetting acts to remove impurities from the interface.
- Preparation of the faying surfaces is not critical except for large parts that may require a bevel to initiate flashing.
- The heat-affected zones of flash welds are much narrower than those of upset welds.
- The parts to be joined need an almost identical cross section.

- Costly maintenance of equipment due to flashing.
- Electric power and upsetting force in available equipment limit the weldable size.
- Removal of flash and upset metal is generally necessary and may require special equipment.

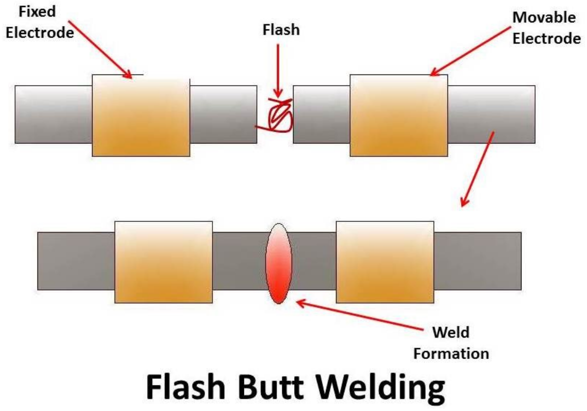

Figure 6: *Flash welding process.*

Special ERW methods

Other resistance welding methods are mostly specialized for a specific goal or application. Examples are: Cross-wire welding, percussion welding, butt seam welding, etc [7] . Cross-wire welding is used for welding wires on top of each other. The shape of the wire actually acts like a natural projection because the wires are only in contact at a small area, focusing the generated heat. Generally, a projection or spot welding machine will both be able to make these welds.

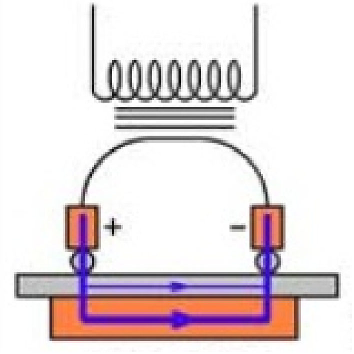

Figure 7: *Cross-wire welding layout. The arrows show the path the current takes.*

Percussion welding is similar to flash welding, but uses higher currents for a shorter time. The parts to be welded are placed end to end at a predetermined distance. With a rapid discharge of stored electrical energy, arcs heat the abutting surfaces. During and after the discharge, pressure is applied to form the weld. With this welding method, substances of entirely dissimilar characteristics can be welded while keeping the HAZ close to the surface. It must be remembered that the total area that can be joined is limited to 0.5 $inch^2$ [7]. Also similar metals can be joined more economically with other welding techniques.

Butt seam welding is a combination of flash welding and seam welding. Two parallel discs represent the electrodes and move along the part creating slight flashes. The heated material is pressed together afterwards, forging the ends together as shown Figure 8. This method is generally used when the part cannot be accessed from the other side and has a long and (almost) straight path.

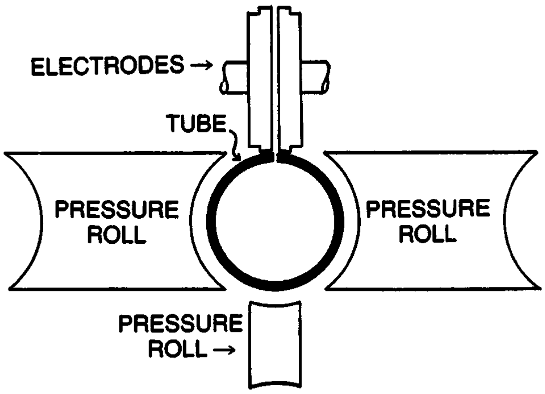

Figure 8: *Butt seam welding machine setup.*

Using the gathered advantages and limitations, a decision tree can be made to find the right method for every scenario, shown in Figure 9.

3.2 Welding machines

For high weld quality, the characteristics of a welding machine are very important. Low inertia for fast follow-up behaviour, high stiffness, and low friction are all essential for welding machine design.

Some welding methods can have multiple machine layouts, designed for different applications or products. Especially RSW, RPW and RSEW machines can have multiple setups.

The machines mentioned below could all be mounted on a robotic arm if needed unless stated otherwise. Also are RSW and RPW machines almost interchangeable. The layouts are the same except for a faster follow-up mechanism in RPW machines.

Resistance spot welding

The most common spot welding machine is the direct RSW machine. The electrodes are positioned co-linear at both sides of the metal sheets. The schematic setup is shown in Figure 10 [7]. Figure 1 was also an example of direct RSW welding.

Generally there are two different machines for direct welding: the C-type and the X-type. The C-type (Figure 11) offers high stiffness and the actuation, pneumatic or servo driven, is directly connected to the moving electrode. The downside is that the range is quite short and can thus only weld

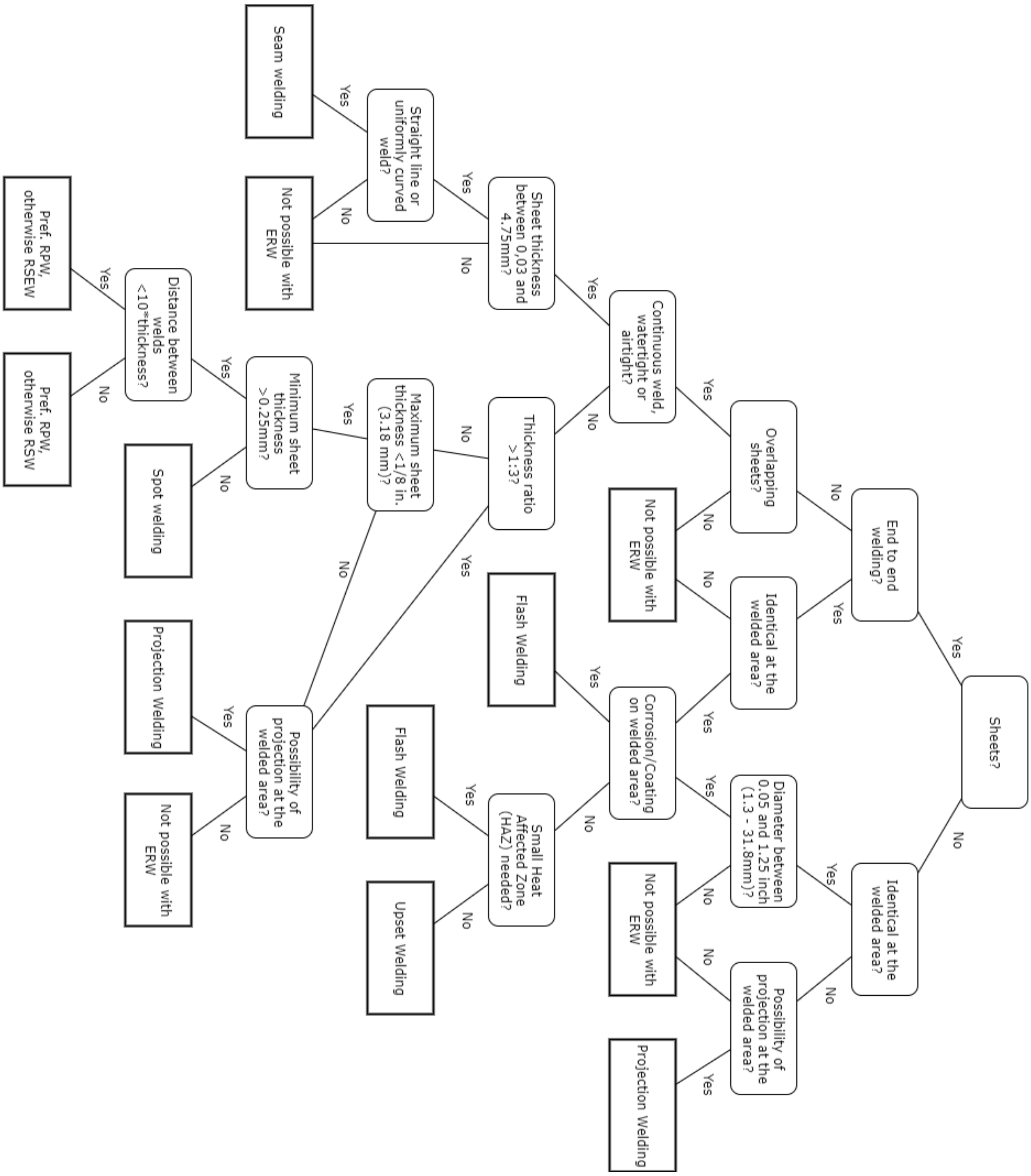
Sheets?
Yes
No
End to end welding?
Identical at the welded area?
Yes
No
Overlapping sheets?
Identical at the welded area?
Diameter between 0,05 and 1,25 inch (1,3 - 31,8mm)?
Possibility of projection at the welded area?
Not possible with ERW
Not possible with ERW
Projection Welding
Continuous weld, watertight or airtight?
Corrosion/Coating on welded area?
Flash Welding
Small Heat Affected Zone (HAZ) needed?
Flash Welding
Upset Welding
Sheet thickness between 0,03 and 4,75mm?
Thickness ratio >1:3?
Straight line or uniformly curved weld?
Seam welding
Not possible with ERW
Maximum sheet thickness <1/8 in. (3,18 mm)?
Minimum sheet thickness >0,25mm?
Distance between welds <10*thickness?
Pref. RPW, otherwise RSEW
Pref. RPW, otherwise RSW
Spot welding
Possibility of projection at the welded area?
Projection Welding
Not possible with ERW

Figure 9: *Resistance wethod decision tree. Starting from the top and ending in a ERW method if possible. Sometimes two methods are possible, but one is preferred (indicated with Pref.) over the other.*

close to the sides of a product or sheet.

The X-type (Figure 12) offers a larger range at the expense of some stiffness. It is more versatile in the places it can reach, especially if it is mounted on a robotic arm.

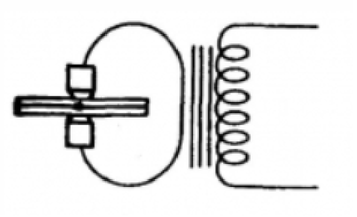

Figure 10: *Schematic layout of direct welding.*

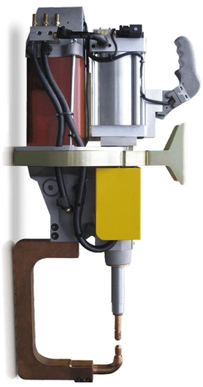

Figure 11: *Example of a C-type welding head [21].*

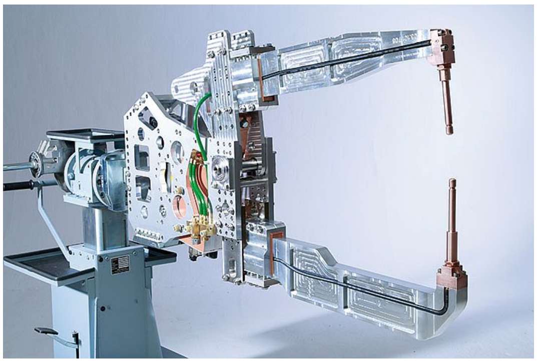

Figure 12: *Example of a X-type welding gun [22].*

An indirect weld, shown in Figure 13, can be made using one contoured and one flat electrode. The contoured electrode focuses the current on a smaller area while the flat pick up conductor is only a surface where the current can return. The advantage is that there is no need for an electrode on the other side. A disadvantage is the shunting current which goes directly through the top sheet back to the pick up conductor.

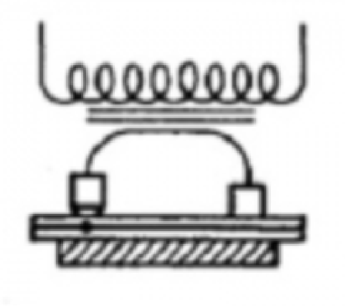

Figure 13: *Schematic layout for indirect welding [7].*

A series weld, or parallel weld, is almost the same as an indirect weld. The major difference is that both electrodes are contoured, creating a weld at both electrode locations. This technique is mostly used if only one side of the product is accessible and multiple welds have to be made at the same time.

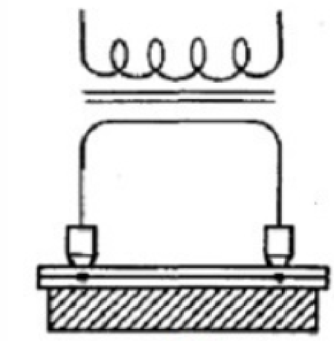

Figure 14: *Schematic layout for series or parallel welding [7].*

A push-pull weld is similar to series welding, but now electrodes are also placed on the other side of the metal sheets. The second circuit provides extra voltage, improving the welding current to shunting current ratio. This arrangement is often used on large panels to reduce secondary cable lengths and the adverse effect of inductance.

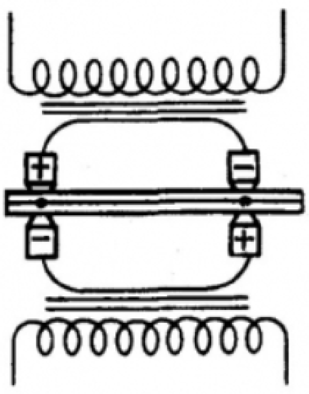

Figure 15: *Schematic layout for push-pull welding [7].*

The decision tree for RSW machines can now be created and is shown in Figure 16. It is assumed that at least one side of the metal sheets is accessible. A suitable RSW machine should be the outcome of this decision tree

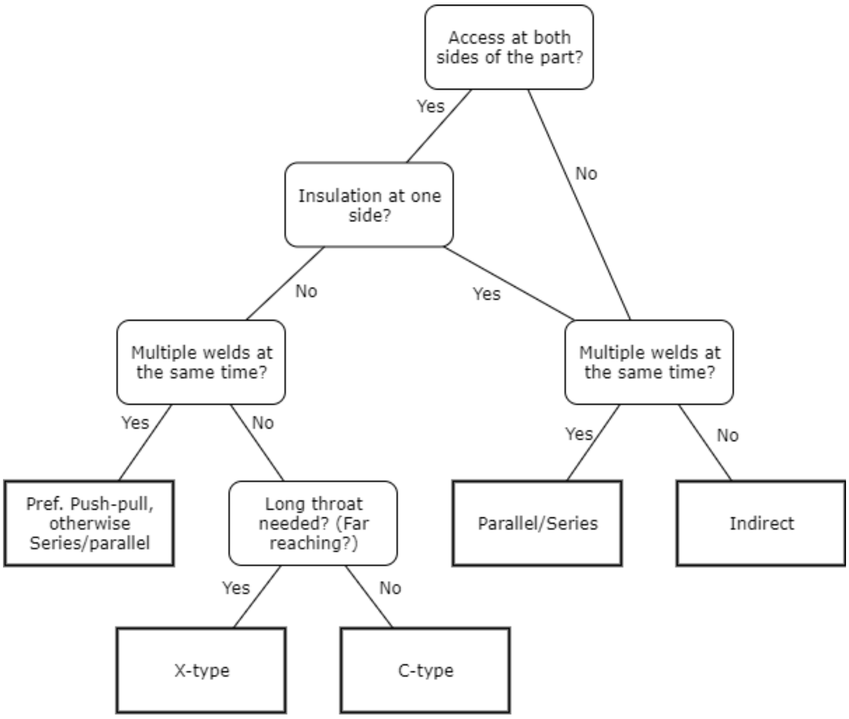
Access at both sides of the part?
Yes
No
Insulation at one side?
No
Yes
Multiple welds at the same time?
Yes
No
Multiple welds at the same time?
Yes
No
Pref. Push-pull, otherwise Series/parallel
Long throat needed? (Far reaching?)
Parallel/Series
Indirect
Yes
No
X-type
C-type

Figure 16: *Decision tree for RSW machines. Starting from the top and ending in a suitable RSW machine. Sometimes two machine setups are possible, but one is preferred (indicated with Pref.) over the other.*

Resistance projection welding

As mentioned before are the machine types of RSW and RPW almost interchangeable. Only indirect welding is not possible anymore. This is because in RSW the electrodes are always contoured to focus the heat generation and the flat electrodes used to be only a pick up conductor.

But in RPW, the heat generation is already focused because of the projection in the metal sheet. Therefore are the flat electrodes enough to make a weld. A small gap between the metal sheets also stops the current from returning to the electrodes at other locations than where projections are placed.

For these reasons the decision tree for RPW machine is similar to the decision tree for RSW machines, but lacks the indirect welding machine. This is shown in Figure 17.

Resistance seam welding

With RSEW two aspects can be varied: the way current is supplied and the amount of wheels. The current can be supplied continuous or pulsating. With pulsating current a choice has to made between overlapping welds or a roll stop motion for closely spaced individual welds (Figure 18). The continuous and overlapping welds provide an airtight or watertight seal. Continuous welding is not always possible for materials which need high welding currents because of the shunting current through the previous welds.

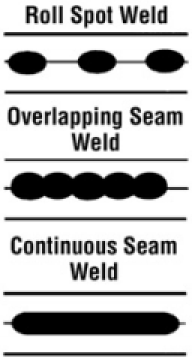
Roll Spot Weld
Overlapping Seam Weld
Continuous Seam Weld

Figure 18: *Different ways to supply current with seam welding [15].*

The other aspect which can be varied are the amount of wheels. The common RSEW machine has two rotating wheels attached to thongs and the metal sheets have to be moved along the wheels. This machine could be attached to a robotic arm if needed, but stationary RSEW machines are preferred for their rigidity. Figure 19 shows a longitudinal and a circular setup for a RSEW machine with two wheels [23].

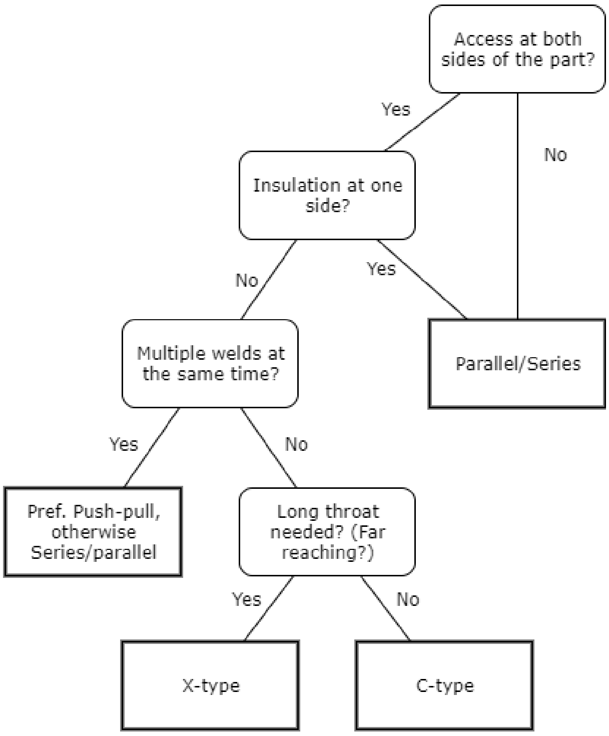
Access at both sides of the part?
Yes
No
Insulation at one side?
No
Yes
Multiple welds at the same time?
Parallel/Series
Yes
No
Pref. Push-pull, otherwise Series/parallel
Long throat needed? (Far reaching?)
Yes
No
X-type
C-type

Figure 17: *Decision tree for RPW machines. Starting from the top and ending in a suitable RPW machine. Sometimes two machine setups are possible, but one is preferred (indicated with Pref.) over the other.*

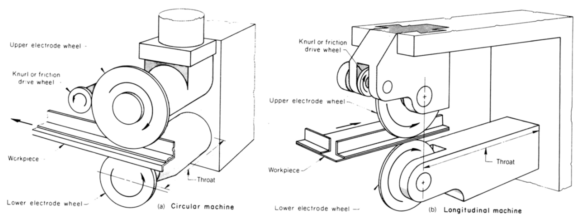
Upper electrode wheel
Knurl or friction drive wheel
Workpiece
Throat
Lower electrode wheel
(a) Circular machine
Knurl or friction drive wheel
Upper electrode wheel
Workpiece
Throat
Lower electrode wheel
(b) Longitudinal machine

Figure 19: *Two different setups for stationary RSEW machines with two rotating wheels.*

If the thongs holding the wheels cannot reach both sides of the metal sheets, a mandrel with a fixed electrode could be used (Figure 20). With this setup generally the wheel is moved along the mandrel, often resulting in large machines for precise movement along the weld line.

The decision tree for resistance seam welding machines can be seen in Figure 21.

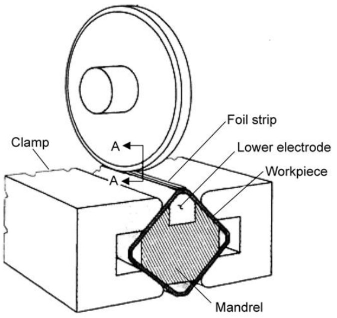
Foil strip
Clamp
A
Lower electrode
A
Workpiece
Mandrel

Figure 20: *RSEW machine with one moving wheel and a mandrel holding the second electrode [23].*

Upset and flash welding

Upset and flash welding are very similar welding techniques and therefore also have very similar machines. The machine design does not vary a lot, only the electrode clamps have to be designed to fit the parts as can be seen in Figure 22 [7]. Therefore no decision tree was made for UW and FW machines.

FW and UW machines require a high stability and upset force, and are generally not used for parts with intricate obstructions. Attaching a FW or UW welding head to a robotic arm is therefore unnecessary.

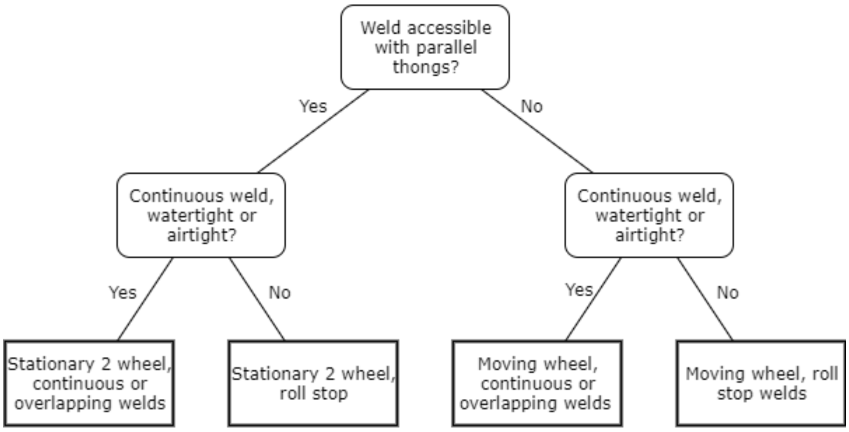
Weld accessible with parallel thongs?
Yes
No
Continuous weld, watertight or airtight?
Yes
No
Continuous weld, watertight or airtight?
Yes
No
Stationary 2 wheel, continuous or overlapping welds
Stationary 2 wheel, roll stop
Moving wheel, continuous or overlapping welds
Moving wheel, roll stop welds

Figure 21: *Decision tree for RSEW machines. Starting from the top and ending in a suitable RSEW machine.*

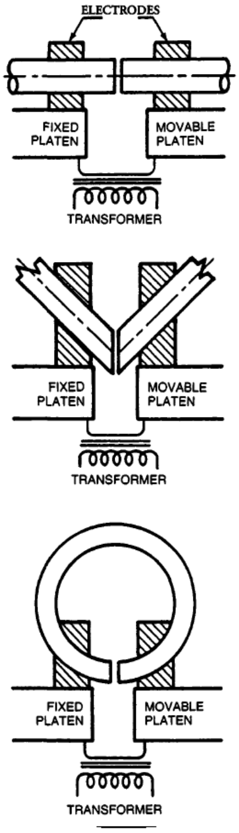
ELECTRODES
FIXED PLATEN
MOVABLE PLATEN
TRANSFORMER
FIXED PLATEN
MOVABLE PLATEN
TRANSFORMER
FIXED PLATEN
MOVABLE PLATEN
TRANSFORMER

Figure 22: *The different setups for UW and FW machines.*

4 Discussion

The decision trees presented in this study show the questions an engineer would have to ask himself when deciding on a ERW method and machine. An engineer or customer with only a basic understanding of ERW could use these decision trees to quickly find the right solution.

The decision trees have been subjected to multiple possible and impossible applications and always resulted in a generally accepted correct solution. It has not and probably can't implement every possible exception for all ERW melding methods and machine. There have been cases for example where spot welding and seam welding were used for mild steel sheet up to 20 mm thick. It requires high currents and expensive equipment, but it can be done [14]. In general however it is accepted that 1/8 inch is the upper limit for spot welding.

The decision trees only takes the geometry and the application of the product into account. The user of the decision tree still has to check if the materials of the parts can be welded with the advised welding method and machine, which can be done with the work of [14] and [13].

Future research could include more exceptions and the choice of materials could be included in the decision trees. Decision trees for other branches of welding process could also be interesting.

5 Conclusion

Resistance welding methods and machines have already been researched thoroughly. But in order to find the correct ERW machine for a specific application, the costumer or engineer will need the advice of an expert.

The decision trees developed in this study combined the results of many previous studies and can be used to find a suitable welding method and/or machine. Even if the person in question has almost no prior knowledge of resistance welding.

The decision trees are based on the geometry and the application of the parts. They do not yet include the material of the parts, so this should be taken into account. Future researchers could integrate the influence of material choice when deciding which ERW method and machine to use.

References

[1] H. Zhang and J. Senkara. *Resistance welding: fundamentals and applications.* Fla: CRC Press, Boca Raton, 2006.

[2] W. Lucas and S. Westgate. 10 - welding and soldering. In M.A. Laughton and D.J. Warne, editors, *Electrical Engineer's Reference Book (Sixteenth Edition)*, pages 10–1 – 10–51. Newnes, Oxford, sixteenth edition edition, 2003. ISBN 978-0-7506-4637-6. doi: https://doi.org/10.1016/B978-075064637-6/50010-1.

[3] E. N. Gregory A. R. Hutchinson D. B. Richardson, T. Z. Blanzymski and L. M. Wyatt. 16 - manufacturing methods. In Edward H. Smith, editor, *Mechanical Engineer's Reference Book (Twelfth Edition)*, pages 16–1 – 16–112. Butterworth-Heinemann, twelfth edition edition, 1994. ISBN 978-0-7506-1195-4. doi: https://doi.org/10.1016/B978-0-7506-1195-4.50020-8.

[4] Richard LeSar and Richard LeSar. Materials selection and design. In *Introduction to Computational Materials Science*. 2013. doi: 10.1017/cbo9781139033398.015.

[5] R.H. Todd, D.K. Allen, and L. Alting. *Manufacturing Processes Reference Guide*. Industrial Press, 1994. ISBN 9780831130497.

[6] P.N. Rao. *Manufacturing Technology*. Number v. 1. McGraw Hill Education, 2013. ISBN 9781259062575.

[7] Resistance Welder Manufacturers' Association and J.F. Deffenbaugh. *Resistance Welding Manual*. Resistance Welder Manufactures assn, 2003. ISBN 9780962438219.

[8] W.H. Cubberly, R. Bakerjian, and Society of Manufacturing Engineers. *Tool and Manufacturing Engineers Handbook Desk Edition*. Desk Edition. Society of Manufacturing Engineers, 1989. ISBN 9780872633513.

[9] J.A. Schey. *Introduction to Manufacturing Processes*. Industrial engineering series. McGraw-Hill, 1987. ISBN 9780070552791.

[10] Zygmunt Mikno, Mariusz Stepien, and Boguslaw Grzesik. Optimization of resistance welding by using electric servo actuator. *Welding in the World*, 2017. ISSN 00432288. doi: 10.1007/s40194-017-0437-x.

[11] Z. Mikno. Projection welding with pneumatic and servomechanical electrode operating force systems this research achieved an improvement in projection welding. *Welding Journal*, 2016. ISSN 00432296.

[12] Yasuharu Sakuma and Hatsuhiko Oikawa. Factors to determine static strengths of spot-weld for high strength steel sheets and developments of high-strength steel sheets with strong and stable welding characteristics. *Nippon Steel Technical Report*, 2003. ISSN 0300306X.

[13] S. M. Darwish, A. Al Tamimi, and S. Al-Habdan. A knowledge base for metal welding process selection. *International Journal of Machine Tools and Manufacture*, 1997. ISSN 08906955. doi: 10.1016/S0890-6955(96)00073-9.

[14] K. G. Swift and J. D. Booker. *Manufacturing Process Selection Handbook*. 2013. ISBN 9780080993607. doi: 10.1016/C2011-0-07343-X.

[15] Amada. Fundamentals of small parts resistance welding, 2013. URL http://www.amadamiyachi.com/servlet/servlet.FileDownload?retURL=%2Fapex%2Feducationalresources_articles&file=01530000000Jybm.

[16] David Löveborn. *3D FE Simulations of Resistance Spot Welding*. PhD thesis, KTH Royal Institute of Technology, 2016.

[17] H. Chang and Hyungsuck Cho. A study on the shunt effect in resistance spot welding. *Welding Journal*, 1990. ISSN 0043-2296.

[18] A.Goens. Spot welding vs. projection welding, 2019. URL https://www.norstaninc.com/blog/spot-welding/.

[19] What is seam welding and how it works, 2018. URL https://www.theweldingmaster.com/what-is-seam-welding/.

[20] S. Westgate. Resistance seam welding, 2001. URL http://www.ansatt.hig.no/henningj/materialteknologi/Lettvektdesign/joining%20methods/joining-welding-resistance%20seam%20welding.htm.

[21] URL https://www.wpitaiwan.com/product/suspended-portable-spot-welding/c-gun.html.

[22] URL https://www.nimak.de/en/spotweldinggun/multiframegun/.

[23] T.J. Lienert, ASM International. Handbook Committee, T. Lienert, and American Society for Metals. Joining Division. *Welding Fundamentals and Processes*. ASM Handbook. ASM International, 2011. ISBN 9781615031337. URL https://books.google.nl/books?id=BULGmwEACAAJ.

4 Modelling and testing of welding machines

4.1 Modeling of welding machines

Römer, Press and Krause [] were the first to make a mathematical model of the welding process. They wanted to find the main influencing machine parameters before, during and after welding. A mass-spring-damper system was used to model the welding machine with a C-type frame [13].

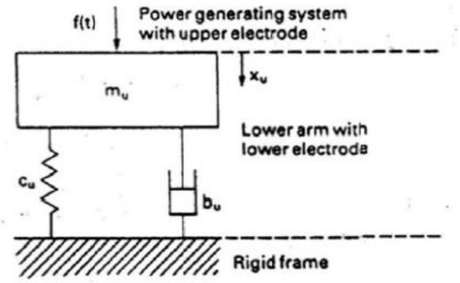
f(t)
Power generating system with upper electrode
m_u
x_u
Lower arm with lower electrode
c_u
b_u
Rigid frame

Figure 4.1: Mass-spring-damper model of a lower arm of a welding gun.

Using the derived differential solutions for touching and follow-up, theoretical optimal values can be determined. Table 4.1 summarizes these optimal values and especially for the lower electrode, the results are sometimes contradictory meaning trade-offs have to be made.

Table 4.1: Theoretical best mass, damping and stiffnesses for upper and lower electrode for spot welding machines [13].

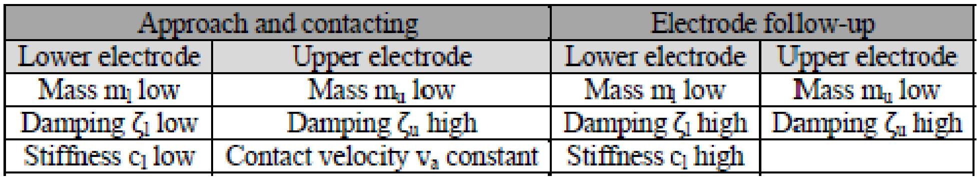

Approach and contacting		Electrode follow-up	
Lower electrode	Upper electrode	Lower electrode	Upper electrode
Mass m_l low	Mass m_u low	Mass m_l low	Mass m_u low
Damping ζ_l low	Damping ζ_u high	Damping ζ_l high	Damping ζ_u high
Stiffness c_l low	Contact velocity v_a constant	Stiffness c_l high	

Chen et al used the model shown in figure 4.2 to made a Simulink model and used displacement and force measurements to calculate the machine characteristics [14]. The downside is that the machine had to be taken apart and all parts had to be weighted to find the lumped mass, the way of modeling and calculating the stiffness and damping factor is interesting though. Experiments also validated his approach .

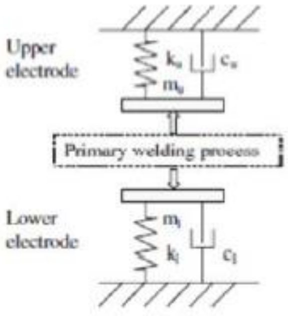

Figure 4.2: Model used by Chen to simulate the welding process [14].

Rymenant et al modeled and tested multiple resistance welding guns, one of them a spot/projection welding gun with a spring coupling between the actuator piston and the moving mass. This spring reduces the mass needed to accelerate during follow-up, but introduces another spring constant in the model. The new model made by Rymenant is shown in figure 4.3 [15].

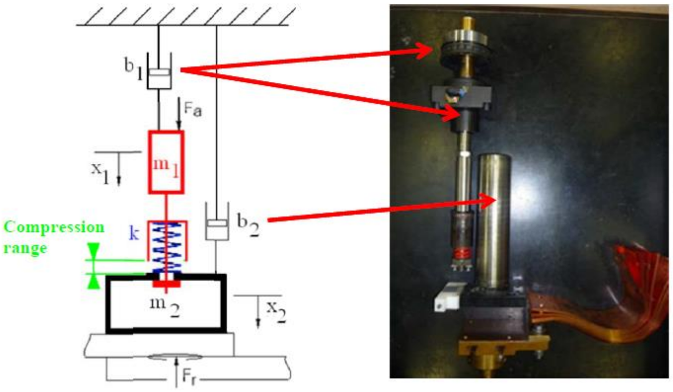

Figure 4.3: The model of the upper weld head of a projection welding machine with a follow-up spring[15].

This kind of setup, with a coupling spring, is recommended in applications where follow-up is important, which is especially relevant for projection welding guns.

4.2 Testing

Rymenant and Wu developed two methods to measure the machine characteristics called the free fracture test and the explosion test [15], [16]. These tests are meant to find the in-situ machine characteristics without disassembling the whole machine and weighing/testing the individual parts. Both tests measure the force in the lower weld head and the relative displacement between the electrodes.

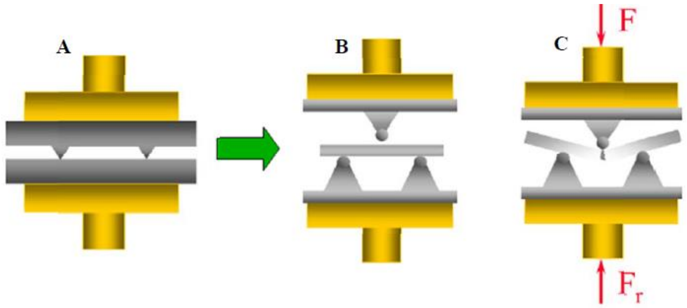

Figure 4.4: Free fracture test. A shows a regular projection weld. B and C show how a free fall is simulated by adding a rod made to break at a certain force [16].

In the free fracture test, shown in fig 4.4, a rod with the property of fracturing at a certain force is used to analyze the free fall of the upper weld head after fracturing. During a free fall, the reaction forces Fr become zero for a short time. Thus, the machine characteristics can be calculated by solving eq. 4.1.

$$m\frac{d^2x}{dt^2} + b\frac{dx}{dt} + kx = F - F_r \tag{0.1}$$

where m is the mass, b is the damping, k the stiffness, x is the relative displacement between the upper and lower electrode, and F the force. [Wu] studied the free breaking test and to find the machine characteristics, he used the time interval where the reaction force has dropped and solved the numeric matrix representation in that time interval.

The explosion test, shown in fig 4.5, is similar to the free fracture test but instead of a rod that fractures, a small ball or button is placed between the electrodes. The ball or button has similar height to the projection height and explodes after the current is applied. The explosion results in a free fall of the upper weld head, simulating a step response. Rymenant determined the mechanical characteristics by analyzing the movement of the upper electrode and fitting it with the recorded data. The resulting equation to fit to are eq. 4.2 and eq. 4.3 .

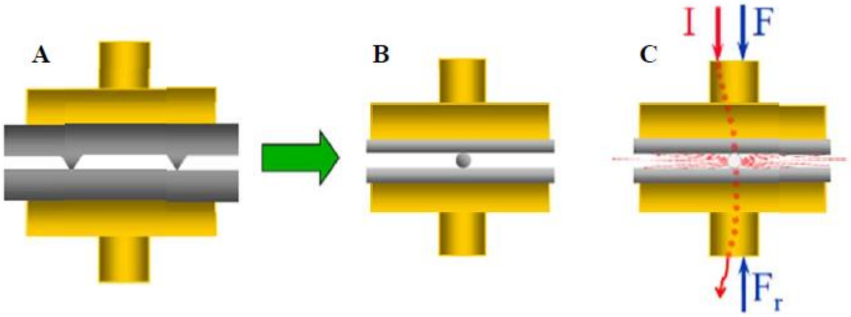

Figure 4.5: Explosion test. A shows a regular projection weld. B and C show how a free fall is simulated by sending current through a small sphere or button. This sacrificial sphere "explodes" due to the high current and heat generation [15].

$$x_{th}(t) = -\frac{F_{fracture}m}{b}\left(e^{-\frac{b}{m}(t+t_0)} + \frac{b}{m}(t + t_0) - 1\right) \tag{0.2}$$

$$v_{th}(t) = -\left[-\frac{F_{fracture}}{b}\left(e^{-\frac{b}{m}t} - 1\right) - \left(v_0 e^{-\frac{b}{m}t}\right)\right] \tag{0.3}$$

5 Factors influencing weld quality

To determine if a weld is strong enough a method has to be used to grade the weld. Although there are no universal accepted standards, an acceptable weld is defined as "a weld that meets the applicable requirements". The quality parameters to test, and which testing technique to use, are determined by the supplier and customer.

Different dimensions and characteristics can classify the formed nugget. The most common parameters for the quality of a weld are:

- Nugget size
- Penetration
- Indentation
- Cracks (internal and surface)
- Porosity/voids
- Sheet separation
- Surface appearance

These parameters are depicted in figure 5.1. Generally, nugget width and penetration are the decisive parameters because they are the easiest parameters to measure and are directly connected to weld strength [17]. For Arplas, surface appearance and indentation are also important quality parameters as the invisibility of the weld is their trademark.

Other characteristics such as cracks or porosity are also important parameters for the quality of a weld. Two welds can have the same nugget size, but if one has many cracks and the other has not, the nugget with cracks will be of lesser quality and will fail under lower stresses [3].

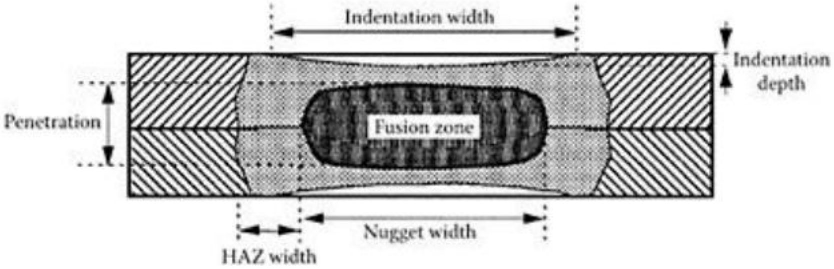

Figure 5.1: The different dimensions used for quality control of a weld [18].

Factors influencing the weld quality are of course the weld parameters electrode force, welding current and welding time, but also some underlying physical aspects due to high currents and rapid heat generation. Furthermore do welding machine characteristics and follow-up characteristics significantly influence the weld quality as well.

5.1 Physical influences

The physical influences discussed in this chapter are:

- Thermal expansion
- Lorentz forces
- Shunt effect

Other effects such as the Peltier effect and the dynamic electrical resistance are explained in Appendix A.1

5.1.1 Thermal expansion

During welding, the metals will locally expand and compress because of the changes in temperature. Metals with a high thermal expansion coefficient will experience higher local stresses.

For some metals like aluminum, the thermal expansion coefficient strongly depends on the temperature itself. Fig. 5.2 shows how the thermal expansion coefficient changes due to an increase in temperature. This changing thermal expansion coefficient makes predicting weld behavior of aluminum in particular hard.

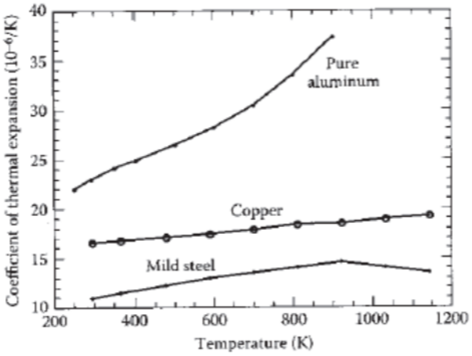

Figure 5.2: Thermal expansion coefficient changing with temperature for aluminum, steel and copper [3].

5.1.2 Lorentz forces

Williams et al noticed cyclic variations in the force while welding with AC current [19]. Williams attributed these cyclic forces to electromagnetic attraction and repulsion. They estimated these forces with the Lorentz force equation:

$$F = \frac{\mu \, I_1 \, I_2 \, L}{2\pi \, a} \tag{5.1}$$

With $\mu = 4\pi$ e-7, $I_1 = I_2$, L the throat length and a the distance between the electrode arms. Fujimoto et al confirmed the observations made by Williams [20]. Fujimoto et al mentioned that these variations in force adversely affect the welding process and depend on the machine characteristics.

Wu et al investigated these Lorentz forces as well [16]. He made a schematic overview of the secondary circuit path, shown in figure 5.3a and made a simplified model of this circuit (fig 5.3b). Wu used this model to calculate the Lorentz forces present in the system.

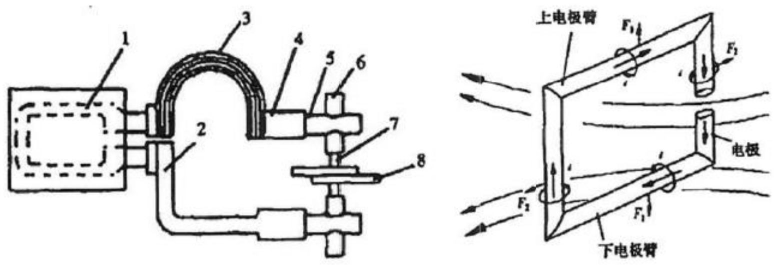

Figure 5.3: Schematic representation of the welding machine circuit to calculate Lorentz forces in a welding machine

5.1.3 Shunt effect

In industrial applications, welds can be placed in a sequence next to each other. These welds, or shunt welds, conduct some of the current provided by the electrodes. Therefore the current density through the shunted weld is reduced resulting in less heat being generated, and affecting the quality of the shunted weld. Chang showed that a shunted weld could lose up to 32% of the supplied current for steel welds that are very close together. Figure 5.4 shows the path of the current when a shunt weld is close. [Chang]

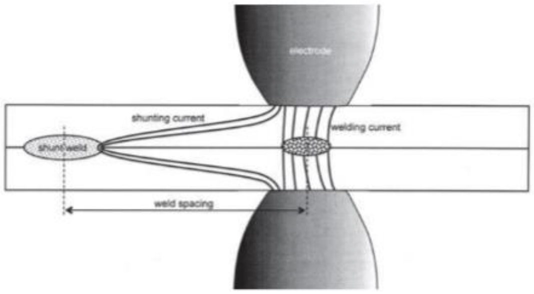

Figure 5.4: Shunt effect [3].

5.2 Weld tests

Multiple methods are possible for the testing of a weld, some destructive and some non-destructive. All test methods are explained in Appendix A.3. The company Arplas uses the peel test, a destructive test method.

The peel test can be done with a roller or a pliers which removes one sheet to make the weld button visible. Figure 5.5 shows how one sheet can be peeled loose to examine the weld button. The average of the maximum and minimum diameter is used for the quality control of the weld.

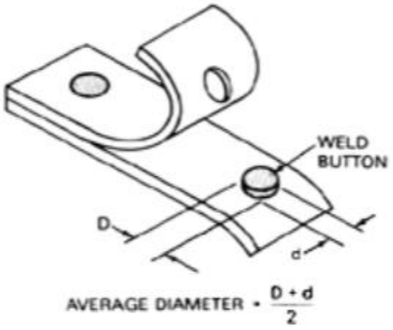

Figure 5.5: The peel test to check the size of the weld button . [21]

After the nugget inspection, new samples are welded for tension and shear strength tests.

The peel test could also be replaced with the chisel test, another destructive testing method. Non-destructive methods are ultrasonic testing, visual inspection, dye penetrant inspection, magnetic particle inspection, eddy current inspection, acoustic emission testing, and radiographic inspection [22].

6 Machine design research

The literature survey about the machine design can be split into two subjects: the equipment used and the general machine characteristics of the machine. Both are connected in some way of course but they have their own sections in this literature study.

6.1 Weld equipment

As already mentioned in section 2.3, the weld equipment can be divided into three categories: the mechanical, electrical, and hydraulic system. Each of these systems contribute to the quality of the weld in their own way.

The mechanical system was mostly already described, where the shape of the arms, a C-type or X-type, will change the behavior for the machine. C-type machines have more stiffness but less reachability whereas the X-type has low rigidity but can reach into tight places.

The choice of actuator can also influence the welding behavior especially for spot welding machines. Generally, either pneumatic or servo actuation is used as they provide high force in a short time. Pneumatic systems were popular back in the days and are still widely used, but servo actuation has become faster and more exact over the years. Servo actuation also produce less noise and has the ability to use force-control. The weld quality also increases significantly when using servo actuation, creating uniform nuggets more efficiently [23], [24].

The choice of which type of electrodes to use is important for both the mechanical and the electrical system. The electrodes are loaded with high electrode forces so they should be strong enough to handle the forces. They are also the focal point for the current to pass through. When welding consecutively, the electrodes will start to heat up due to the contact resistance between the workpiece and the electrode. The electrodes will therefore experience high forces, high currents and higher and higher temperatures.

Choosing the right electrode material is crucial for the lifetime of the electrodes and special care should be taken when welding dissimilar materials. Correcting the heat balance for these kind of situation can be done by using different materials for the lower and upper electrode as shown in figure 6.1.

Electrode degradation is also an important aspect of weld quality. With each welding cycle, the tip of the electrode is being affected by the heat and alloying with the workpiece. Softening, recrystallization, alloy formation, tip diameter growth and pitting are all types of degradation. Maintenance in the form of tip dressing, coatings and/or lubrication can significantly increase electrode lifetime, especially when aluminum or alloyed steels [25]–[27].

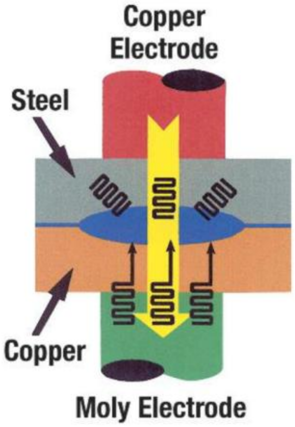

Figure 6.1: The image shows how the electrode materials should be chosen if dissimilar materials are welded [2].

For the electrical system, the right transformer should also be chosen carefully. The transformer applies the welding current but a choice will have to be made between welding with AC or DC. Welding with DC is preferred when fast rise times are necessary. These are therefore generally used for welding thin foils or fine wires. AC current is preferred when welding current is applied for a longer duration and is therefore more popular for spot welding than projection welding. The middle ground between the two is a mid-frequency DC (MFDC) inverter. These use pulse width modulation (PWM) to reach fast rise times. In projection welding these are typically used as they have excellent control and a high current capacity [2], [28].

The final piece of equipment is the hydraulics system which was also already discussed. As the electrodes heat up when welding rapidly, cooling is necessary. Water flows through small tubes inside the electrode to keep them at a stable operating temperature. Especially when welding conductive materials such as aluminum or copper, water cooling is a must have.

6.2 Mechanical characteristics

Many studies have focused on modeling, testing and determining the (best) mechanical characteristics. The process is complex and the optimal machine characteristics are sometimes contradictory. Therefore, to optimize the welding gun, trade-offs are necessary. Below are the combined results of the literature study about the machine characteristics. The results are categorized into four different aspects: weld quality, electrode life, touching behavior and follow-up behavior [29]–[34].

Note however that most research has been done on spot welding machines and not on projection welding machines. The operating principle is very similar but for projection welding follow-up is a lot more important.

Appendix A.6 contains a summary and small conclusion of each individual study for those interested.

6.2.1 Quality

- In all cases, moving mass exerted little effect on the nugget diameter.
- Moving mass has no clear influence on weld quality or follow-up.
- Stiffness and friction have the most significant influence on weld quality. This is due to the change in mean electrode force during follow-up.
- High stiffness reduces electrode misalignment.
- The expulsion limit is increased with an increasing stiffness.
- Higher stiffness also increases the forging effect after follow-up
- Friction is generally unfavorable for the weld quality and should be minimized
- In types C and D (indirect actuation) the nugget has a more elliptical shape.
- It was found that lower moving mass and lower stiffness resulted in a reduction of scatter of the strength value.

Low mass and low friction are recommended for the best weld quality. A tradeoff has to be made for the stiffness as high stiffness is better for electrode misalignment, the expulsion limit and forging effect, while a lower stiffness reduces the scatter in weld strength. The recommendation made in this study is therefore to have a high enough stiffness in order to have the most benefits, but not have an unnecessary high stiffness. Especially for projection welding machines care should be taken with the stiffness when designing a machine because of the necessary fast follow-up.

6.2.2 Electrode life

- Electrode life is dependent on impact energy, which is influenced by the moving mass, friction and stiffness.
- It was noticed that when rigidity was low (types B, C, and D) moving mass and friction had less effect on the electrode life. This was explained by the low rigidity absorbing the other effects.
- Moving mass should be minimized in order to reduce the impact at touching for improved electrode life.

To improve the electrode life, moving mass should be minimized. The influence of moving mass and friction become less noticeable when electrode arm stiffness is reduced.

6.2.3 Touching

- Changes in the moving mass and stiffness of the electrode arms significantly influence the static mechanical properties and dynamic touching behavior.
- Low moving mass improves contacting.
- Force is faster stabilized with low moving mass and high damping in the upper electrode arm.
- When the electrode arms have low rigidity (types B, C, and D), the influence of friction is small
- Lower stiffness of the lower electrode arm improves contact (short oscillations of electrode force), but increases bouncing effects
- Low friction worsens contacting.

- Theoretically low stiffness, low mass, high damping in upper arm and low damping in lower arm are preferable.

For the best touching behavior, the moving mass should be low and the damping in the upper arm high. However, when machines with a large throat length are used, the stiffness in the arms reduces and the effect of friction becomes less visible.

6.2.4 Follow-up

- With spot welding guns, the bending of the electrode arms primarily influences follow-up.
- In type A, the influence of friction is considerable.
- When the electrode arms have low rigidity (types B, C, and D), the influence of friction is small
- Lower stiffness of the lower electrode arm improves follow-up behavior (short oscillations of electrode force), but increases bouncing effects
- Moving mass has a lower impact on follow-up behavior below the splash limit.
- To stabilize the force quickly during/after follow-up, upper electrode mass should be low and damping should be high.
- Low friction improves follow-up.
- Low moving mass has no clear influence on follow-up.
- Theoretically, high stiffness, high damping and low mass are preferable.

For fast follow-up low friction is preferred, but high damping on the other hand could stabilize the force faster. Moving mass does not significantly influence the follow-up behavior for spot welding machines, but since projection welding machines have a larger distance where follow-up occurs, lower moving mass will have a larger impact on the follow-up behavior. For the stiffness the results are inconclusive, theoretically high stiffness is preferred, but some references concluded that lower stiffness is preferable for follow-up.

Table 6.1: Summary of the literature about the optimal machine characteristics.

	Weld quality		Electrode life		Touching		Follow-up	
Electrode	*Upper*	*Lower*	*Upper*	*Lower*	*Upper*	*Lower*	*Upper*	*Lower*
Mass	Low	-	Low	Low	Low	Low	Low	Low
Stiffness	High	High	-	-	Low	-	-	Low/High
Damping	-	Low	-	-	High	Low	Low/High	High

Part II: Testing the current C-type

7 Introduction

Since the company has not designed an X-type machine before, and to get similar weld results as with a C-type gun, some tests need to be performed on the current C-type system. The results will provide a starting point for the mechanical requirements of the X-type gun and can also be used to assess and compare the X-type results.

The literature review has given insight in the modelling and testing of C- and X-type spot welding guns nowadays, and gives some additional requirements. Although spot welding machines and projection welding machines are very similar in principle, projection welding machines have very different follow-up characteristics. Thus is follow-up important to measure for the Arplas C-type welding machine.

7.1 Goal

The goal of this test is to help make a list of requirements for this future X-type machine design. Tests are performed to find the mechanical characteristics of the current C-type, in particular the follow-up and structural characteristics. Additionally will the model be validated. Parameters of interest are:

- Machine stiffness
- Damping coefficient
- Effective masses of the system
- Maximum follow-up acceleration
- Welding stiffness

A schematic model of the C-type machine will make clear how the C-type machine behaves, and which parameters to measure. An analysis of the welding process will help understand how the system changes during the process.

Since the welding machines of Arplas weld both steel and aluminum sheets, the follow-up characteristics of both materials will be tested.

In addition, the influence of the metal sheets on these characteristics are tested and analyzed.

7.2 Analysis of Arplas system

The current system that is analyzed is a C-type projection welding machine from Arplas Systems, shown in figure 7.1. The machine uses a pneumatic actuator to apply pressure and a spring system with a mechanical stop provides the ability to regulate the electrode force.

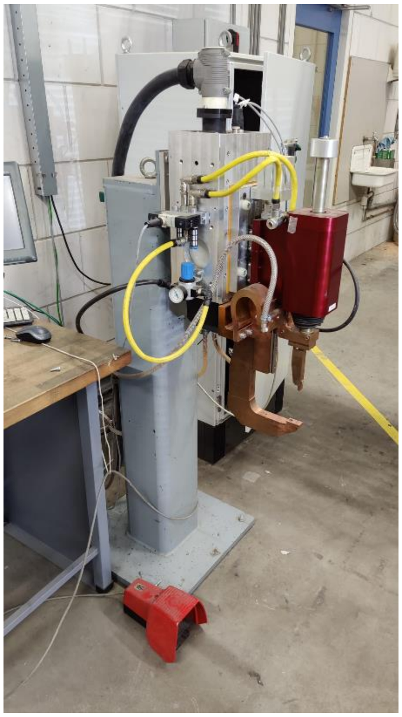

Figure 7.1: Photo of Arplas's current C-type that will be tested.

The upper weld head is connected to a linear guiding rail and the parts on both sides of the spring are separately connected to the guiding rails. The lower weld head is a copper frame bolted to the rigid machine or robotic arm.

Table 7.1: Arplas C-type machine specifications.

Force system	Pneumatic	Spring follow-up system
Electrode force	Min. 300 N	> 3000 N
Throat gap *e*, and length *l*	*e* = 150 mm	*l* = 300 mm
Mass of movable parts	3.41 kg	Electrode assembly + slide
	1.48 kg	Piston rod + spring assembly
	1.86 kg	Flexible lead
Coupling spring	200.000 N/m	

7.2.1 Welding procedure

First, a projection has to be made in a metal sheet on the locations of a weld. Arplas uses a separate machine for this step of the process and afterwards the sheets are placed within the range of the welding robot. The welding robot has to approach the product and the welding gun has to open its arms to place the electrodes on both sides of projection. The arms of the welding gun then must move towards each other until the product is detected. In the end position, the electrodes have to be collinear for the most effective welding.

The next step is to add the necessary electrode force without overdeflecting the structure to keep the electrodes collinear. When the applied force is stabilized, a current is sent through the electrodes, generating the heat necessary for welding. Quickly after the current is being applied, the projection collapses. In the short time the projection collapses, the welding gun has to keep contact to both sides of the product so the current loop remains closed.

When enough current is provided, the welding gun needs to keep pressure for a short cooling time. Afterwards the weld is finished and the welding robot can move to the next position.

Summarizing the welding process:

1. The welding machine is at standstill, no pressure is applied and the gun is open. Pressure is applied and the upper arm with integrated spring is moving down with some dynamic friction. It should be noted that this moving mass is actually two moving masses connected by a coupling spring, but acts as one moving mass at this stage.
2. The upper electrode touches the steel or aluminum sheets and starts to build up the necessary electrode force. This electrode force is regulated by moving the mechanical stop for the spring up or down, limiting the distance the spring is allowed to compress.
3. A stabilizing time ensures that the electrode force is stable before welding.
4. Current is applied and welding occurs. The projection collapses and the welding machine follows the material with a moving mass located between the spring and lower arm.
5. After a short forging time, the electrode force is removed and the gun opens.

These steps are also shown figure 7.2.

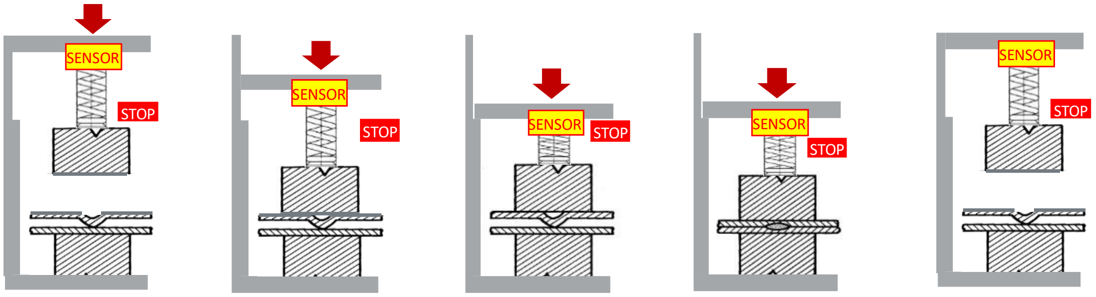

Figure 7.2: 1 Upper weld head moves down. 2 The weld head touches the lower electrode. 3 Electrode force is applied through the spring system until the mechanical stop is hit. 4 Welding current is applied, follow-up occurs, and a weld is made. 5 Upper electrode arm moves upwards. Pictures provided by Arplas.

7.2.2 Model of welding gun

To be able to determine machine characteristics from data, a model of the machine is important. Multiple studies have already modeled resistance welding machines and verified their results. The basic model was already developed by Römer et al [], where the lower weld head can be modeled as a mass-spring-damper system. The upper weld head was modeled as a mass-damper system when in motion. Rynemant [] also added that the structural damping of the lower weld head low is, which is also taken account in the model of Gould [].

The welding gun in use by Arplas has a spring coupling between the force actuator and the moving mass. Rymenant [] also analyzed a similar welding gun with a spring coupling and the model was shown in figure 4.3. To explain the change of the model during the welding process when a spring coupling is present, the different stages are analyzed.

At the start, the system is open and standing still. When the upper weld head moves downwards, the mass is accelerated M_u but experiences some frictional forces. Therefore, the upper weld head can be seen as a mass-damper system at this stage. The damping factor depends on the frictional forces in the bearing, linear guides, etc. The model of this stage is shown in figure 7.3a.

In the first step of the process, the whole weld head (with integrated spring) is moving down as one mass M_u. However, as soon as contact is made with the lower weld head, the system gets more complicated. The upper head splits into two masses, M_1 and M_2. A spring is placed between M_1 and M_2 to represent the coupling spring in the machine. Since both masses M_1 and M_2 slides separately over the same guiding rails, a damping factor connecting to the outside world are connected for both M_1 and M_2.

The sheets have not been modeled in previous literature yet, but with projection welding the sheets could have a compliance due to the projection in the sheets. For now, it is assumed that the mass of the sheets are irrelevant in this test because the test samples are small and lightweight. If it adds a stiffness, it could be modeled by a spring only. The model for the touching behavior can be seen in fig 7.3b .

After touching the sheets, the electrode force is being applied and the coupling spring gets compressed. The actuator applies force until the needed electrode force is obtained in the coupling spring element k_s. The actuator force does not need to be controlled because of the manually adjusted mechanical stop. The spring also lowers the moving mass during the welding stage where follow-up is extremely important.

When the electrode force is fully built up, mass M_1 is pushed against the mechanical stop and is therefore practically locked in place. Thus, the model for the follow-up stage is a bit simpler and is shown in fig 7.3c.

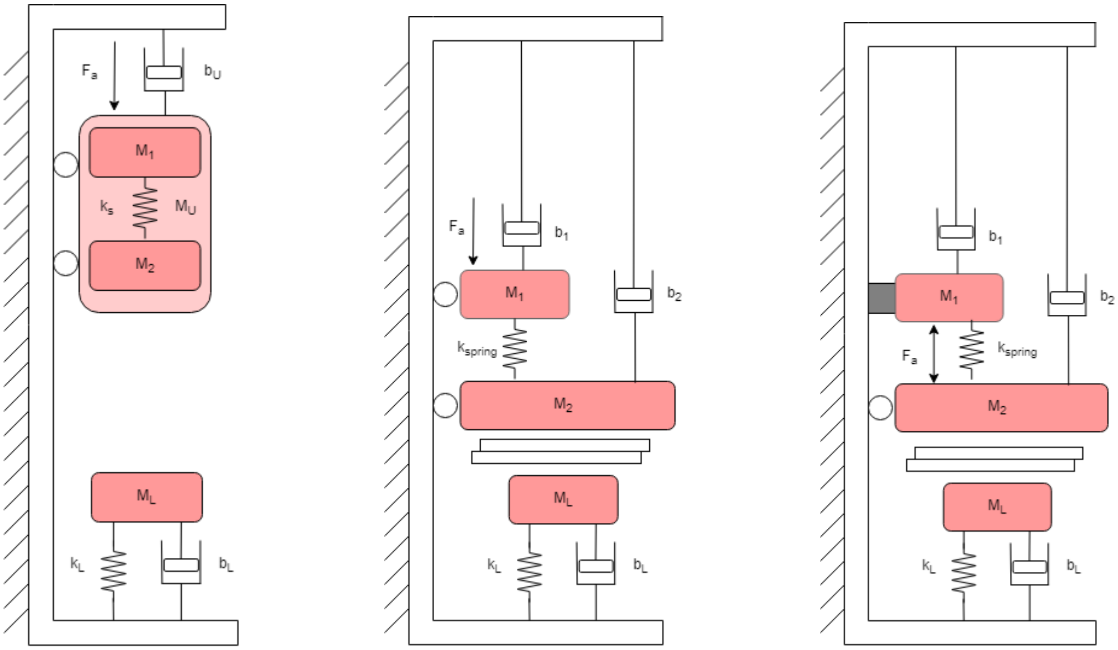

(a) (b) (c)

Figure 7.3: Models of the different steps in the welding process. A) Model when upper weld head is moving up or down. B) Model when upper weld head touches the lower weld head. C) Model for follow-up, M_1 is now rigid.

7.2.3 Frequency analysis of the model

To find the eigenfrequencies of the system, the models of figure 7.3 are further analyzed. During touching, all components of the system are excited, resulting in a frequency analysis capable of predicting the eigenfrequencies as functions of the masses and stiffnesses. These eigenfrequencies can later be measured to validate the model.

For the frequency analysis, the sheets in model B and C could be modelled either as a rigid body or as a spring stiffness. The spring stiffness indicating that the sheets are compressible due to the Young's modulus the sheet material. If so, the eigenfrequency of the lower arm may be possible to see too. Both models will be further investigated.

Analyzing the welding stage should confirm the results made in the touching phase.

Model B

First, we model B with the sheets as rigid body. M_L and M_2 will become connected and will act as a single mass. The single mass, M_{23} is than connected to the lower arm stiffness k_L and the coupling spring k_S.

Setting up the mass and stiffness matrix and solving eq. 7.1 gives us the two eigenfrequencies:

$$\omega = \sqrt{\frac{M_1 + M_{23}}{2M_1M_{23}}k_s + \frac{k_L}{2M_1} \pm \sqrt{\left[\frac{M_1 + M_{23}}{2M_1M_{23}}k_s + \frac{k_L}{2M_1}\right]^2 - \frac{k_sk_L}{M_1M_1}}} \tag{7.1}$$

Secondly, model B is analyzed with the sheets as stiffness, k_w. M_2 and M_L will now be disconnected.

The resulting stiffness and mass matrix become:

$$\begin{bmatrix} k_s & -k_s & 0 \\ -k_s & k_s + k_w & -k_w \\ 0 & -k_w & k_w + k_L \end{bmatrix} \tag{7.2}$$

$$\begin{bmatrix} M_1 & 0 & 0 \\ 0 & M_2 & 0 \\ 0 & 0 & M_L \end{bmatrix} \tag{7.3}$$

The masses M_1 and M_2 can both be measured by taking apart the welding machine and weighting the components, the results were already shown in Table 7.1, 1.48 kg and 3.41 kg respectively. The flexible lead will only be partly contributing to M_2, how much has not been tested yet.

The lower arm effective mass is hard to measure with a simple weight scale. Therefore it is assumed that the lower arm acts as a cantilever, having an effective mass of:

$$m_{eff} = \frac{33}{140}m \tag{7.4}$$

And an eigenfrequency of

$$\omega_L = 1.029\frac{h}{L^2}\sqrt{\frac{E}{\rho}} \tag{7.5}$$

E=124GPa, ρ = 8960 kg/m^3 , W = 30mm, h = 55mm, L = 150mm

The stiffness of the coupling spring is known but the effective spring stiffness of the lower arm and sheets are yet unknown. These will need to be measured during the experiments in chapter 8.

Model C

During welding M_1 is locked in place, meaning that the resulting frequency analysis is just as single mass between two springs if the sheets are assumed to be solid ($\omega = \sqrt{\frac{k_s+k_L}{m_{23}}}$).

If the sheets are assumed to be springs, two eigenfrequencies will be visible by solving with stiffness and mass matrices:

$$\begin{bmatrix} k_s + k_w & -k_w \\ -k_w & k_w + k_L \end{bmatrix} \tag{7.6}$$

$$\begin{bmatrix} M_2 & 0 \\ 0 & M_L \end{bmatrix} \tag{7.7}$$

8 Method

The tests that will be performed are used to find the kinematics, the machine characteristics and the follow-up characteristics of the current C-type welding gun of Arplas. These results will be used to have a starting point for future design of welding guns and they can be used to compare and validate new welding guns.

Principles used in previous literature will be applied to find the mechanical characteristics of the welding machine. The follow-up characteristics are found by analyzing the acquired data. A second method, a frequency analysis derived in section 7.2, will could also be applied to validate the model and machine characteristics.

8.1 Experiment setup

The machine characteristics can be found by measuring the displacement and force. In the literature [Wu,Rymenant] a force sensor is placed on the lower weld head, and a displacement sensor between the two electrodes. The velocity and acceleration can be numerically derived from the displacement data.

In the Arplas welding gun, a force sensor is already integrated in the upper weld head, so this sensor will be used in the tests instead of a force sensor on the lower weld head. The displacement sensor is placed at the top of the welding gun, measuring the displacement of the dynamic electrode. The schematic overview and picture of the setup are found in figure 8.1.

The way Arplas has designed their welding gun, a rod is visible at the top which is directly connected to the upper electrode. This way, the sensor cannot be damaged by flying hot metal during welding, while still accurately measuring the upper electrode displacement.

The displacement sensor does not measure the distance *between* the two electrodes, but only the displacement of the upper electrode. The lower weld head is assumed to be significantly stiffer than the upper weld head, and therefore have low displacements relative to the upper weld head. This still has to be taken into account when processing the data.

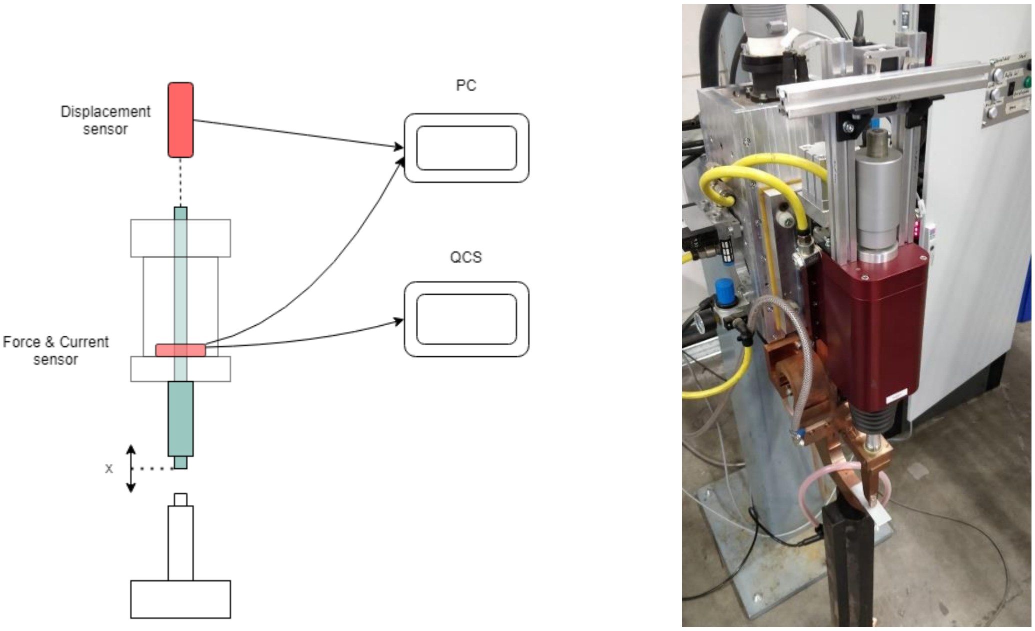

(a) (b)

Figure 8.1: Experimental setup for tests. (a) Schematic representation of setup and sensors. (b) Picture taken from setup.

Equipment used for the tests:

Force sensor	Kistler 9103 A	
Displacement sensor	Keyence LK-H052 fine target laser sensor	Range +-3mm, acc 0.02\mu m
Sensor controller	Keyence LG-G5001	125.000Hz?
Data Acquisition system	National Instruments NI USB-6211	250.000Hz

In the schematic overview in figure 8.1a it can be seen that the force and current measurements are not only stored on the pc, but also the QCS. The QCS is the weld controller provided by Arplas, using the force and current data to control the welding process. The QCS sample frequency is low compared to the data acquisition (1000Hz vs 125.000 Hz), and therefore the results of the data acquisition system will be preferred. Especially since follow-up happens in a few milliseconds.

8.2 Experiment 1: Touching behavior

The goal of this experiment is to find the machine characteristics of the touching behavior and the influence of material/samples between the electrodes. With the measured machine characteristics, model B is validated as well.

8.2.1 Lower arm stiffness

To determine the lower arm stiffness from touching behavior of the welding gun, the time response of the displacement sensor will be analyzed. The lower weld head bends when the electrode force is applied which can be seen with the linearly increasing displacement when electrode force is built up. This characteristic can be used to find the effective stiffness of the lower arm (and compression of sample material) during touching using the equation

$$k_L = \frac{\Delta F}{\Delta x} \tag{8.1}$$

In the section explaining the model (section 7.2), a note was already made that the structural damping of the lower head is low. Therefore the effective damping ratio is mainly governed by the damping ratio of the upper weld head/moving mass.

To find the damping ratio of the upper weld head, a response analysis after touching can be performed. Since the displacement sensor measures the position of the upper weld head plus the position of the lower weld head, the influence of the lower weld head on the displacement measurement has to be removed.

The lower weld head displacement is technically just the bending of the arm. Knowing the stiffness of the machine and the force applied to the system, the bending influence can be eliminated with the equation:

$$x_m = x_u + x_l \tag{8.2}$$

$$x_u = x_m - \frac{F}{k_L} \tag{8.3}$$

8.2.2 Sheet stiffness

To find the influence of the sheet stiffness, the touching behavior is analyzed for tests without any sample, increasing thickness steel samples and increasing thickness aluminum samples. The samples that will be used are:

- No sample
- Steel 0.8mm
- Steel 1.6mm
- Aluminum 0.8mm
- Aluminum 1.5mm

Increasing the thickness should result in a more clearly visible change in the measured upper electrode displacement. Thicker sheets have more material that is compressible. If significant changes are visible in the displacement, the sheet stiffness cannot be disregarded in the models.

Important to note is that the samples used in this test do NOT have dimples. This could be analyzed in further research.

The sheet stiffness can be measured with the upper electrode displacement during force buildup. By comparing the bending of the lower without any sample with those with the steel and aluminum sample. The sheet compression extra displacement with a sample by applying eq. 8.4.

$$k_{measure} = \frac{1}{\left(\frac{1}{k_{sheet}} + \frac{1}{k_L}\right)} \tag{8.4}$$

K_L is the result of this test without any sample between the electrodes.

8.2.3 Total stiffness acting on workpiece

It can be seen in the model made in section 7.2 for touching, model B, all the spring stiffnesses are in series. Since only the upper weld head is able to move, the total stiffness acting on the part can be found by calculating the effective stiffness with all springs in series. Therefore, the total stiffness acting on the workpiece is calculated with:

$$k_{measure} = \frac{1}{\left(\frac{1}{k_s} + \frac{1}{k_{sheet}} + \frac{1}{k_L}\right)} \tag{8.5}$$

Where k_{sheets} goes to infinity if sheets are rigid bodies. k_s is already known as the coupling spring is always tested separately before being assembled in the welding gun.

8.2.4 Damping of the system

The damping factor, zeta, can be found by measuring the decrement of the oscillation peaks and applying:

$$\zeta = \frac{\delta}{\sqrt{\delta^2 + (2\pi)^2}} \text{ where } \delta = \ln\frac{x_0}{x_1}$$

With x_0 being the amplitude of the first overshoot peak and x_1 being the amplitude of the second oscillation peak.

Alternatively, the damping can be found by fitting the envelope of the impulse response. Since the impulse response for an underdamped system is

$$Y = Ae^{-\zeta\omega_0 t}\sin(\omega_d t) \tag{8.6}$$

Where $e^{-\zeta\omega_0 t}$ represents the damping of the system. Fitting a first order exponential to the peaks of the response gives us the damping factor as well. Since the distance between the peaks reveals the damped frequency and the system stiffness has just been calculated, the mass can be calculated with

$$m = \frac{k}{{\omega_0}^2} \tag{8.7}$$

The damping coefficient is then calculated with the natural frequency as follows:

$$b = 2\zeta m w_n \tag{8.8}$$

8.2.5 Model B validation

A Fourier transform of the oscillations when touching should validate the model when all parameters are inserted into the modal analysis of model B.

8.3 Experiment 2: Welding behavior

The goal of this experiment is to find the weld characteristics:

- Stiffness during welding/ stiffness acting on workpiece
- Follow-up acceleration
- Model C validation

The same method as in the previous experiment can be used to find the machine characteristics. A step response analysis will result in the effective stiffness, damping factor and mass during follow-up.

Multiple tests will be done where a successful weld is made. The initial conditions such as electrode force, welding current, and current duration are changed for different metal sheets to ensure a good weld. The conditions are listed in the table below:

Table 8.1: Welding parameters used in the tests.

Material and sheet thickness	**Electrode force**	**Current time**	**Current amplitude peak**
Steel 0.8 mm	1000 N	5 ms	16 kA
Steel 1.6 mm	1300 N	7 ms	21 kA
Aluminum 0.8 mm	2300 N	25 ms / 15 ms downslope	43 kA
Aluminum 1.5mm	2500 N	40/20	43 kA

During this test the follow up characteristics will be analyzed. The projection used for the steel sheets is 0.7mm in height and for the aluminum sheets the projection height is 0.45mm.

8.3.1 Continuous measurement of mechanical characteristics

A second method will be used to try to verify the results and if this method is successful, will give the machine characteristics not only during follow-up but also throughout the whole process.

This method uses the same principle as Wu [] used in his analysis. Wu performed a free fracture test to simulate a complete drop of the reaction force and solved eq. 8.9 in the time interval where the reaction force has dropped.

$$m\frac{d^2x}{dt^2} + b\frac{dx}{dt} + kx = F - F_r \tag{8.9}$$

In this research not only the time interval during welding is considered. Instead, the machine characteristics will be measured and calculated throughout the whole welding process.

Having the force, displacement, velocity and acceleration during the whole process, the mass, damping and stiffness can be calculated. However, because the system is changing during the welding process, as was shown by the different models for the different stages, the calculated effective masses, damping factors and stiffnesses will also change. Therefore the data will be split in blocks with a short time interval. The machine characteristics will be calculated for each of these time blocks to analyze the changes in the system during the whole process and find the corresponding machine characteristics for those systems.

The difference between Wu and this research is that in this research a continuous analysis of the process is made instead of between a specific time interval. Another difference is that Wu and Remenant both need a sacrificial part to simulate the step response while in this research any part that is usually welded can be analyzed.

The lack of a lower arm force sensor and not using a sacrificial part could prove problematic though. If successful, this method could make the testing of welding machines extremely easy. If not successful, the step analysis will be used which is a bit more complicated but still remove the need for extra sensors and sacrificial parts.

8.3.2 Machine characteristics Rymenant method

Rymenant used in his tests a sacrificial part to invoke a step response on the upper weld head. By fitting eq. 8.10 on his velocity data he calculated the machine characteristics. This method will also be used in the tests on the C-type machine. No sacrificial part will be used, since the small projection for the Arplas welds does already function as an initiator of a step response. The results of this method will be used to compare with the other calculated machine characteristics.

$$v_{th}(t) = -\left[-\frac{F_{fracture}}{b}\left(e^{-\frac{b}{m}t} - 1\right) - \left(v_0 e^{-\frac{b}{m}t}\right)\right] \tag{8.10}$$

8.3.3 Stiffness during welding

The force drop and displacement drop can be used to calculate the stiffness during welding. Again all springs contribute during the welding process, meaning that we should be able to verify the stiffness acting in the workpiece, which we calculated with the Touching experiment. Using the same equation as for the calculation of the lower arm stiffness, the effective stiffness can be measured:

$$k_{weld} = \frac{\Delta F_{drop}}{\Delta x_{drop}} \tag{8.11}$$

8.3.4 Follow-up acceleration

With the numerically derived acceleration from the displacement, the acceleration during welding can be found. The acceleration is an indication of how fast the weld collapses and how fast the system responds to the collapse.

8.3.5 Model C validation

As with the Model B validation, a Fourier transform of the follow-up displacement should give us the visible eigenfrequencies of the system. Filling in the parameters in the modal analysis of model C, the calculated frequencies and measured frequencies should be similar.

9 Results

Figure 9.1 shows the result of a welding cycle of the C-type machine. At first the weld head is at standstill, then a small force impulse accelerates the weld head towards the samples. When contact is made with the lower weld head a small force impulse is seen again and the electrode force is applied. After the force has stabilized, welding is initiated and a drop in force and displacement can be seen.

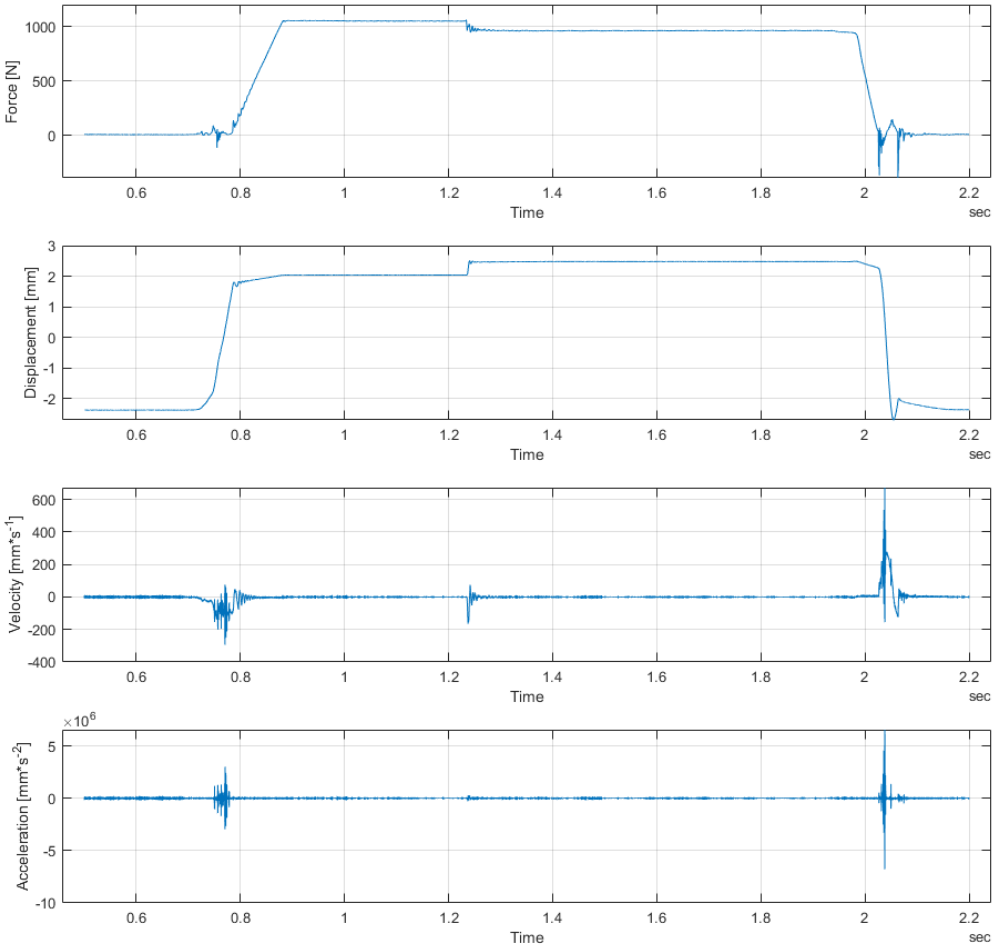

Figure 9.1: Resulting measurements of a welding process.

9.1 Experiment 1: Touching

In figure 9.2 below, the results for one of the tests without welding and without any workpiece is shown. The data was smoothed by a moving average with the "smoothdata" function of Matlab. The velocity and acceleration are numerically determined as explained in section 8.1.

What can be seen in the figure is that at first the system is at standstill and starts moving down. When contact is made between the upper and lower weld head, another small impact peak in force is visible. Immediately afterwards, the electrode force is built up. This can be seen by the increasing force and the slowly increasing displacement. The system becomes stable and with no welding occurring, the system moves back to its initial position with the gun arms open.

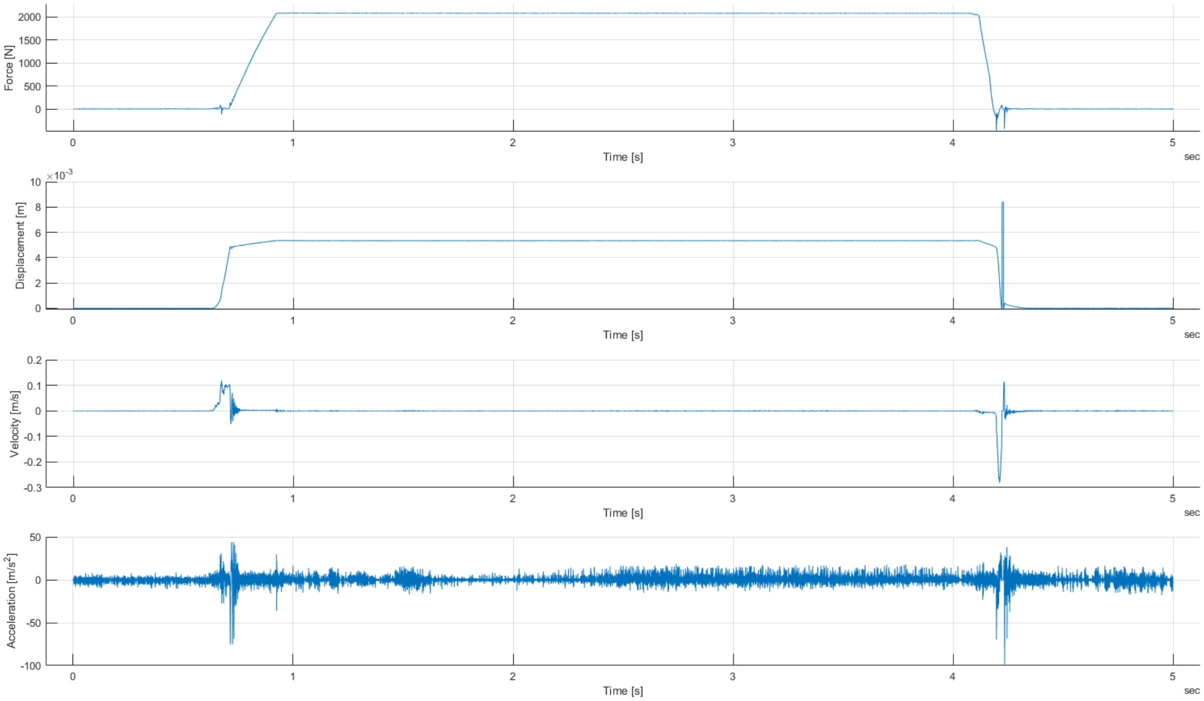

Figure 9.2: Typical response of the displacement, velocity, acceleration and force for touching and building up electrode force. The different stages of the process, gun close – build up force – release force – gun open, can clearly be identified.

Figure 9.3 shows a zoomed view of this time interval where the system moves downwards and applies the electrode force. The system starts moving at t=0.64s, but the max pneumatic pressure is applied at t=0.67s where the small peak in force (~85N) can be seen.

At t=0.72s the impact force peak is visible but is dwarfed by the electrode force buildup.

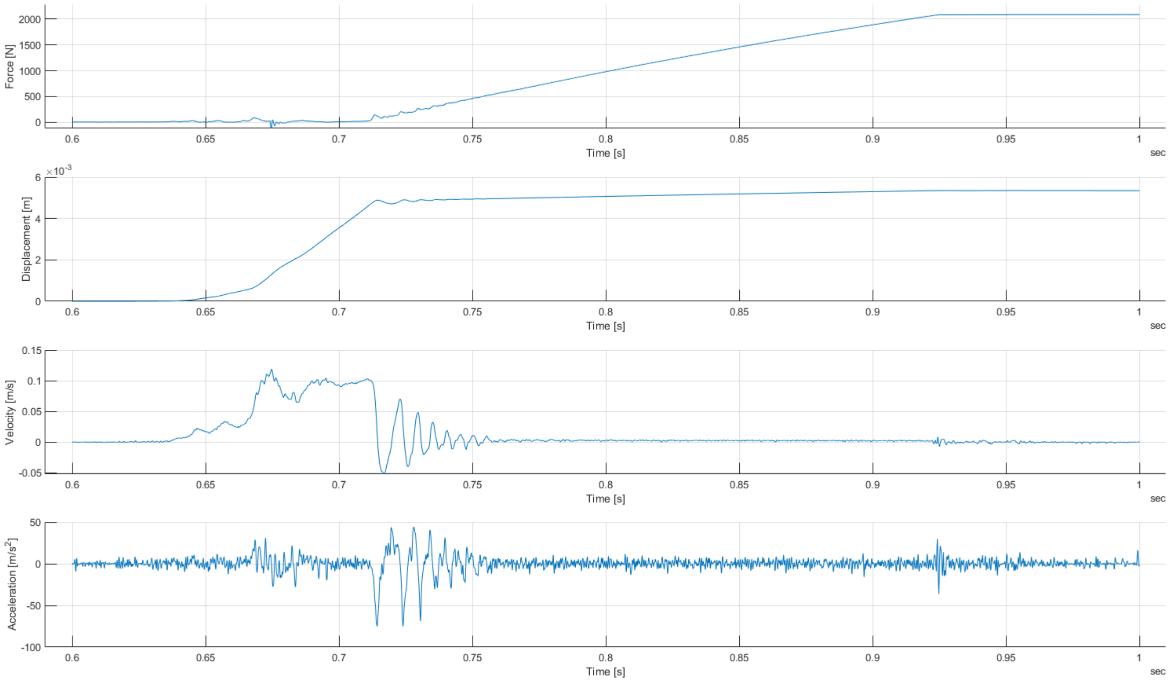

Figure 9.3: Zoomed view of free stroke and touching behavior.

9.1.1 Lower arm stiffness

The stiffness of the lower arm can be determined by calculating the steepness of the linear increase of the displacement due to the electrode force. In the region where the electrode force is built up, the effective stiffness is calculated with eq. 8.1. No material is placed between the electrodes to find the pure lower arm stiffness. The results are shown in table 9.1.

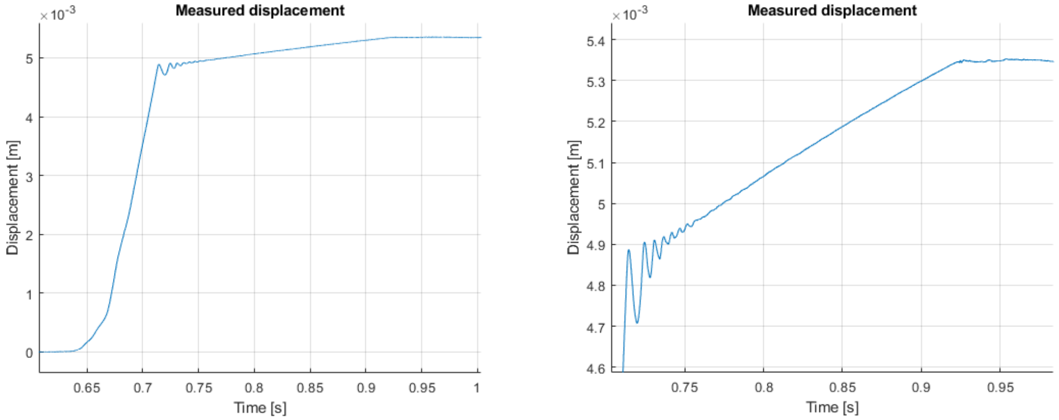

Figure 9.4: a) Zoomed view of free stroke and touching behavior. b) Zoomed view of touching behavior.

Table 9.1: Measured lower arm stiffness

	K (N/mm)
Test 1	3411.4
Test 2	3599
Test 3	4008.4
Test 4	3777.2

9.1.2 Sheet stiffness

The process shown for the lower arm stiffness is done with and without sample sheets between the electrodes. The results are shown in figure 9.5 and can also be found in table (damping). Averages are taken and compared to find the sheet stiffness of each sample, shown in table 9.2 .

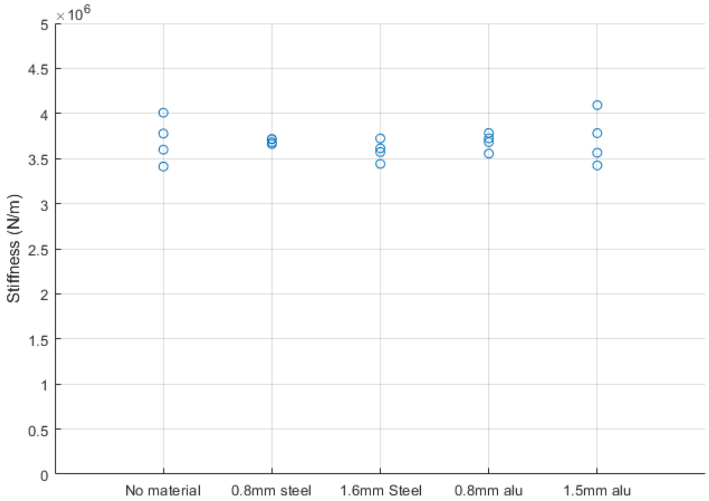

Figure 9.5: Graph with the measured lower arm stiffnesses for tests with and without samples between the electrodes

Table 9.2: Mean values of the measured stiffnesses.

	Average total lower arm stiffness (N/m)	Sheet stiffness (N/m)
No material	$3.814 * 10^6$	-
0.8mm steel	$3.791 * 10^6$	$2.54 * 10^9$
1.6mm steel	$3.805 * 10^6$	$1.19 * 10^8$
0.8mm aluminum	$3.741 * 10^6$	$1.08 * 10^9$
1.5mm aluminum	$3.660 * 10^6$	$-8.3 * 10^8$

9.1.3 Total stiffness acting on workpiece

Having the total lower arm stiffness, eq. 8.5 can be applied and the total stiffness is calculated, shown in table 9.3.

Table 9.3: Calculated total stiffness acting on the workpiece.

	Total stiffness acting on workpiece (N/m)
No material	$1.89740 * 10^5$
0.8mm steel	$1.89730 * 10^5$
1.6mm steel	$1.89440 * 10^5$
0.8mm aluminum	$1.89710 * 10^5$
1.5mm aluminum	$1.89780 * 10^5$

9.1.4 Damping of the system

Removing the displacement of the lower arm with eq. 8.3, the linear increase of the force buildup is removed. The response left is shown in figure 9.6.

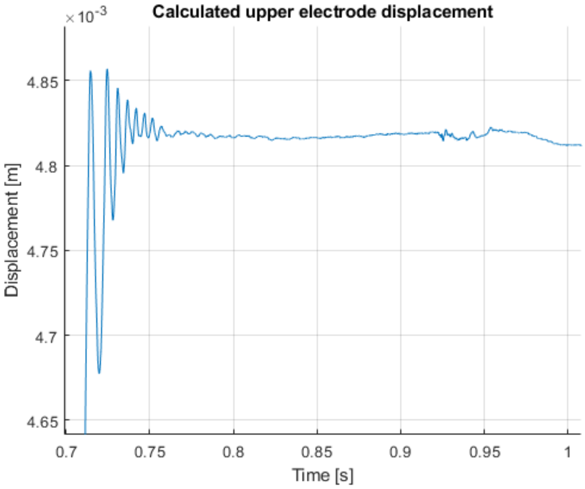

Figure 9.6: Calculated displacement of the upper electrode during touching.

With a third order detrend function in Matlab, the oscillations of the touching behavior is isolated. Fitting a first order exponential function, ae^{bt}, on the peaks resulted in the damping ratio. The filtered touching response with the fitted damping lines can be seen in figure 9.7.

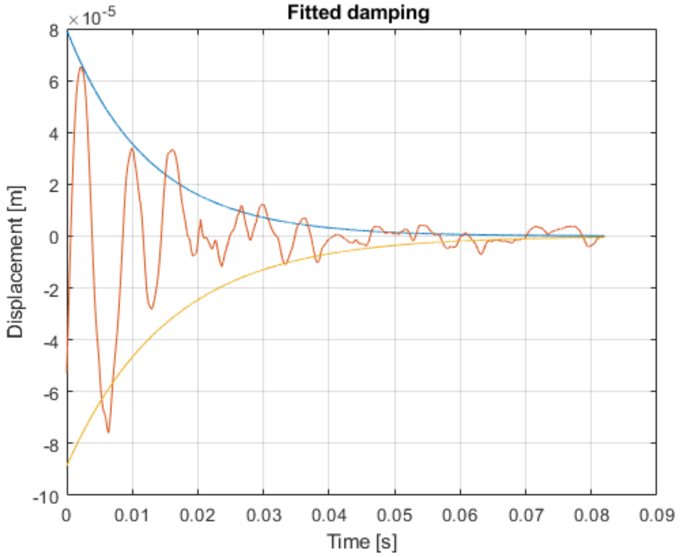

Figure 9.7: Fitted exponential curve to the peaks of the touching response.

The results from the upper and lower fit with corresponding calculated machine characteristics are shown in table 9.4 and 9.5 respectively.

Table 9.4: Upper peaks fit derived machine characteristics.

Material	Thickness (mm)	K (N/mm)	M (kg)	Damping (kg/s)	ω_0 (Hz)
No sample	-	3411.4	4.25	461.8	142.5
No sample	-	3599	5.64	691.8	127.1
No sample	-	4008.4	6.68	1090.6	123.3
No sample	-	3777.2	5.89	662	127.4
Steel	0.8	3681.3	6.34	960.5	121.3
Steel	0.8	3660.8	6.66	1392.5	118.0
Steel	0.8	3718.7	7.21	1604.4	114.3
Steel	0.8	3713.7	6.79	1244.3	117.7
Steel	1.6	3572	7.27	825.9	111.6
Steel	1.6	3440.8	6.91	673.3	112.3
Steel	1.6	3723.1	7.78	589.6	110.1
Steel	1.6	3613.2	8.23	546.6	105.5
Aluminum	0.8	3555.5	5.92	1120	123.3
Aluminum	0.8	3682.4	5.97	1218	125.0
Aluminum	0.8	3783.2	6.08	1104.2	125.5
Aluminum	0.8	3724.4	6.17	1107.3	123.6
Aluminum	1.5	3564.5	6.72	1164.4	115.9
Aluminum	1.5	3423.7	5.84	942	121.9
Aluminum	1.5	4092.3	5.40	626.2	138.5
Aluminum	1.5	3781.4	5.90	937.6	127.4

Table 9.5: Lower peaks fit derived machine characteristics.

Material	Thickness (mm)	K (N/mm)	M (kg)	Damping	W_n (Hz)
No sample	-	3411.4	4.29	521.5	142.0
No sample	-	3599	5.75	857.1	125.9
No sample	-	4008.4	6.61	974.3	124.0
No sample	-	3777.2	5.93	721.7	127.0
Steel	0.8	3681.3	6.20	753.1	122.6
Steel	0.8	3660.8	6.24	763.5	121.9
Steel	0.8	3718.7	6.72	905.2	118.4
Steel	0.8	3713.7	6.57	915.1	119.7
Steel	1.6	3572	7.44	1064.5	110.3
Steel	1.6	3440.8	7.18	1045.8	110.2
Steel	1.6	3723.1	8.25	1241.1	106.9
Steel	1.6	3613.2	8.62	1063.3	103.1
Aluminum	0.8	3555.5	5.77	877.2	125.0
Aluminum	0.8	3682.4	5.79	925.1	127.0
Aluminum	0.8	3783.2	5.81	672.5	128.4
Aluminum	0.8	3724.4	6.34	1360.8	122.0
Aluminum	1.5	3564.5	6.29	537.6	119.8
Aluminum	1.5	3423.7	5.86	982.3	121.6
Aluminum	1.5	4092.3	5.54	858.5	136.8
Aluminum	1.5	3781.4	5.65	532.6	130.2

Interesting to note is the change in natural frequency after a few milliseconds. The first two peaks seem to be one sinusoid with a frequency of 100-140Hz. After about 10ms, it seems to change to two sinusoids, one with a higher frequency and one with a lower frequency, thereby changing the calculated masses and damping coefficients. This indicates that the system is changing rapidly after touching.

It is likely that the upper weld head moves and touches the lower arm as one mass at first, and only later the two masses in the upper arm start to vibrate individually.

9.2 Experiment 2: Welding behavior

9.2.1 Continuous measurement of machine characteristics

Figure 9.8 shows the result of a the continuous analysis of the machine characteristics. It contains a lot of noise and the graphs are hard to read. The results seem of a completely different order than expected and seem not to adhere to the models made in section 7.2.

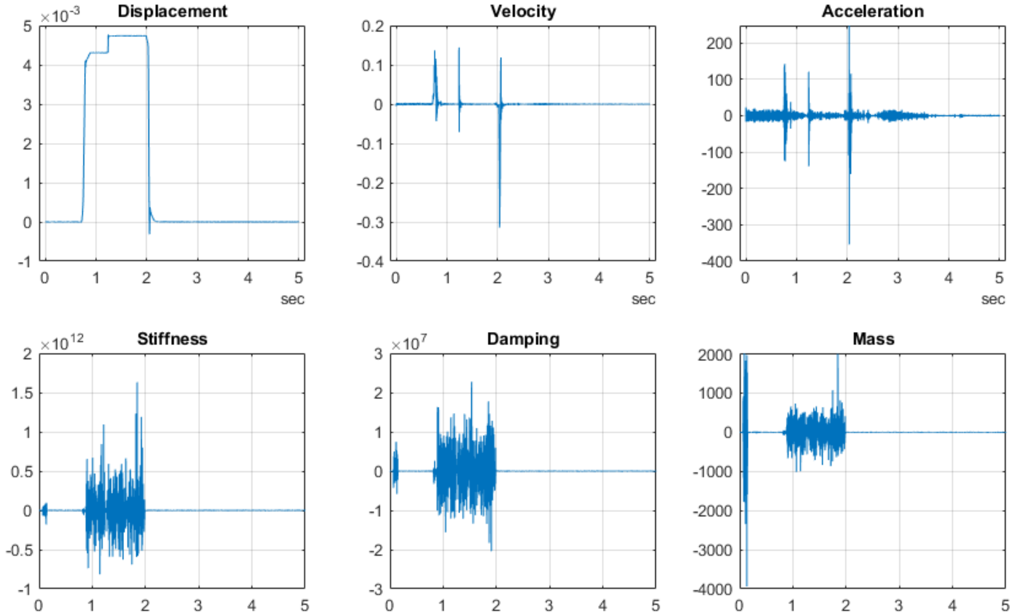

Figure 9.8: Graph of the continuous measurement of the machine characteristics. With displacement in m, velocity in m/s, acceleration in m/s2, stiffness in N/m, damping in kg/s and mass in kg.

Changing block size and overlap did not influence the result, as did other filtering and smoothing functions. This method was therefore not used anymore.

9.2.2 Machine characteristics Rymenant method

In figure 9.9, the fit with the function provided by Rymenant is plotted. The fitting is done with the lsqcurvefit function in the MATLAB toolbox. The fit does not start off well, but later approximates the graph okay. Table 9.6 contains the resulting mass and damping coefficient gained by the fitting. The results were far off from the actual values and were not consistent at all. Therefore only the steel weld have been fitted. Time was not spent on isolating the aluminum weld data and fitting since the fits were so unsuccessful for the steel welds.

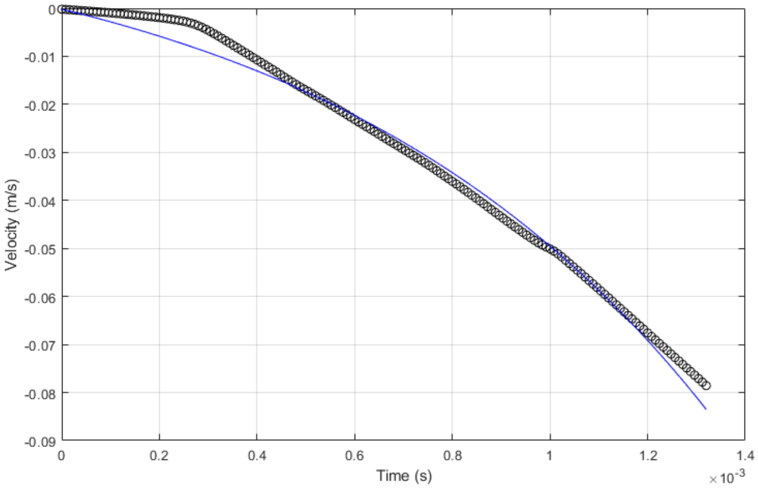

Figure 9.9: Collapse of steel weld with the fitted line as recommended by Rymenant.

Table 9.6: Mass and damping coefficient calculated with the fitting model of Rymenant.

Sample	Mass (kg)	Damping (kg/s)
Steel 0.8mm	46.31	-61188
Steel 0.8mm	156.3	-409520
Steel 1.6mm	15.86	-40965

9.2.3 Stiffness during welding

The time interval of the weld is isolated and analyzed. Below, in figure 9.10 a zoomed view of the weld is shown. Interesting to see is the time it takes to weld steel is a lot shorter than welding aluminum. Steel welds are one clear drop in force and displacement, while aluminum can have up to three drops before stabilizing. Also does the aluminum weld first collapse, then grow larger (seen by the increasing displacement after the first drop), then a second drop (with sometimes a small third drop), before slowly stabilizing. The welding stiffnesses have been calculated with eq. 8.11 with the results shown in table 9.7.

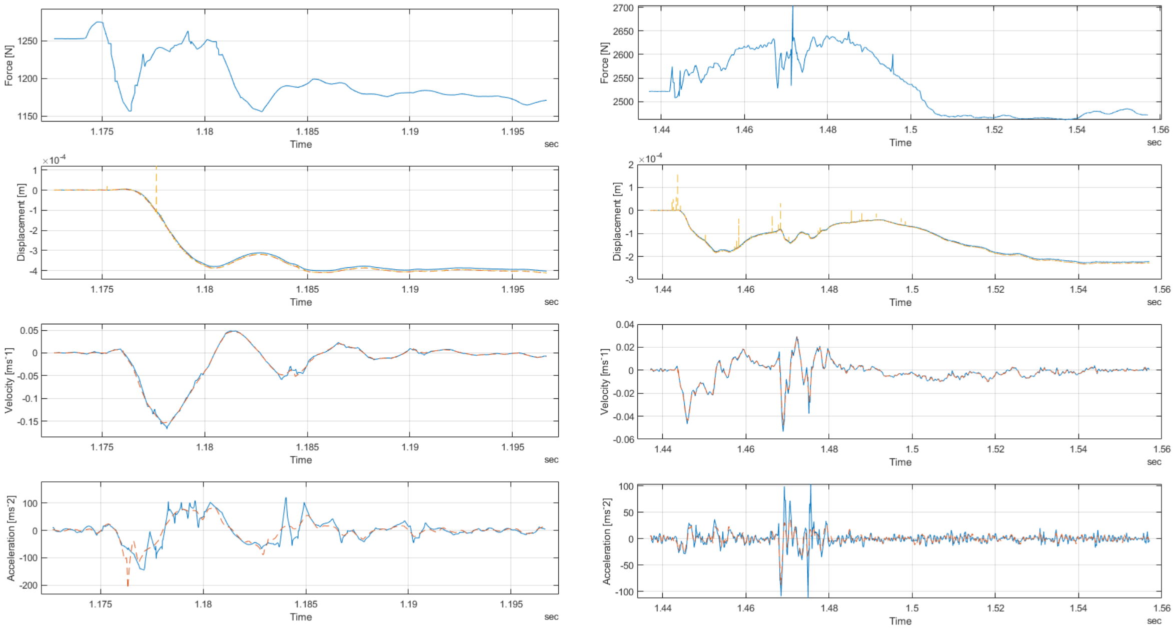

(a) (b)

Figure 9.10: Zoomed view of welding interval for steel (a) and aluminum (b). Force, displacement velocity and acceleration are shown.

Table 9.7: Displacement drop and force drop measurements with the calculated welding stiffness.

Material	**Sheet thickness**	**Force drop (N)**	**Displacement drop (mm)**	**Welding stiffness (N/mm)**
Steel	0.8mm	82.8638	0.434	188.9
Steel	0.8mm	82.8101	0.424	193.4
Steel	1.6mm	82.1861	0.422	186.7
Aluminum	0.8mm	17.5708	0.099	172.1
Aluminum	1.5mm	48.1348	0.272	176.6
Aluminum	1.5mm	53.1205	0.2820	185.7

Even with bad welds the force and displacement drop result in the expected welding stiffness:

Table 9.8: Displacement drop and force drop measurements with the calculated welding stiffness for bad welds.

Material	**Sheet thickness**	**Force drop (N)**	**Displacement drop (mm)**	**Welding stiffness (N/mm)**
Steel	0.8mm	70.7	0.322	205.382
Steel	1.6mm	60.5	0.307	184.359

Being curious of the influence of a projection for the touching stiffness, this was calculated for the welding samples as well. The results were very interesting. Using the calculated sample stiffness, the loss of dimple by material deformation due to the electrode force can be calculated as well:

Table 9.9: Calculation of the sheet stiffness for sheets with a dimple. The loss of dimple height is also shown.

Material	Sheet thickness	Stiffness touching (N/m)	Stiffness sample (N/m)	Loss of dimple (mm)
Steel	0.8mm	$3.314 *10^6$	$2.529 *10^7$	0.0388
Steel	0.8mm	$3.216 *10^6$	$2.051 *10^7$	0.0478
Steel	1.6mm	$3.250 *10^6$	$2.199 *10^7$	0.0570
Aluminum	0.8mm	$2.036 *10^6$	$0.437 *10^7$	0.4093
Aluminum	1.5mm	$2.983 *10^6$	$1.369 *10^7$	0.1842
Aluminum	1.5mm	$3.035 *10^6$	$1.487 *10^7$	0.1866

9.2.4 Follow-up acceleration

In figure 9.1, the acceleration of the follow-up mechanism is also shown. A lot of noise is present in the signal, even with the displacement having been averaged. A second averaging was applied to the acceleration data and was compared to filtering the noisy data with a lowpass filter. Both filtering methods sometimes resulted in accurate results while giving inaccurate results in other cases (surprisingly, when one method gave inaccurate results the other method proved to be accurate). Therefore, maximum acceleration results from both filters are shown. Note that some maximum acceleration peaks had to be ignored due to inaccurate filtering. For the 1.6mm steel sample, a second acceleration is added as it had a second drop which is rare for steel, but could not be ignored.

Table 9.10: Measured follow-up acceleration.

Material	Sheet thickness	Acceleration (m/s^2) Lowpass filter	Acceleration (m/s^2) Averaging
Steel	0.8mm	115.6	104.9.8
Steel	0.8mm	111	91.25
Steel	1.6mm	1st 100.3, 2nd 162.9	98.96
Aluminum	0.8mm	53.34	50.34
Aluminum	1.5mm	105.9	87.28
Aluminum	1.5mm	119.4	104.8

10 Discussion

10.1 Experiment 1

The bending of the lower arm was clearly visible in the displacement graphs. The resulting lower arm stiffnesses were close to the expected value, as the machine was designed to bend only a few tenths of a millimeter. High lower arm stiffness results in good electrode alignment and low stresses acting on fixed workpieces.

The sheet stiffness influenced the total stiffness acting on the workpiece with a maximum of 0.2%. Therefore, it can be assumed that the sheet stiffness can be neglected when calculating the machine stiffness. If an accurate calculation of the total lower arm stiffness is required, the sheet stiffness of thick aluminum parts should be taken into account. Since Arplas does not weld aluminum sheets thicker than 2mm, the sheet stiffness with aluminum can always be neglected. Steel has no influence whatsoever.

BUT, when welding parts with a projection in them, the sheet stiffness definitely plays a role. Low thickness aluminum sheets reduced the arm stiffness by almost 50%. This will influence the touching behavior, but more importantly, the projection height is reduced because of the elastic and maybe even plastic deformation. However, since the projection collapses during welding, the sheets lose its stiffness anyway. This means that the welding stiffness causing the drop force is not influenced by the sheet stiffness, which is confirmed by the measurements with welding.

For the damping of the system, the reduction in oscillation amplitude was analyzed. The linear increase in displacement with increasing electrode force was removed with eq. 8.3. Although the linear increase was removed, it can be seen that the response is not just an impulse or step response. The “stable” value is only reached after a few milliseconds. An explanation is that as touching occurs not an impulse or step response is present but a ramp response due to the linear increasing force. A first order ramp response is a delayed response to a steady state increase. An example of a unit ramp response is shown in fig 10.1. Looking at the displacement response in figure 9.4b, it seems that the stable linear increase due to the stiffness of the lower arm is only reached after ~10ms. Therefore, a delayed response due to the ramp input of the electrode force is quite possible.

Fitting functions for this delayed response did not fit well and, in consultation with the supervisors, it was decided as out of the scope for this research and was not investigated further. The influence of the delayed response was removed with a detrend function in Matlab.

By analyzing the reduction in oscillations, an indication of the damping factor could be obtained. From the results it can be concluded that since the oscillations are slowly stabilizing, the damping factor is low and therefore, the friction in the system is low. The calculated masses are also close to the actual values, indicating that this method was quite successful in measuring the machine characteristics.

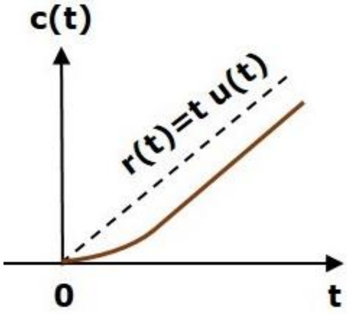

Figure 10.1: Example of a unit ramp response showing a delayed response to a steady state linear increase. r(t) is the unit ramp signal and c(t) is the unit ramp response.

10.2 Results. Analysis and Evaluation Experiment 2

The method of both Wu and Rymenant did not result in an accurate analysis of the machine characteristics. The main reason for this is probably the lack of a sacrificial part. The welds made with a projection were actual welds, and not overheated, exploding balls or buttons. The slower response and the lack of a simulated “freefall” resulted in mass and damping coefficients that were highly inconsistent and inaccurate. If time allowed it, I would have done extra tests with sacrificial parts, but for now it is postponed for further research.

The welding stiffness measured with the drop force and displacement are close to the values calculated in Experiment 1 with the total stiffness acting in the workpiece. This was to be expected as the machine was designed to have this stiffness when welding.

The follow-up accelerations measured were hard to read from the graphs as the measured displacement was not a smooth drop. In the end were the accelerations for both steel and aluminum quite similar and of similar order Rymenant measured in his tests. Rymentant also measured the accelerations with his breaking and exploding tests and measured stable accelerations of 250m/s^2. Since his tests simulated a freefall, and the tests conducted in this thesis are actual welds, the lower weld accelerations are expected

Models B and C are verified by comparing the measured welding stiffness and the calculated stiffness acting on the workpiece. Both represent the total machine stiffness. Since the measured stiffness (183.92 N/mm) and the calculated stiffness (189.68 N/mm) are very similar, the models are assumed to be correct.

There was no time left for a thorough analysis of the Fourier transforms, and using that for the validation of the models.

11 Conclusion

Although the test methods provided by Wu and Rymenant from the literature did not result in accurate machine characteristics during actual welding, the machine characteristics and other parameters of interest were still obtained using alternative methods. The correct use of Wu and Rymenant, with the use of sacrifial parts, are recommended for further research.

The obtained machine characteristics match with the models made in section 6.2 and can be used for future tests on C-type machines.

Sheet stiffness did not influence the lower arm stiffness when flat sheets are used. However, when dimples are added in the sheets this does influence the lower arm stiffness which can be used to calculate the loss of dimple height. Alternatively, the deflection of the lower arm without samples can be compared to the deflection when a sample is added.

When welding thin sheets of aluminum, the projection is already significantly reduced in height due to the electrode force. Because of that, the drop force is harder to measure. If the welding stiffness is increased, the drop force will become more noticeable. The downside is that this also influence the welding behavior of steel welds. To make the drop force of steel and aluminum comparable, a follow-up spring of increasing stiffness could be used for future designs.

For more accurate results of the machine characteristics, investigating the ramp response when touching is recommended for future research. The fitting software used in this thesis did not result in good approximations of this delayed response.

Lastly, the models were not used yet to predict responses given a certain input force. If the response can be predicted accurately, the C-type machine characteristics could be fine-tuned for optimal touching and welding responses.

11.1 Mechanical characteristics

The mechanical characteristics of the current C-type machine were successfully obtained with the described methods. The masses, stiffnesses and damping coefficient resulted in:

- Calculated stiffness acting on workpiece: 189.68 N/mm
- Measured stiffness acting on workpiece: 183.92 N/mm
- Lower arm stiffness: 3814 N/mm
- A moving mass of 3.41 kg
- Average damping coefficient: 913.4 kg/s
- Follow-up acceleration ranges between 53.34 and 162.9 m/s^2

11.2 Requirement distillation

The results from the literature in chapter 6 gives insight in what other researchers recommend for the machine characteristics. However, most of the literature recommendations are recommendations for spot welding guns. Some ideal requirements for spot welding machines are not necessarily ideal for projection welding. These will have to be filtered out.

The result from the literature was:

	Weld quality		**Electrode life**		**Touching**		**Follow-up**	
Electrode	Upper	Lower	Upper	Lower	Upper	Lower	Upper	Lower
Mass	Low	-	Low	Low	Low	Low	Low	Low
Stiffness	High	High	-	-	Low	-	-	Low/High
Damping	-	Low	-	-	High	Low	Low/High	High

Where high stiffness is required for good electrode alignment, resulting in high weld quality. For touching, low contact stiffness is required for a longer electrode lifetime. Making the tradeoff between high precision and low touching impact is important although weld quality usually takes priority. For spot welding machines, high stiffnesses in both arms are preferred.

Projection welding machines however, need to make sure contact is kept between the workpiece and electrodes. The stiffness of projection welding machines is critical for the follow-up. If the stiffness is too high, the spring will be fully extended before the projection has completely collapsed, resulting in loss of contact. This is the reason why most projection welding machines have a follow-up spring with a relatively low stiffness compared to the structural stiffness of the machine. The follow-up spring reduces the moving mass during welding but most of all, it allows for keeping contact during follow-up while guiding rails provide the electrode alignment.

Low moving masses are preferred for a low touching impact and high follow-up accelerations. Damping should be low for fast follow-up, but high damping is preferred for the best touching behavior and damping the vibrations after welding. Friction has a negative influence on the weld quality, and since friction is the main contributor to damping, damping should be minimized for best weld quality.

From the tests conducted in the experiments, requirements to take over in future designs for similar weld characteristics are:

- A total stiffness acting on workpiece of 183.92 N/mm
- Capable of follow-up acceleration up to 163 m/s^2
- A moving mass of approximately 3.4 kg
- Low friction

Part III: Designing the X-type

12 Introduction

Arplas Technology B.V. specializes in welding equipment mainly for the automotive industry. In this industry, the common materials used are sheets of steel or aluminum. Arplas makes use of resistance projection welding to join these sheets together.

What makes Arplas stand out from the other welding equipment suppliers is that Arplas has the ability to make almost invisible welds on the sheet without dimple. In the automotive industry this is perfect for parts that are visible to the customer, for example a window frame or gutter. In the past, these parts had to be covered with plastic sheets to hide the ugly spot welds, but with this technique that won’t be necessary anymore.

Arplas’ current machines are all C-type machines, either stationary, robotic or manual. Currently, the C-type machine is the only variation on the market for projection welding machines. The armature of the lower arm can be adapted to the wishes of the customer, but the motor will remain in-line with and close to the electrodes. Figure 12.1 shows the different armatures for different applications.

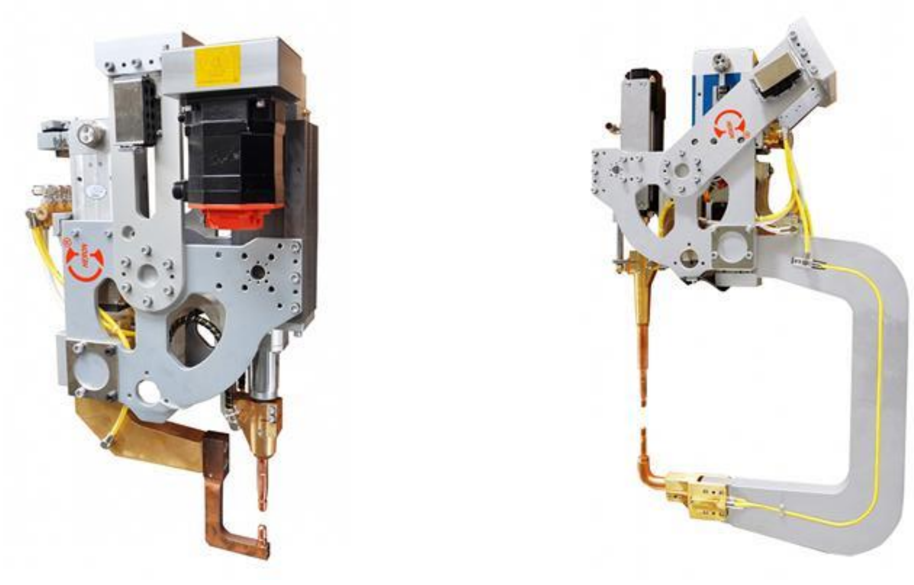

(a) (b)

Figure 12.1: Different sizes of C-type lower arm armature. (a) Small armature. (b) Large armature. It can also be seen that the actuator is directly connected to the upper electrode [35].

Spot welding machines are already available as X-type designs, but projection welding machines need faster follow-up response, so no X-type *projection* welding machines exist on the market yet. An X-type RPW gun would be a great addition to the Arplas product portfolio.

X-type machines have a large throat length, making it possible to reach weld locations a C-type cannot reach. The actuation is usually placed close to the base of the welding gun and not necessarily in-line with the upper electrode. Examples of X-types are shown in fig 12.2. An X-type welding gun, especially if mounted on a robotic arm, offers a larger range at the expense of some stiffness.

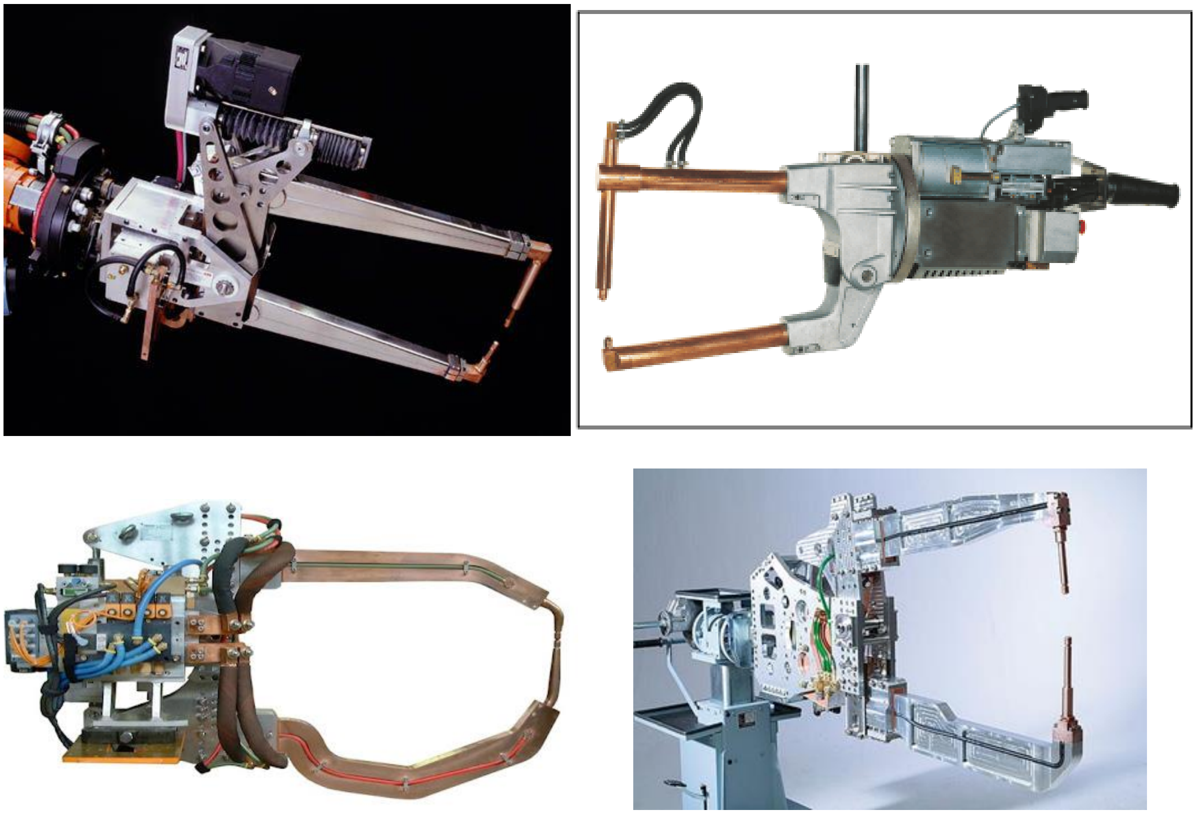

Figure 12.2: Different designs of X-type machines for spot welding. It can also be seen that the actuator is not directly connected to the upper electrode but rather rotates the full upper and/or lower arm [5], [36]–[38].

12.1 Design problem

Arplas has requested to research the feasibility of a far-reaching, or X-type, welding gun. The welding gun should be able to weld both steel and aluminum sheets, and implements the Arplas technology. Their current C-type welding gun works smoothly and a lot of testing and weld optimization has been performed. To be able to use that knowledge in the X-type as well, the assignment will be to:

“Design a robot mounted far-reaching projection welding machine, using the Arplas technology, having similar mechanical characteristics as their current welding machine.”

The initial throat length is set to be 500mm, but a configuration tool will be developed in section 15.5 to change the throat length and other relevant parameters, while still meeting all the requirements.

12.2 Functions and requirements

To create a list of requirements, it important to know the functions the welding gun has to perform. The whole process of making a weld has already been analyzed in section 7.2. This section will focus on distinguishing functions. The design process starts with the identification of the need, followed by the main and sub-functions.

The machine will need to perform projection welding at any given location in any given orientation. Automation of the process will require a robot mounting, sensors and a controller. Given these requirements, the definition of the need takes the form of:

> “A user-friendly machine controlled by an intelligent supervisory control system supported by a sensory system that operates in six degrees of freedom and achieves welding in a 3-D working envelope.”

The main and its decomposed main sub-functions can be quickly distinguished as:

Table 12.1: Main function with the corresponding decomposed sub-functions.

Main function	Decomposed main sub-functions
Intelligent resistance projection welding robot	1. Intelligent supervisory control system 2. 3-D working envelope positioning robot 3. Resistance projection welding machine 4. User interface module 5. Sensory system

Each of these of these sub functions can be decomposed into even smaller and simpler functions. In this thesis, it is assumed that a 6 DOF robot, control system and user interface are already available since Arplas has already developed these for their current welding guns. Therefore, only sub functions 3 and 5 will be further investigated in table 12.2 and 12.3.

Table 12.2: Decomposed sub-functions of main sub-function Resistance projection welding machine.

Main sub function	Decomposed sub-functions
Resistance projection welding machine	3.1 Projection weld 3.2 Weld quality 3.3 Weld validation 3.4 Activities manager

Table 12.3: Decomposed sub-functions of main sub-function of the sensory system.

Main sub function	Decomposed sub-functions
Sensory system	5.1 Force measurements 5.2 Current measurements

The decomposed sub-functions translate to requirements. This is shown in table 12.4. Note however that the suspension stiffness, or follow-up stiffness was adjusted form the measured value of 189 N/mm to 200 N/mm. This was discussed with the company and they preferred 200 N/mm.

Table 12.4: Requirement distillation from decomposed sub-functions.

Main sub-function	**Sub-function**	**Sub-sub-function**	**Strategy/Func req.**	**Design specs**
Resistance projection machine	Projection weld	Contact pressure	Electrode force	3000 N
		Follow-up	Acceleration Suspension	Up to m/s^2 200.000 N/m
		Welding current	Current amplitude Current duration	Max. 50 kA Max 50ms
	Weld quality	Concentric electrodes	Rotational align Horizontal In-plane bending	±1.5° <0.5 mm <0.5 mm
		Weld strength	Nugget size Tensile force Shear force	Similar to C-type
		Surface appearance	Indentation Marks of welding	Similar to C-type
	Weld validation	Dimple collapse distance	Drop force Sheet separation?	Similar to C-type
Sensory system	Force measurements	Elec force check Drop force check	Force range Accuracy	*0-3000 N* < 1N
	Current measurements	Weld current check	Current range Accuracy	0 – 60kA < 10A

The precision of the tips is essential to the weld quality. Requirements from the company are a maximum electrode misalignment of ±1.5° and 0.5 mm under maximum load of 3000N electrode force. Figure 12.3 shows this graphically. Structural bending will be the main contributor to these misalignments.

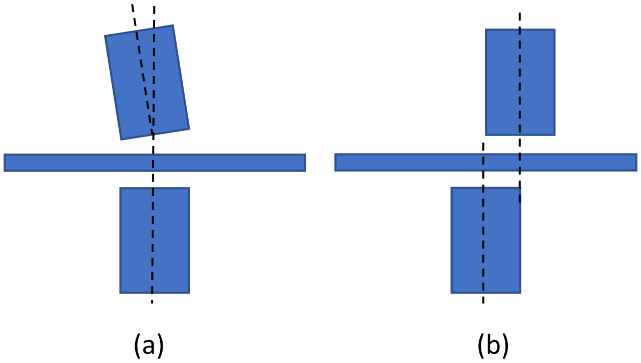

Figure 12.3: Electrode misalignment requirements. (a) Rotational misalignment requirement: max. ±1.5°. (b) Parallel axis misalignment requirement: max 0.5 mm.

Downward deflection is also part of the precision requirement. Just as the parallel misalignment, is the downward deflection restricted to 0.5 mm. Because the workpiece is fixed, downward deflection puts local stresses on the workpiece.

The heat generation when sending current through the metal sheets can increase the temperature of the welding gun significantly. This means that cooling is necessary in the arms of the welding gun when welding with large currents and many welds per second.

In addition, the electrode tips have to be replaceable as they wear with every weld. Cleaning the electrode tips requires removing and polishing the top layer, resulting a smaller electrode after every cleaning process. Eventually the electrodes need to be replaced as they become too short. Other key components prone to failure should be easily replaceable as well.

The welding gun also has to meet requirements set by the company: weight, costs, safety, outer dimensions, minimum amount of welds per minute, and reliability. Lastly are some requirements from the working environment too, for example the available resources at the site, mounting on the robot, etc. All these secondary requirements can be found in table 12.5.

Table 12.5: Secondary requirements.

	Requirement	**Value**
Maintenance	Simple system Replaceable key components Use of standard components	
Robot connection	Lightweight	Max. 125 kg
	Compact	
Sequential welding	Max heat accumulation Easy replaceable electrode tips	
Budget	Easy to acquire prats Total budget	
Modular	Easy replaceable parts and assemblies	

12.3 MosCoW requirements

The MoSCoW method will be used to prioritize the requirements. Starting with the *Must haves*, which are the essential key requirements for the design. The *Should haves* compose of the requirements that are important for the design to work but are often not as critical as the *Must haves*.

The *Could haves* are the desirable requirements but not necessary and can be used to preference certain design choices. The *Would haves* are the last priority and can be added to the design if the time and resources allow it.

Must haves:

- Long throat (> 500mm)
- Provide electrode force
- Can provide weld current
- Concentric electrodes
- Fast follow-up
- Noticeable force drop after welding

Should haves:

- Be able to make strong welds
- Leave no indentation
- No excessive heat accumulation at 20 welds/min
- Able to weld a flange of 15mm
- Max height < 200mm
- Replaceable key components
- Compact
- Easy to acquire parts

Could haves:

- Lightweight
- Low budget
- Flexible robot mount
- Minimal misalignment on visible side
- Simple system

Would haves:

- Quick exchangeable armature (modular)

13 Concept generation

Having distilled the functions and requirements, the concept generation can now start. The functions and requirements translate to an array of solutions. Combinations of these solutions will result in viable concepts.

13.1 Possible solutions for each function

Let us start with the electrode force requirement. The electrode force has to be applied at the tips. Two options are possible: an actuator located at the tips, or an actuator located at the base combined with a mechanism transferring the force to the tips. An example of such a mechanism is a lever. Figure 13.1 shows the five different possible solutions for an actuator located at the base.

Since the welding gun has to open and close with relative large distances, one of these mechanisms is necessary anyway. Separating the open and close actuator with the electrode force actuator could be one of the concepts.

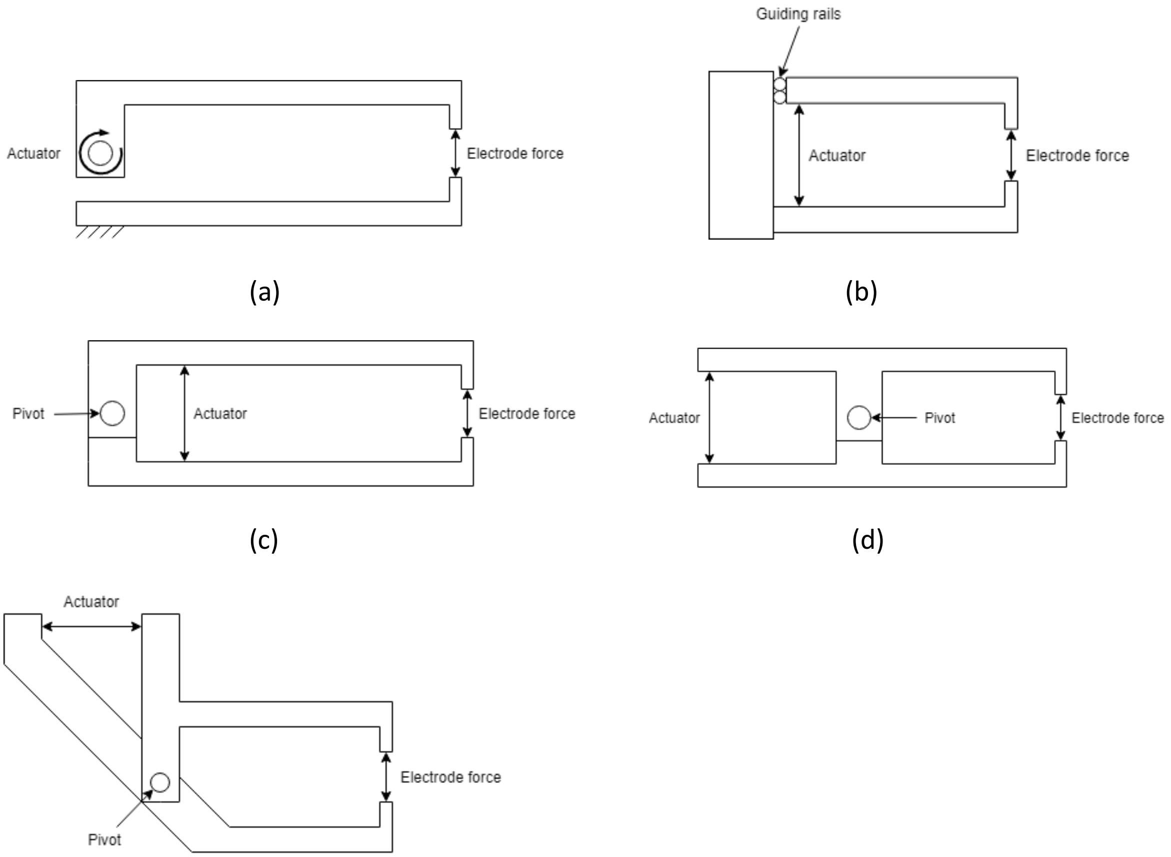
Actuator
Electrode force
Guiding rails
Actuator
Electrode force
Pivot
Actuator
Electrode force
Actuator
Pivot
Electrode force
Actuator
Electrode force
Pivot

(a) (b)

(c) (d)

(e)

Figure 13.1: Mechanisms transferring actuator force to tips. (a) Rotational motor input, actuator located at pivot. (b) Slider on rails, actuation is placed at the slider. (c) Lever with actuator and tips at the same side of pivot. (d) Lever with actuator and tips at opposite sides of rotation point. (e) Lever with actuator above pivot point.

For follow-up either a separate suspension or a fast-response actuator is necessary. The suspension can be placed at the electrodes, at the base (if electrode force actuator is chosen at the base and not at the tips), or solely natural bending stiffness in the arms can be used.

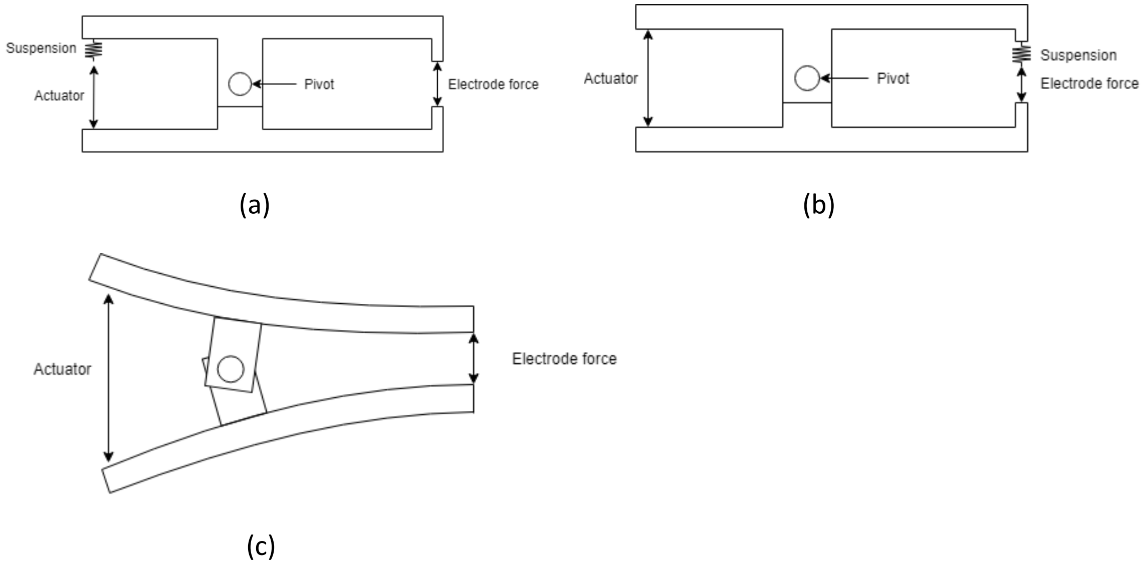

(a)

(b)

(c)

Figure 13.2: Three different ways to add suspension to a design. The design from figure 13.1d has been used as example. (a) Suspension at the base. (b) Suspension at the tips. (c) Bending stiffness as suspension.

The alignment requirements are also very strict. Structural stiffness will be important to keep the electrodes within the misalignment requirements. A small angle offset in the electrodes could be introduced, anticipating certain tip rotations.

Adding a compensation mechanism is also possible. This can be in the form of a small attachment on the tips. The mechanism compensates the deflection and rotation due to structural bending. Examples are flexible couplings or spherical/cylindrical joints. The Sarrus mechanism is also an example of a compliant mechanism that could function as angle compensation.

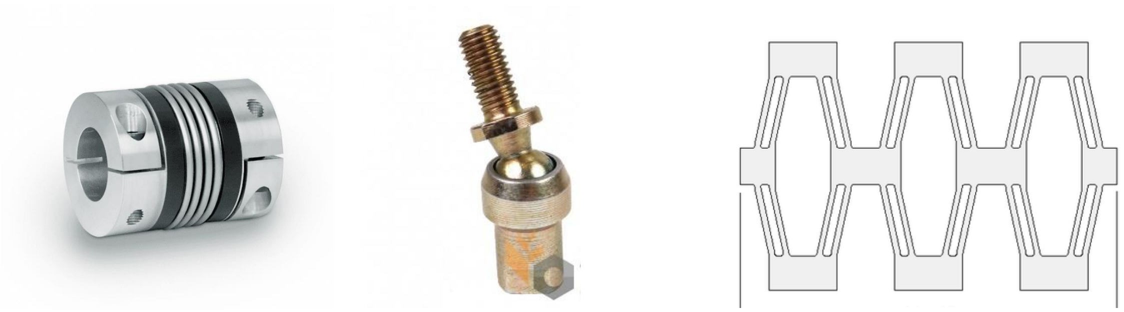

Figure 13.3: Examples of angle compensation tools. Left a flexible coupling, middle a joint, right a Sarrus mechanism.

Another solution for misalignment compensation is a remote center of motion mechanism (RCM mechanism). The mechanisms use parallelograms and other linkages to create a remote fixed point around which a mechanism or part can rotate. Examples are shown in fig 13.4. Some mechanisms can change a single rotation RCM to a 1 rotation and 1 translation RCM with only minor adjustments.

The RCM mechanisms are active misalignment compensation mechanisms requiring sensors to measure the misalignment and then move to the correct orientation. If the misalignment can be predicted, this system can be made passive.

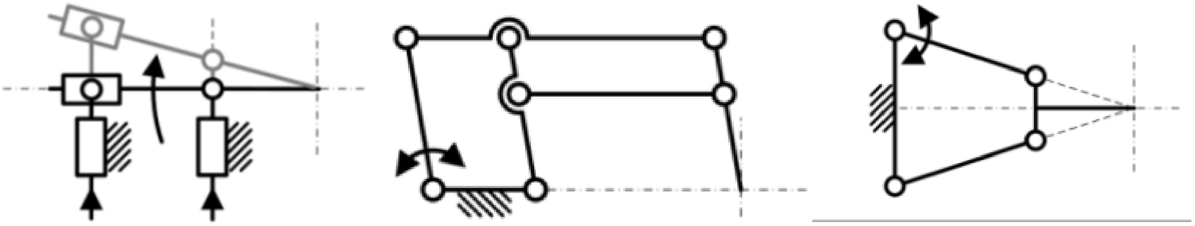

Figure 13.4: Remote Center of Motion Mechanism examples. (a) Parallel manipulators. (b) Parallelogram. (c) Four bar mechanism. [Janeau Janssen, Compliant Remote Center of Motion Mechanism Optimized for Energy Dispersive Spectroscopy, 2018]

Summarizing section 13.1, there are three main design choices to be made:

- The location of the actuation.
- If and where the suspension is placed.
- If and where misalignment compensation should be placed.

A morphological overview presents these possible solutions in a structured way. Each combination results in a different design. Every design has been sketched to increase the chance of finding new and innovative designs. Fig 7.5 depicts the final morphological overview

Function	**Solutions**						
Actuator	Moment at pivot 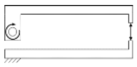	Parallel 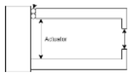	V 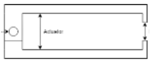	X (side) 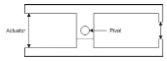	X (top) 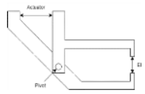		
Suspension	None, use fast-response actuator	At the tips 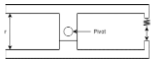	At the base 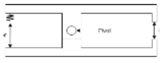	Bending energy (flexural energy) 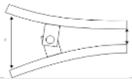			
	Passive				**Active**		
Misalignment compensation	None, structural stiffness	Angled electrodes	Ball/roller bearing 	Flexible coupling 	RCM mechanism 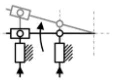	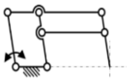	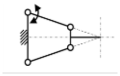

Figure 13.5: Morphological overview of all the possible design choices. Choosing one solution from each row results in a design.

For example, following the green line in fig 13.6 would result in a concept looking like shown in fig 13.7

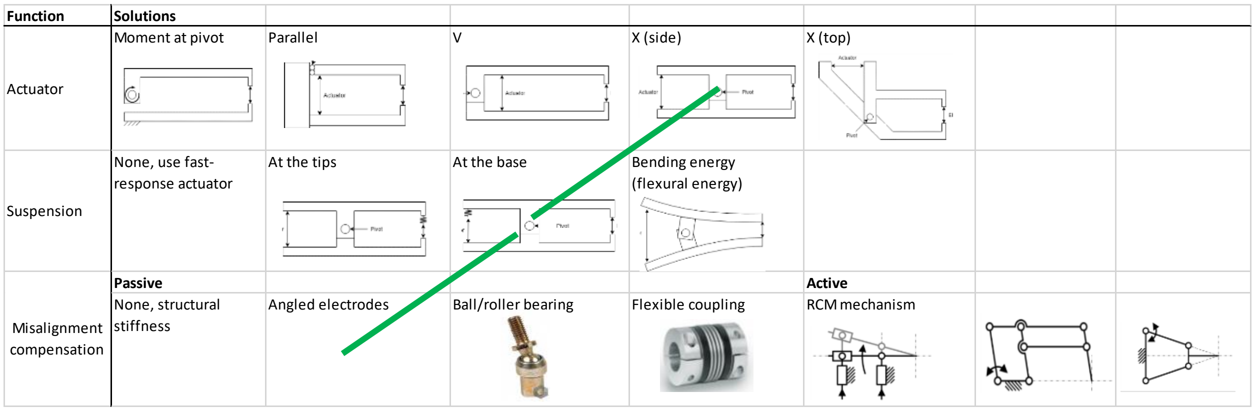

Function	Solutions						
Actuator	Moment at pivot	Parallel	V	X (side)	X (top)		
Suspension	None, use fast-response actuator	At the tips	At the base	Bending energy (flexural energy)			
Misalignment compensation	**Passive**				**Active**		
	None, structural stiffness	Angled electrodes	Ball/roller bearing	Flexible coupling	RCM mechanism		

Actuator
Pivot

Figure 13.6: Using the morphological overview to generate concepts. The green lines choose one solution from each row. Combining these solutions could result in a design like figure 13.7.

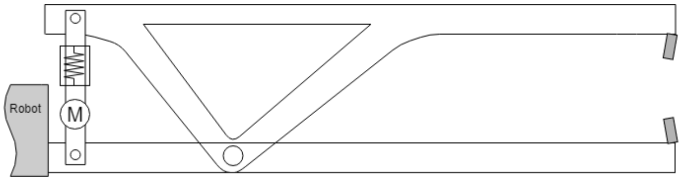

Figure 13.7: Possible design using the morphological overview. The actuator and suspension are located at the opposite side from the tips and as misalignment compensation angled electrodes are added.

Appendix B.1 contains all sketches made using the morphological overview.

14 Concept selection

A wide range of possible concepts is now generated. The next step is to find the best (few) concepts. Normally, a few feasible concepts are picked and based on design criteria together with for example a multi-criteria analysis, the best one is chosen.

It was decided not to pick only a few concepts this time since almost all the different designs are feasible. Instead, design criteria and multi criteria analyses are applied to each function to choose the best solution individually. This way, the final concept also still has some design freedom for the detailed design phase.

14.1 Design criteria

Based on the requirements, design criteria can be set up. The criteria compare and rate the different solutions, making it easier to identify the pros and cons of the solutions.

First, the design criteria for the placing of the actuator are established. Table 14.1 contains the translation of requirements to design criteria. Fig 14.1 shows an example of how the compact requirement translates to space occupation criteria.

Table 14.1: Translation of requirements to design criteria for the placing of the actuator.

Relevant requirements	**Corresponding design criteria**
Provide electrode force Min throat length Max throat height	Good mechanical advantage
Alignment/Precision	High bending moment of inertia
Follow-up	Low mass moment inertia/low moving mass Low friction
Compact	Low total space occupation
Simple system	Low amount of parts Easy fabrication
Reliability	Low exposure to harmful contamination Few moving parts
Lightweight	Low mass

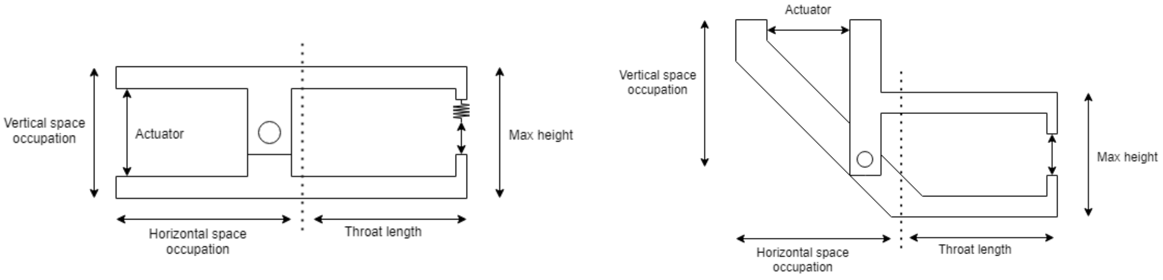
Vertical space occupation
Actuator
Max height
Horizontal space occupation
Throat length
Actuator
Vertical space occupation
Max height
Horizontal space occupation
Throat length

(a) (b)

Figure 14.1: Representation of some design criteria. (a) and (b) are representations of the criteria for the X-type with the actuation at the side and top respectively.

All design criteria for the placing of the actuator are now established. A grading table, like in table 14.2, is used to grade the solutions at a later stage. Defining 4 grades, - - being the most negative and + + the most positive, will give a reproduceable method of selecting the best solutions to our design problem.

Table 14.2: Grading table for the design criteria. - - is the most negative, + + the most positive.

Grade	Mechanical advantage	Dynamic capabilities	Horizontal space occupation	Vertical space occupation	Strength potential in arms (stiffness)	Protection of the actuator	Complexity system	Fabrication
++	Small actuator with high leverage possibility (>1:1 ratio)	Low moving mass potential and low friction	No space occupation	Does not increase height more than max height	Easy design for stiff arms with high bending moment inertia	-	Mechanical system is a simple and robust design with few moving parts	Few, small and easy produced/acquired parts. No special treatments/processes
+	Medium actuator with good leverage possibility (≈1:1 ratio)	Medium moving mass potential, low friction	Minimal hor. space (0-20% of throat length)	Minimal increase in total height (0-20% of max height)	Potential design for stiff arms with high bending moment inertia	No housing necessary, structure between actuator and welding process	System containing a couple of subsystems and some moving parts	Some small and medium parts. Easily produced. Few may need special processes
-	Large actuator with small leverage (<1:1 ratio)	Medium moving mass potential, high friction	Some hor. space (20-50% of throat length)	Moderate increase in total height (20-50% of max height)	Low potential design for stiff arms with high bending moment inertia	Actuator exposed to welding process	Intricate system with sub systems and multiple moving parts	Many parts, some medium or large. Some hard to produce/acquire. Few may need special materials or processes
--	No leverage possible	High moving mass potential, high friction	A lot of space (>50% of throat length)	Significant increase in height (>50%)	Design does not allow for a stiff structure and high bending moment	-	System is highly complex with many subsystems and many moving parts	Many different components with large, specialized parts, treatments and/or production processes

Second are the design criteria for the suspension. Table 14.3 shows the translation of requirements to criteria and table 14.4 the grading table for the criteria.

Table 14.3: Translation of requirements to design criteria for the suspension spring.

Relevant requirements	Corresponding design criteria
Noticeable force drop	Noticeable force drop
Able to weld a flange of 15mm	Minimize "dead" space at tips
Follow-up	Low mass moment inertia/low moving mass Low friction

Simple system	Low amount of parts Easy fabrication
Reliability	Low exposure to harmful contamination Few moving parts
Compact	Low total space occupation

Table 14.4: Grading table for the design criteria. - - is the most negative, + + the most positive.

Grade	Low moving mass	Force drop	Dead space at tips	Complexity system	Fabrication
++	Moving mass can be reduced to a moving tip only	Force drop can easily be controlled and is visibly present	No dead space (0-5mm)	Mechanical system is a simple, predictable, controllable and robust design with few moving parts	Few, small and easy produced/acquired parts. No special treatments/processes
+	Moving mass can be reduced to tip with some extra components	Force drop can be controlled but is not visibly present	Dead space is 5-10mm	Simple system, relatively predictable and controllable	Some small and medium parts. Easily produced. Few may need special processes
-	Moving mass is reduced to moving frame and tip	Force drop is hard to control but is visibly present	Dead space is 10-15mm	System containing a couple of subsystems with moving parts. Controllable but hard to predict	Many parts, some medium or large. Some hard to produce/acquire. Few may need special materials or processes
--	No moving mass reduction	No force drop is present and can't be controlled	Dead space >15mm	Intricate system with sub systems and multiple moving parts. Uncontrollable and hard to predict	Many different components with large, specialized parts, treatments and/or production processes

Third and last are the design criteria with corresponding grading table for the misalignment compensation, shown in table 14.5 and 14.6.

Table 14.5: Translation of requirements to design criteria for the angle misalignment.

Relevant requirements	Corresponding design criteria
Provide electrode force Weld with high currents	Robust
Alignment/Precision	Effectiveness
Follow-up	Low friction
Simple system	Low amount of parts Easy fabrication
Reliability	Low exposure to harmful contamination Few moving parts
Compact	Low total space occupation
Lightweight	Low total mass

Table 14.6: Grading table for the design criteria. - - is the most negative, + + the most positive.

Grade	Effectiveness	Dead space at tips	Complexity system	Fabrication
++	Passive compensation, both angle and translational	Electrode tips can be located at the very end of the arms and has no dead space (0-5mm)	Mechanical system is a simple, predictable, controllable and robust design with few moving parts	Few, small and easy produced/acquired parts. No special treatments/processes
+	Active compensation, both angle and translational	Dead space is 5-10mm	Simple system, relatively predictable and controllable	Some small and medium parts. Easily produced. Few may need special processes
-	Passive or active compensation, only angle or only translational	Dead space is 10-15mm	System containing a couple of subsystems with moving parts. Controllable but hard to predict	Many parts, some medium or large. Some hard to produce/acquire. Few may need special materials or processes
--	Misalignment will generally be within the range, but in special cases go outside.	Dead space >15mm	Intricate system with sub systems and multiple moving parts. Uncontrollable and hard to predict	Many different components with large, specialized parts, treatments and/or production processes

14.2 Multi Criteria Analysis

A multi criteria analyses (MCA) is excellent for decision-making based on criteria. Based on the criteria and grading tables established in section 14.1, each solution will receive a total score. Weighting factors are added to prioritize some criteria above others.

In the grading tables, plusses and minuses are used for grading. In the MCA, this shows at a glance where the different solutions compare better relative to the others. To define a score, the numbers 1 to 4 are used, 1 representing the double minus and 4 representing the double plus. The solution with the highest score can be assumed the best solution for that function.

For the first function, the placing of the actuator, the MCA is shown in table 14.7. Comparing the total scores, the best solution is using an X shape with the placement of the motor above the pivot point.

Table 14.8 is the MCA for the suspension. The solution of having a spring at the base has the best score and is therefore chosen as final solution. From table 14.9 the final solution for the misalignment compensation is derived. No misalignment compensation came out as the best solution. If absolutely necessary, angled electrodes can be used as a backup.

The actuator placement of the actuator at the pivot point was left out. The concept was not feasible since a direct drive motor would have to be huge and heavy. Also it was not preferred by the company.

Table 14.7: MCA for the placement of the actuator.

Placement motor	Weighting factor 1-4	X (side)	X (top)	V	Parallel /Slider
Mechanical advantage	4	++	++	+	--
Dynamic capabilities	4	-	+	+	-
Strength potential in arms (stiffness)	4	+	++	+	--
Horizontal space occupation	3	--	+	+	+
Vertical space occupation	3	+	--	+	+
Complexity system	2	+	+	+	-
Safety of the actuator during welding	1	+	+	-	-
Fabrication	1	-	-	+	-
Total		63	67	65	42

Table 14.8: MCA of the location for the suspension spring.

Suspension	Weighting factor	No spring	Spring at base	Spring at tips	Bending energy
Moving mass	4	--	-	++	+
Force drop	3	--	++	++	-
Dead space at tips	3	++	++	--	++
Complexity	2	++	+	+	-
Fabrication	1	++	+	-	-
Total		31	41	36	36

Table 14.9: MCA of the misalignment compensation.

Misalignment compensation	Weighting factor	No compensation	Angled electrodes	Joints	Flexible coupling	RCM mechanism
Effectiveness	4	--	-	-	++	++
Dead space at tips	3	++	++	+	-	+
Complexity	2	++	++	+	-	--
Fabrication	1	++	++	+	-	--
Total		28	32	26	28	28

14.3 Final concept

Resulting from the multi criteria analyses, a final concept can be introduced. The best solutions following this selection process would be:

- Actuator placement above the pivot point
- Suspension at the base
- No misalignment

There are still multiple variations for this concept, but these will be addressed in the detailed design. Some of the variations are shown in fig 14.2. Important to note from the variations is the difference between single moving arm and double moving arm. As the names already suggest either one or both arm can be moved with the actuator. With the single moving arm, the stationary arm is rigidly connected to the robot. With a double moving arm, usually the main pivot connection is also the connection to the robot, leaving both arm free to rotate.

The final concept is used as basis for the detailed design.

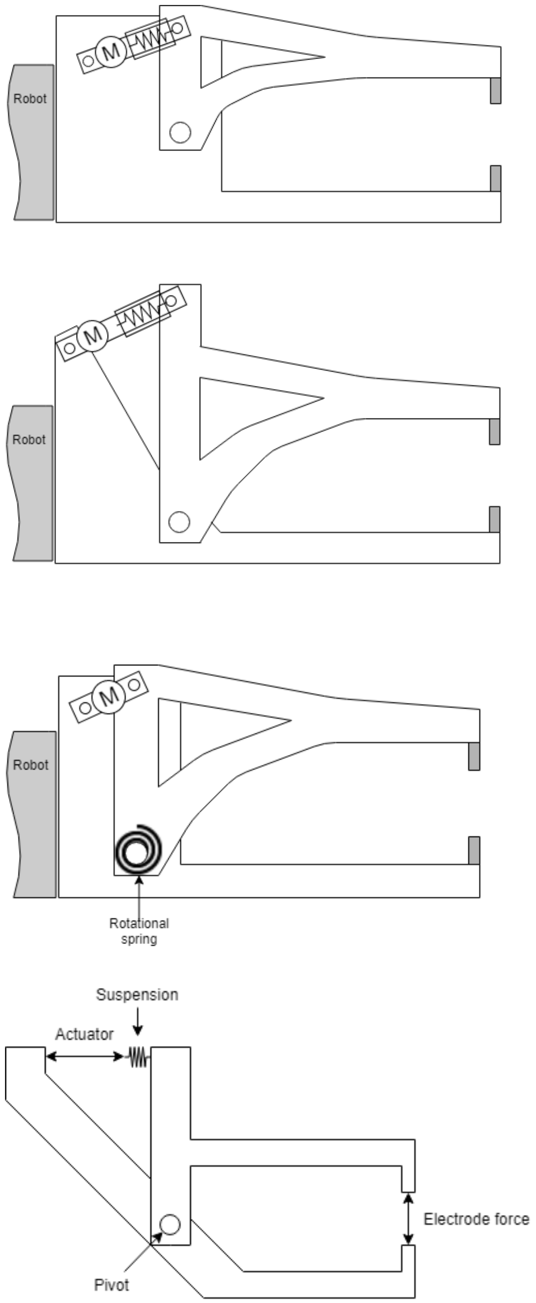
M
Robot
M
Robot
M
Robot
Rotational spring
Suspension
Actuator
Electrode force
Pivot

Figure 14.2: Possible interpretations of the final concept. The first three concepts have a single dynamic arm while the last is a double dynamic arm.

15 Detailed design

After many revisions, the final detailed design is finished. The design is made as proof of concept and therefore is easy to adjust for later experimentations.

The X-type projection welding gun has a servo actuator to provide the electrode force and a linear suspension for the follow-up. A MFDC transformer provides the necessary welding current through the arms to the tips.

The dimensions of the beams and its connections are chosen to ensure tip alignment. A passive position system keeps the welding gun in initial position when the gun is at rest, though it minimizes its influence while welding.

A force sensor is added for weld validation and the current sensor is integrated in the transformer. The final design is shown in figure 15.1.

The location and details of the components are explain in section 15.1. The working principle is in section 15.2 and the modeling is described in section 15.3. How these design choices were made is explained in section 15.4.

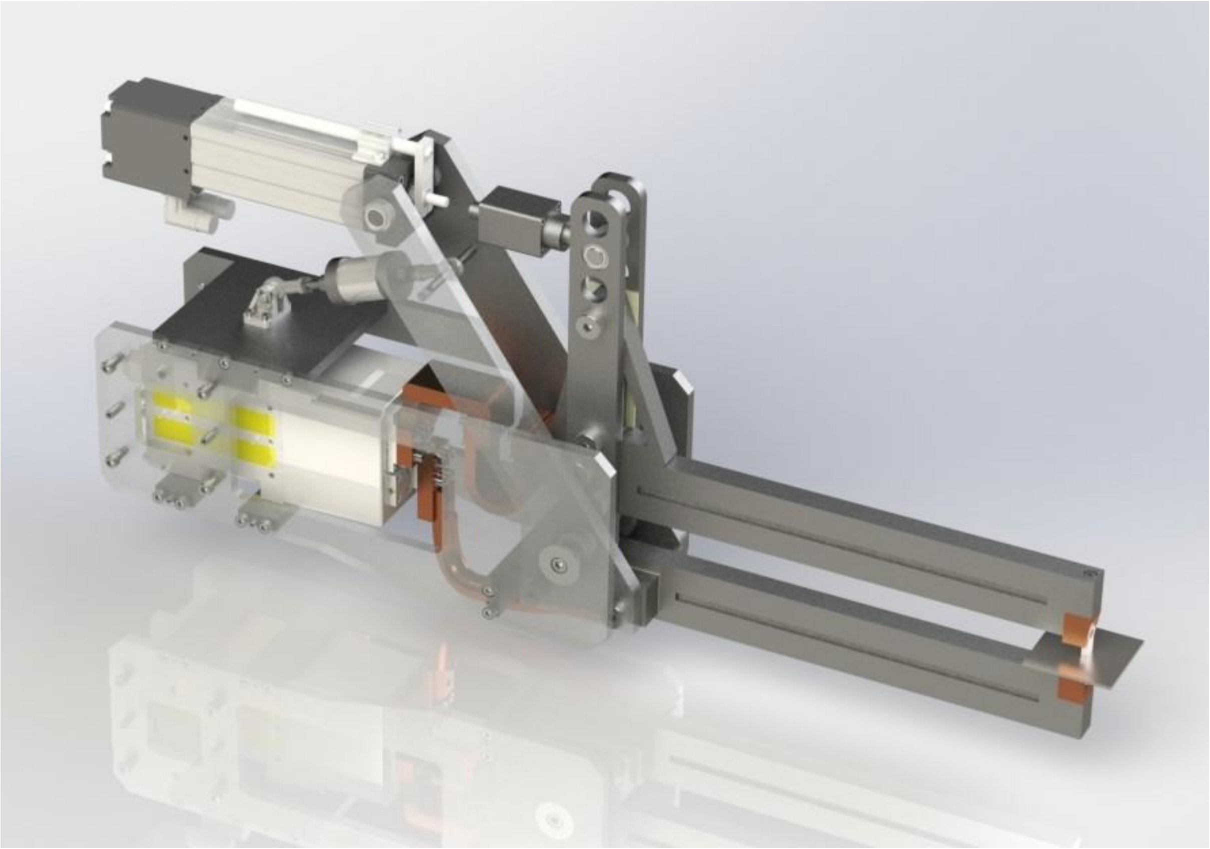

Figure 15.1: Final design of the welding gun.

15.1 Components

The design consists of multiple components and subsystems, shown in figure 15.2. To be able to make a projection weld, electrode force and current are necessary. The servo motor (fig 15.2a) provides the electrode force. The upper and lower arm (fig 15.2 b and c) rotate about a main axis to transfer the motor force to the electrode tips. The transformer with its connections (fig 15.2 h) supplies the welding current.

A suspension system (fig 15.2 d) located in-line with the motor makes sure that contact is maintained during follow-up. A positioning system (fig 15.2 e) consisting of a guided compression spring and a mechanical stop, makes sure that the lower arm is pressed to the mechanical stop when the robot is not welding. This will be further explained in section 15.2.

The enclosure and robot mounting plate (fig 15.2 f and g) connect the welding machine to the robot.

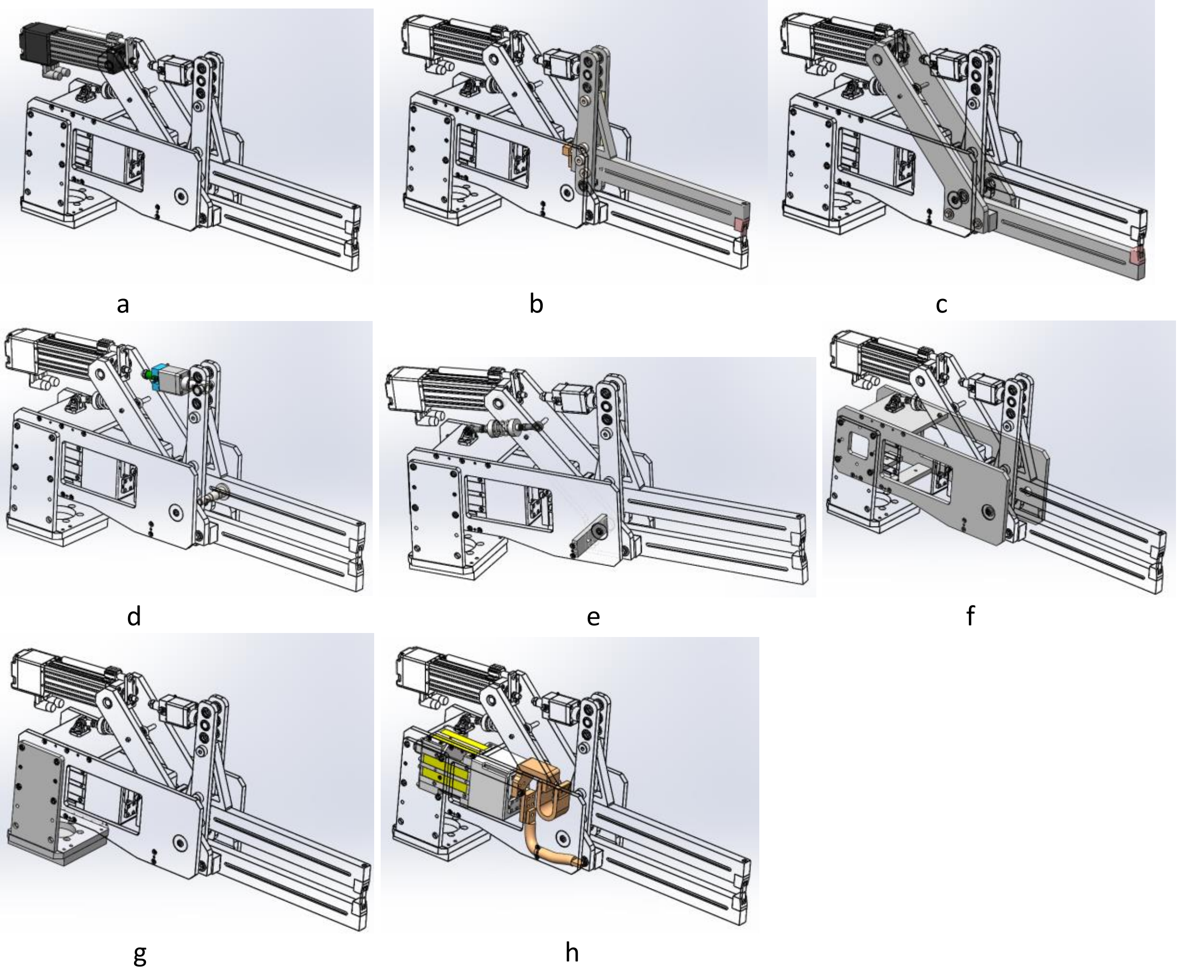

Figure 15.2: Components of the design. a) Motor, b) Upper arm, c) Lower arm, d) suspension system, e) position system, f) enclosure, g) robot mounting, h) transformer with connections.

15.2 Working principle

Just as any other projection welding machine, the X-type welding gun has to fulfill all the steps for welding. In section 7.2, the welding process has already been analyzed for a projection welding machine. The summarized steps are:

1. Welding gun is at rest with the arms open
2. Gun moves towards the desired weld location
3. Gun closes its arms
4. Electrode force is built up and stabilized
5. Welding current is applied
6. The projection collapses
7. Gun opens its arms

When the X-type gun is at rest, the positioning system keeps the arms the arms in initial position. A preloaded compression spring pushes against the lower arm, pushing the lower arm against the mechanical stop. Figure 15.3 shows where the spring and mechanical stop are located with the yellow and red arrow respectively. In this design, the lower arm is pushed against two bolts. These could be replaced for more robust stops in later designs.

The preload is determined with the combined mass and center of gravity of the arms, motor and suspension. The acceleration of the robot when moving to a new location is also taken into account. The preload for the spring is calculated in Appendix D.6 with the result that a preload of ca. 300N should be enough to keep the arms pushed against the stop with a robot acceleration of 3 m/s^2.

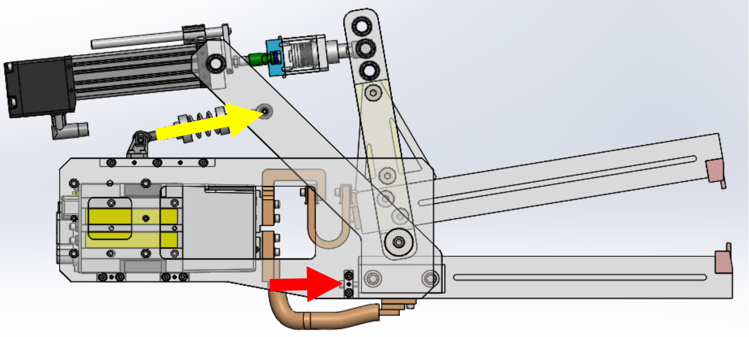

Figure 15.3: Weld gun at rest with the positioning system keeping the arms in initial position. The compression spring pushes the lower arm with a certain preload (yellow arrow) against the mechanical stop (red arrow).

Opening and closing the X-type welding gun is matter of extending and retracting the servomotor. Figure 15.4 shows the X-type in open and closed position at a welding location. The upper arm can rotate 10 degrees, giving an opening of a little over 100mm.

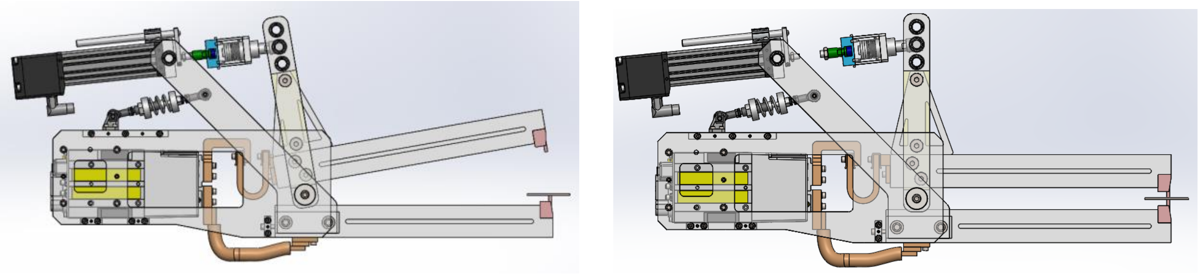

Figure 15.4: *X-type gun in open position (left) and closed position (right).*

Now that the arms are closed at the desired weld location, the electrode force builds up. The motor will start pushing harder resulting in bending in the arms while also compressing the suspension. Note that the motor needs to provide force equal to the leverage ratio times the electrode force. Figure 15.5 depicts the bending of the arms.

Since the design has double moving arms, meaning both upper and lower arms are free to rotate to some extent, the electrode tips will stay centered at the welding location and most of the deflection is at the motor and suspension side.

I can already hear you thinking, we started this section with the positioning system keeping the lower arm in place, how is it free to move now? That is because the preload in the positioning system is low compared to the electrode forces. After the electrode force build-up has reached 400N, the preload in the positioning system is overcome and because of the low spring stiffness, the lower arm is now free to deflect and bend.

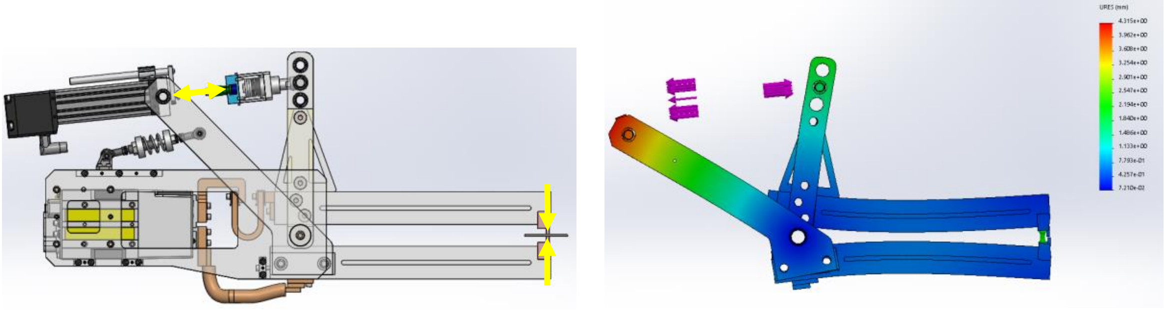

Figure 15.5: Force application and bending of the arms. a) Unloaded b) Max electrode force.

When the electrode force has stabilized, the weld current can be applied. A MFDC transformer supplies the necessary current. A laminated shunt is attached to the upper arm to allow the arm to fully open and close. The arms, made of 7075 aluminum alloy also called Fortal, conduct the current to the electrodes.

Both the lower and the upper arm are insulated to prevent short-circuiting. Figure 15.6 shows the path of the welding current.

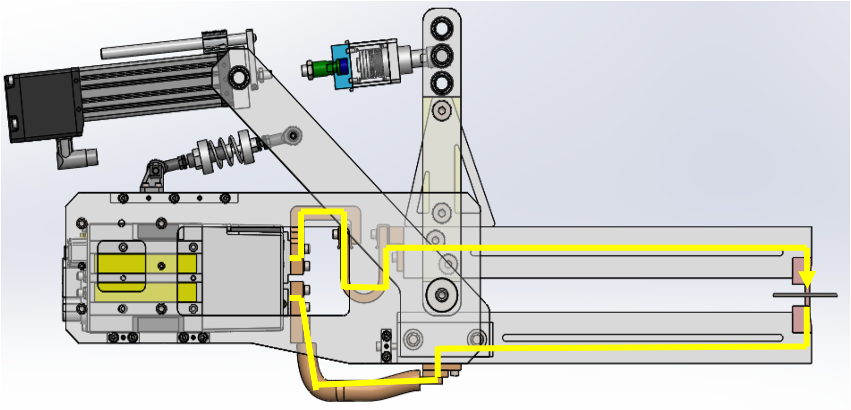

Figure 15.6: Electric path from the transformer to the electrodes shown with the yellow lines.

Shortly after the welding current is applied, the projection collapses and follow-up initiates. For follow-up keeping contact is important, therefore the right suspension felt at the electrodes is important. The combined stiffness of the arm bending and the suspension results in a total suspension, felt at the electrodes, similar to the current C-type welding gun, 203.6 N/mm.

Only a suspension is not enough for follow-up. High tip acceleration is required, meaning that the moving mass or rotating inertia should be within certain limits. This will be further discussed in the dynamic model in section 15.3. The combination of the right suspension and low moving mass result in good follow-up characteristics.

After the weld has collapsed and after the weld current has ceased, the weld is formed and the welding gun can open its arms. The robot can now move to the next location.

15.3 Model of the X-type

The modeling of the X-type gun is essential for the calculations of the suspension stiffness and follow-up acceleration. H. Soemers explains in his book about the difference and significance of two different types of models, a static stiffness model and a dynamic model [39].

The static stiffness model assumes there is no motion and is therefore excellent for the calculation of the suspension stiffness. Having calculated the stiffnesses, the dynamic model can then be used to calculate the follow-up characteristics.

Static stiffness model

For the static stiffness model, shown in figure 9.7, both arms are modeled as rigid beams with a stiffness at the motor side. This bending stiffness can be simulated in Solidworks and is placed at the motor side because the deflection occurs at the motor side. The suspension stiffness is placed between the motor and the upper arm.

The motor force is transferred through the stiffnesses and the rigid beam to the weld location on the sheets. Using ratio b/a, the electrode force at the weld location can be calculated.

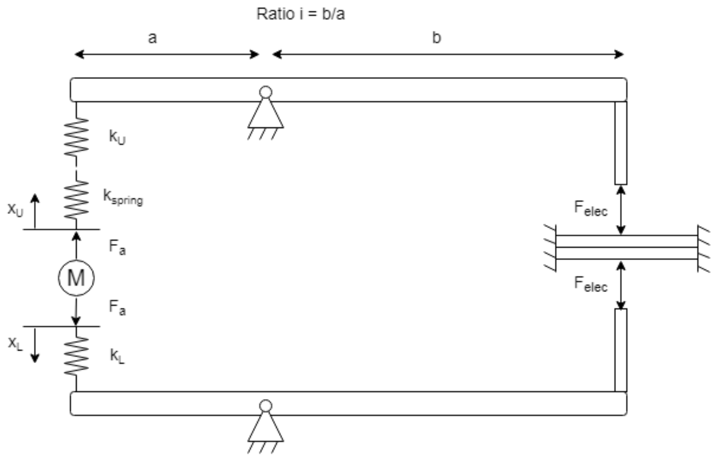

Figure 15.7: Schematic model X-type welding gun. K_U and K_L represent the upper and lower arm bending stiffness, k_{spring} the suspension stiffness. Both arms are pushed against the rigidly supported sheets with a certain electrode force F_{elec}.

A certain suspension felt at the electrode tips is necessary to maintain contact while the projection collapses. The schematic model will have to be modified/simplified a bit to be able to calculate this stiffness felt at the tips. The transmission ratio b/a can be used to find the equivalent stiffness at the electrodes [39]. The equivalent stiffness is calculated with the equation:

$$k'_i = \frac{k_i}{i^2} \tag{15.1}$$

With this knowledge, a new schematic model with the equivalent stiffnesses can be made. In figure 15.8a this new schematic model is shown. Now that the transmission ratio is 1, the equivalent stiffnesses can now also be placed at the tips. This might feel counterintuitive, but since the forces and displacements are now equal on both sides of the beam, both models are correct. Figure 15.8b shows the model with the equivalent stiffnesses at the electrode side.

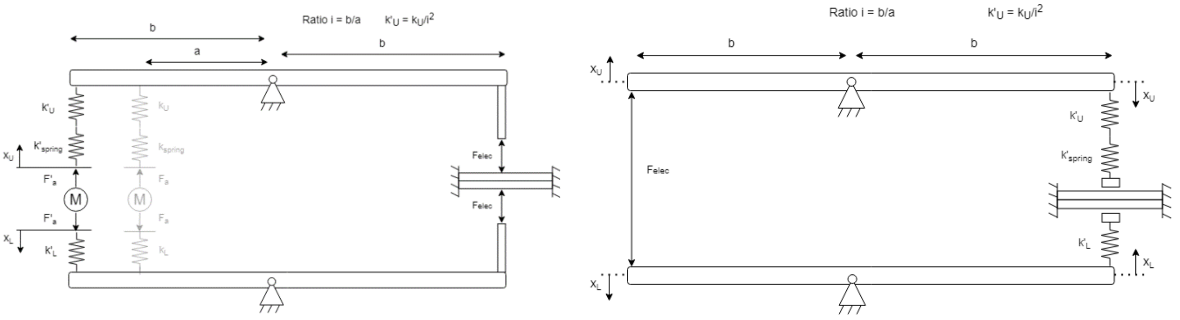
Ratio i = b/a
k'U = kU/i2
b
a
b
kU
k'spring
xU
F'a
M
F'a
xL
k'L
kU
kspring
Fa
M
Fa
kL
Felec
Felec
Ratio i = b/a
k'U = kU/i2
b
b
xU
xU
Felec
k'U
K'spring
K'L
xL
xL

(a) (b)

Figure 15.8: Schematic model of the X-type with equivalent stiffnesses k'_i. (a) with stiffnesses at the motor side, (b) at electrode side.

If we now zoom in on the right side, or electrode side, of the schematic model from figure 9.8, the model could be even further simplified. The resulting model, shown in figure 9.9, becomes a linear system looking very similar to the C-type model. The major differences are the transmission ratio, the upper arm stiffness and the moving lower arm.

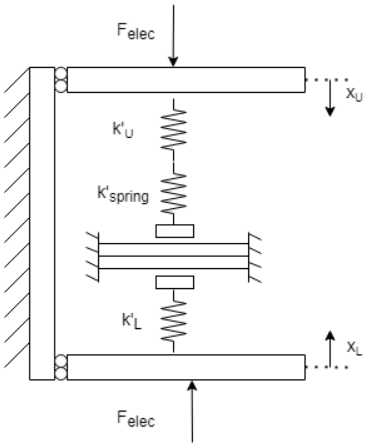
Felec
xU
k'U
k'spring
k'L
xL
Felec

Figure 15.9: Simplified model of the X-type.

Finally, the total stiffness felt at the electrodes and the suspension stiffness can be calculated. The motor pushes both ends outward, meaning that its total displacement is the summation of the upper arm displacement and lower arm displacement. The total stiffness can therefore be calculated with:

$$k'_{tot} = F_a x_{tot} = F_a(x_U + x_L) \tag{15.2}$$

$$x_L = \frac{F_a}{k'_L} \tag{15.3}$$

$$x_U = \frac{F_a}{\frac{1}{k'_{spring}} + \frac{1}{k'_U}} \tag{15.4}$$

$$k'_{tot} = \frac{1}{\frac{1}{k'_i} + \frac{1}{k'_i} + \frac{1}{k'_i}} \tag{15.5}$$

The total stiffness felt at the electrodes k'tot should be equal to the suspension requirement of 200.000N/m. Having the equivalent stiffnesses of the upper and lower arm calculated by Solidworks, equation 15.4 can now be solved.

For the X-type the simulated stiffnesses are k_U = 2582.6 N/mm and k_L = 1564.9 N/mm .The required spring stiffness in the suspension system is calculated to be 125.9 N/mm.

Dynamic model

The dynamic model is necessary to calculate the dynamic response of the X-type. The follow-up characteristics can be obtained from this model. In figure 15.10 the schematic model during the welding process is shown.

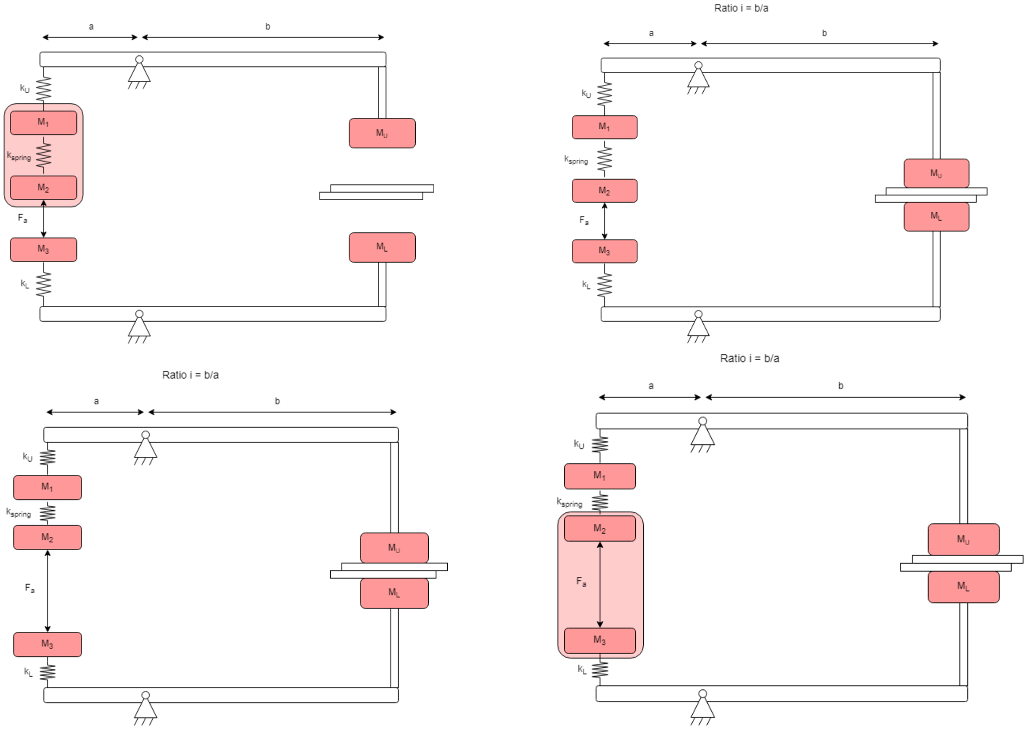
a
b
k_U
M_1
k_{spring}
M_2
F_a
M_3
k_L
M_U
M_L
Ratio i = b/a
a
b
k_U
M_1
k_{spring}
M_2
F_a
M_3
k_L
M_U
M_L
Ratio i = b/a
a
b
k_U
M_1
k_{spring}
M_2
F_a
M_3
k_L
M_U
M_L
Ratio i = b/a
a
b
k_U
M_1
k_{spring}
M_2
F_a
M_3
k_L
M_U
M_L

Figure 15.10: Dynamic schematic model of X-type welding gun throughout the welding process. (a) Gun at rest, arms are open and m1 and m2 act as a single mass. (b) Gun is closed and electrodes touch. (c) Electrode force builds up. (d) Model when welding, m2 and m3 act as a single mass with a rigid connection.

With eq. 15.6, the effective mass of the arms can be calculated. The moments of inertia were calculated with Solidworks, resulting in an upper arm moment of inertia at pivot: = 0.3904 kg*m^2 and for the lower arm: 0.8310 kg*m^2. The distance of the motor and electrodes to the pivot point are r_b = 575 mm and r_a = 350mm, respectively. With Newton's second law, the acceleration is calculated. The calculations are made with the minimal electrode force required for welding steel, 800N.

$$m_{i,eff} = \frac{J_{pivot,i}}{{r_i}^2} \tag{15.6}$$

The resulting effective masses are 1.18 kg and 2.53 kg for the upper and lower arm respectively. The maximum accelerations for the upper and lower arm are therefore respectively 677.5 m/s^2 and 318 m/s^2.

The eigenfrequencies of the system can be found in Appendix C.6.

15.4 Design choices/considerations

During the detailed design process many decisions were made to meet all the set requirements. This section goes into detail about the different solutions and why some of the choices were made.

Single versus double dynamic arm

After the concept selection process, single and double moving arm concepts were drafted as final concept. A single moving arm means that only one of the arms is dynamic and thus free to move while the other arm is fixed. It is a much simpler system than a double dynamic arm where both the arms are free to move.

The current C-type welding gun has only one moving arm, the upper arm. This is possible since large and stiff lower arm armatures can be made. The X-type welding gun does not have that luxury since the throat length is long and the height is limited. Downward deflection, or vertical deflection, becomes excessive with a single dynamic arm. This is shown in figure 15.11.

However, a double dynamic arm leaves the lower arm free to move and therefore free to deflect at the motor side. The advantage is that vertical deflection is no longer an issue and the electrodes will center itself on the weld location. The disadvantage is that the system becomes more complex and since both arms only connect to a rotation point, some mechanism is needed to keep the arms in a known location when the welding gun is at rest.

The advantages outweigh the disadvantages and a double dynamic arms has therefore been chosen.

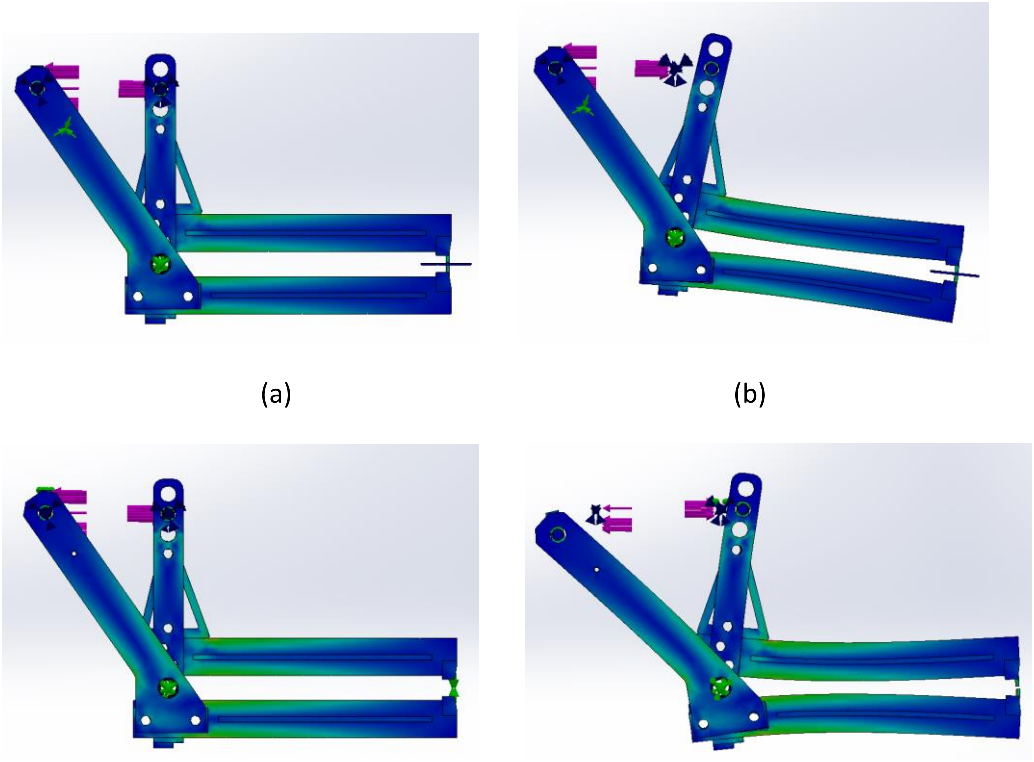

(a) (b)

(c) (d)

Figure 15.11: Comparison of the deflection of a single dynamic arm (a) and (b) versus a double dynamic arm (c) and (d). The colours are the stress distribution.

Material selection

Careful material selection is crucial for some of the components in the X-type machine. Especially the upper and lower arm materials are important since they need to handle high stresses, high currents, and high precision. Fast, consecutive welding can heat the arms so good thermal conductivity and low thermal expansion are taken into account as well.

Using the material database Granta EduPack, previously known as CES Edupack, the best suited material for the arms is the aluminum 7000 series. Since the company Arplas has already worked with aluminum 7075 before, it is readily available and relatively affordable, the arms will be made out of 7075 aluminum.

The main axis also has to handle high loads, and is therefore made of hardened steel C60. The copper parts at the tips are made from Copper Zirconium to increase the yield strength compared to regular copper.

Tip precision

The alignment requirement has been a deciding factor in the dimensioning of the beams. As can be seen in figure 15.12, when the load is applied, the electrodes displace horizontally. In the figure, the tips have deflected from their original location to the right. To reduce this deflection, the beam height and width can be increased. The location of the bolts connecting the main beams also directly influences the horizontal displacement.

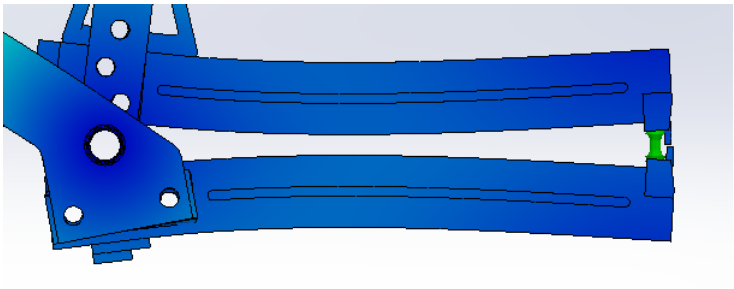

Figure 15.12: SolidWorks simulations of the bending of the lower arm. It can be seen that the horizontal displacement can become quite high.

Addition of stiffener bracket

- Bit more mass
- Increases upper arm stiffness
- Increases useable throat length range
- Bit better electrode precision

Spring choice

As suspension, a spring or something acting like a spring could be used, as long as the correct stiffness can be acquired. Possible solutions for the springs are:

- Single compression spring
- Multiple (different stiffness) compression springs
- Disc springs
- Torsional springs

Stiffness manipulation is not at the order in this research, although this could be interesting for future research. Different stiffnesses in different force ranges could make it possible to control the drop force for aluminum and steel welding individually. Multiple springs with different stiffnesses would be the simplest way of achieving different spring constants at different force levels. A single compression spring with a progressive or regressive spring rate could also achieve the same goal. But since this is not necessary, these springs are not chosen in this design

A torsional spring with the required stiffness rate would take too much space at the already densely filled axis. Additionally, the design would have to use more moving parts to integrate a torsional spring since the motor and spring cannot be attached to the same rotating part. Torsion springs are also harder to replace and adjust. Bending stiffness is better for linear springs since full upper arm be used to reinforce.

A linear spring is therefore chosen. Since the length of the suspension directly influences the size of the lower arm, a short spring is the best solution. The disc springs, or belleville springs, have the characteristic of having high stiffness for their small length. Stacking them in series or parallel affects the total stiffness of the stack. The stiffness needed for this application is ideally suited for disc springs, decreasing the total length of the spring system with almost 85%. Also, the total stiffness can easily be adjusted by changing the stack design.

Disc springs are therefore used in this design, especially as the design is an experimental setup where the ease of replacing and adjusting is important. More information about the selection of the spring can be found in appendix C.3.

Suspension spring enclosure

The spring enclosure needs to keep the housing and spring piston concentric while also providing guidance for the disc springs. Minimizing friction and play will keep the suspension durable and running smoothly.

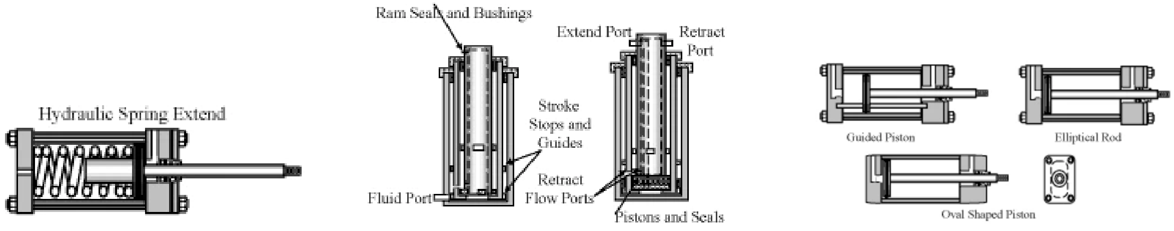

(a) (b) (c)

Figure 15.13: Possible solutions for the enclosure of the suspension spring. (a) D single-acting spring extend cylinder. (b) Single and double-acting telescope cylinders. (c) Guided piston [40].

Telescope cylinders are mostly used for applications where large strokes are necessary. For short strokes, the single-acting spring-extend cylinders are preferred. Guided cylinders, either internal or external, are preferred for cylinders that are not allowed to rotate. It is always best to guide the workpiece externally and only use the cylinder to cycle it [41].

A single-acting spring-extend cylinder is chosen since the stroke is short and rotation of the suspension does not influence its performance. An internal guiding shaft keeps the disc springs neatly aligned. A stack of different size shims keeps the suspension adaptable so a change in suspension stiffness can easily be made. Preload can also be added by increasing the stack of shims.

A shaft misalignment compensation unit is added to compensate for the manufacturing errors. If the motor and spring system are not aligned, the moments acting on the spring system could lead to high static and dynamic friction. Note that this is only an axial alignment coupling and no angular misalignment is compensated. All components of the suspension spring are shown in figure 15.14.

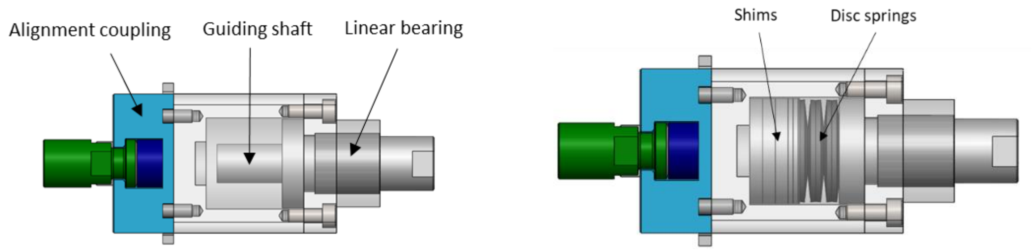

Figure 15.14: Components in the suspension spring.

Bearing choice

The bearings are an important aspect for the functioning of the welding gun. Low friction, high stiffness and good reliability are the main criteria. Bearings are in many shapes and sizes. In the X-type both linear and roller bearings are necessary. The linear bearings are located in both spring systems. Roller bearings are in the upper and lower arms at every rotating joint.

For the linear bearings in the spring systems, plain bearings were chosen as they are a compact, reliable, self-lubricating, and do not depend a lot on the shaft material. They have a slight starting friction but to reduce this, relatively long linear bearings have been selected.

The roller bearings selection also ended in plain bearings. These bearings were at first not preferred, but more research resulted that plain bearings are the best for the type of motion of the X-type. Low running speeds, reciprocating motion instead of full rotations, and heavy static loads resulted in the choice of plain roller bearings. Appendix… has more information about the different bearing types, advantages and disadvantages, and the bearing selection.

Positioning system

Since the upper and lower arm are both only connected to a pivot, one or both of the arms will need a mechanism keeping the arms in a known initial position during rest or robot movement. The positioning system should minimize its influence when the electrode force builds up.

Three possible solutions were found: Two mechanical stops with the motor pulling both arms against the stops, one mechanical stop with a spring pushing one of the arms against the mechanical stop, or having a locking mechanism that can lock one of the arms in initial position while unlocking during welding. These options are shown in figure 15.15.

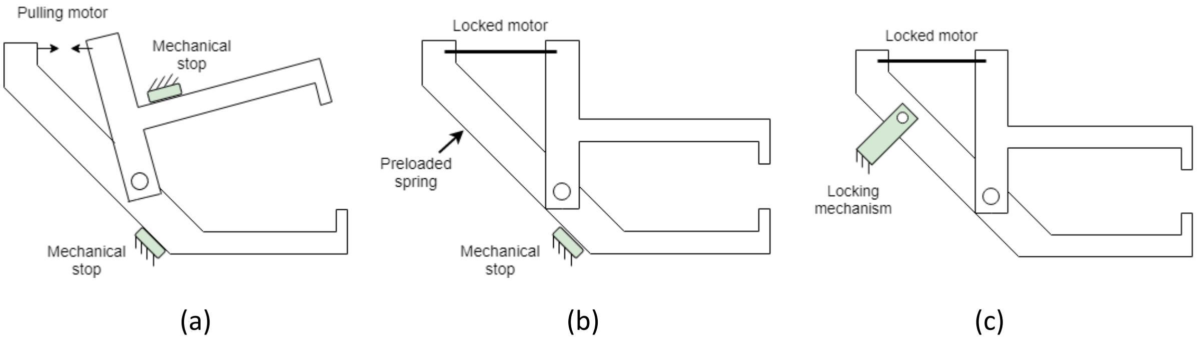

Figure 15.15: Possible solutions for the positioning system. a) Two mechanical stops, b) one mechanical stop with a preloaded spring pushing against the stop, c) a locking mechanism.

The concept from figure 15.15b with the spring pushing the lower arm against a stop is chosen. This system is passive, does not require any control or sensors, and the upper arm can be rotated without losing the initial position. However, the preload in the spring does influence the bending of the arms a little. Solidworks simulations have shown that the downward, or vertical deflection is well within the limits stated by the requirements.

Arm insulation

When current is applied, it is critical that no short-circuiting happens. Good electrical isolation is necessary to make sure the current goes directly through the arms to the electrodes without shunting. Options for the insulation are:

- Insulate outer beams
- Insulate inner beam
- Insulate bearings
- Insulate main axis

Insulated bearings need a special coating and are generally susceptible to high forces and do not have a long durability. Insulating the main axis would require stiff insulating material that can withstand high shear forces. Ceramics are the most common stiff and insulating materials, but these are susceptible to shear loads. Alternatively, compounds such as glass fiber could be used, but these materials are hard to produce and since the main axis is relatively large, the part would become expensive fast. Insulating the inner or outer beams would be the best and cheapest solution.

If the outer beams are insulated, the bolt connecting the parts would carry current. Therefore, also the bolt head would need to be insulated so it will not touch the outer beams. From experience of Arplas, these insulating caps are not very tough. Insulating the inner beam was therefore chosen in consultation with the supplier, Doceram GmbH. These insulating cylinders are made of a special glass fiber having good toughness and stiffness.

Epoxy glass sheets prevent the inner and outer beams from touching, as shown in figure 15.16.

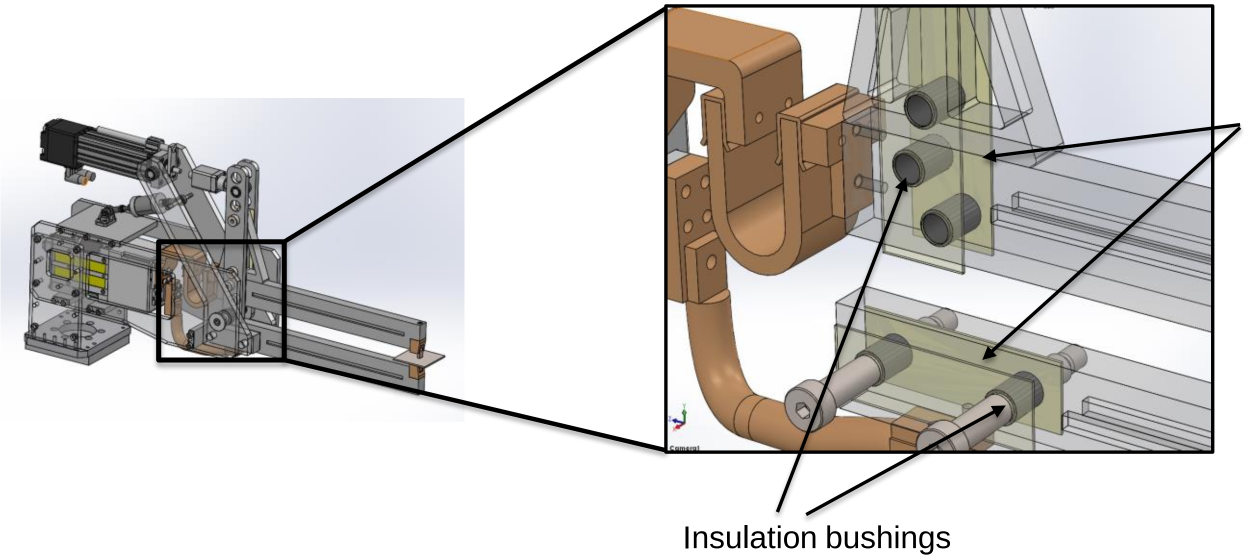

Figure 15.16: Locations of the electrical insulation.

Cooling system sleeves

When currents with the magnitude used in projection welding are applied, the conducting parts heat up, especially at the surfaces where the parts make contact. For fast, consecutive welding, the conducting parts should be water-cooled but this was decided out if the scope for this research. Sleeves were made in the arms so cooling tubes can be added in future tests.

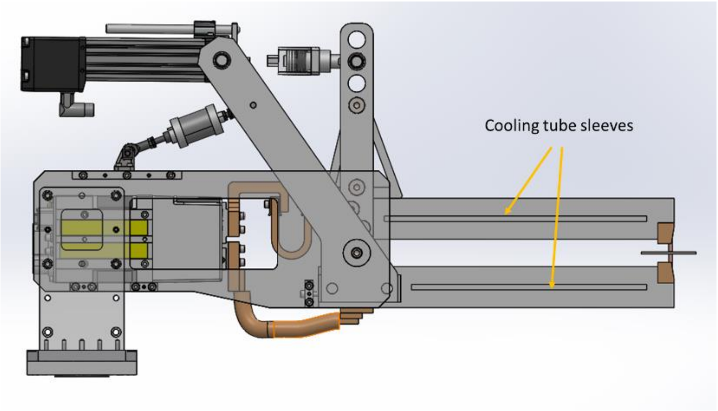

Figure 15.17: 8mm deep sleeves made for cooling tubes.

15.5 Configuration tool

To be able to change the design to adjust for different applications of the X-type welding gun a step-by-step plan is made. There is still some engineering knowledge and SolidWorks simulation skills expected from thee user though.

The first few steps are to set some important parameters which will be the basis for the rest of the design:

1. What electrode force is required?
2. What arm length is required?
3. What motor is used (how much force can it produce) → ratio electrode-motor

Then the general design of the welding gun is determined.

4. Decide placement of motor, above or before pivot point (true X versus above X, chapter 13)
5. Design the upper and lower arms as desired as long as the arms can be made stiff enough to stay within the horizontal bending requirement. Beam height is one of the main factors for tuning this bending deflection, as well as the location of the bolts holding each arm together.
6. Stiffener bracket(s) could be added if bending requirement is hard to reach.

Now that the placement of the motor is known and the arms have been designed, the models made in section 15.3 will be used to calculate the suspension, or follow-up, spring stiffness together with the total stiffness of the design.

7. Use simulation software to predict the bending displacement at the motor side as shown in figure 15.11d.
8. Calculate upper and lower arm stiffness with the simulation software bending displacement and applied force. Also check safety factors of beam stresses and bolt connections.
9. Necessary suspension spring stiffness is calculated with eq. 15.5.
   NOTE: if arm deflections are already too high (or the stiffness too low), the desired total suspension stiffness cannot be obtained unless a tension spring is added. However, increasing arm dimensions and thus arm stiffness is the best solution.

With all the theoretical calculations done, it is time to select parts and piece everything together

10. Spring choice is now made, recommended is a compression spring for stiffness <=500.000, and disc springs >500.000N/m.
11. If disc springs, careful selection is required. h/t should be minimized (for linear spring stiffness) while still strong enough to handle the max motor force. Easiest is to find disc spring which are compressed 75% at max motor force, and choosing the lowest h/t disc spring. These disc springs should be stacked in order to provide the required stiffness. For more information, Appendix C.3 can be used.
12. Arms and suspension design is done, next is the housing. The main axis holding the upper and lower arm should be the only connection to the housing. The rest of the housing is necessary to attach the electrical parts such as the transformer and the MGDM. The other moving parts could be covered with the housing as well.
13. To keep the arms in an initial position, the position spring system is added. A spring with low stiffness as to not interfere with the welding process needs to push the lower arm against a

mechanical stop. Necessary preload in the spring can be calculated with the inverted pendulum model, the parameters obtained from the simulation program and the max acceleration of the robot. This all explained in further detail in Appendix C.5.

14. Mounting of the spring and mechanical stop should be added on the housing and lower arm.
15. Check all previous calculations and assumptions, redesign where needed.
16. Now most of the design is done, adding the electronics, insulation and cooling is the final step.

16Experimental validation

The design of the X-type welding gun will have be tested to see if it meets all the requirements set in table 12.4. The requirements to be tested are shown in table .. . The theoretical values calculated in the design phase are also shown. Since the main objective is the mechanical system, these will be tested first. Making strong and invisible welds is the secondary objective and can usually be perfected with changing the welding parameters and not the machine characteristics. Finally, the X-type is mounted on a robot.

Table 16.1: Requirements to be tested

Criteria	Parameters	Required	Calculated
Contact pressure	Electrode force	800-3000 N	0-3026N
Follow-up	Acceleration	>162 m/s^2	677 m/s^2
	Suspension	ca. 200 N/mm	203.6 N/mm
Concentric electrodes	Electrode parallel misalignment	< 0.5mm	0.004 mm
	Electrode angular misalignment	±1.5°	Upper arm: 0.121° Lower arm: 0.103°
	Lateral displacement	< 0.5mm	Upper arm: 0.416 mm Lower arm: 0.420 mm
	Vertical deflection	< 0.5mm	0.181 mm
Weld strength	Nugget size Tensile force	Similar to C-type	
Surface appearance	Indentation Marks of welding	Similar to C-type	
Weld validation	Drop force	Similar to C-type	

16.1 Method

The X-type welding gun will be tested with four different experiments. The first three will be without welding, the last will be with welding. The same equations as in Part II, the testing of the C-type, will be used. This makes sure the X-type is tested the same way the C-type was tested. Both results can then be compared.

16.1.1 Equipment

Table 16.2: Sensors used for during the tests.

	Supplier	Model type
Displacement sensor 1	Keyence	LK-H022
Displacement sensor 2	Keyence	LK-H052
Force sensor 1	Kistler	9103A
Force sensor 2	Tecna	Force Transducer 200daN
High speed camera	Casio	EX-F1

The Bosch process resistance welding interface (PRI) is used as controller for the welding machine. It is an already developed program that is already used on the current servo C-type machine of Arplas. Its main advantages are:

- Easy control of weld parameters
- Movement and weld execution
- Force calibration
- Current calibration
- Lever ratio

16.1.2 Experiments

Experiment 1: Force check and total machine stiffness

In this test, the maximum force will be applied, checking if the requirement of a maximum force of 3000N electrode force can be applied. Using the Kistler force sensor between the upper arm and suspension spring, the motor force can be measured. A Tecna force transducer will be put between the electrodes to measure the actual electrode force.

The Bosch PRI weld controller has a built-in function for X-types. The lever ratio between the motor and electrodes must be set, and it will automatically convert all data to the electrode displacement and electrode force. It can also be calibrated to compensate for nonlinear behavior of voltage input in the servo and its output electrode force. The Tecna sensor will also be used for the calibration of the force.

Since the output of the weld controller is already converted to force and displacement at the electrode tips, the total machine stiffness check can be done by simply measuring the change in displacement due the force increase:

$$k_{tot} = \frac{\Delta F_{motor}}{\Delta x_{motor}} \tag{16.1}$$

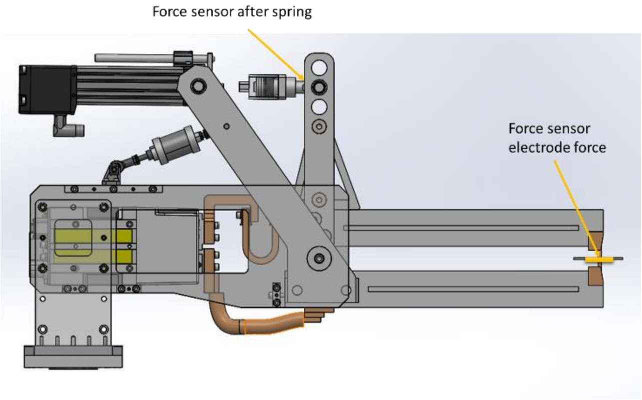

Figure 16.1: Location of force sensors during experiment 1.

Experiment 2: Horizontal misalignment

To check the lateral (horizontal) displacement of the electrode tips, a laser sensor will be positioned at the ends of the electrodes as shown in figure 16.2. The displacement is measured four times for electrode force values increasing from 1000N to 3000N in steps of 500N.

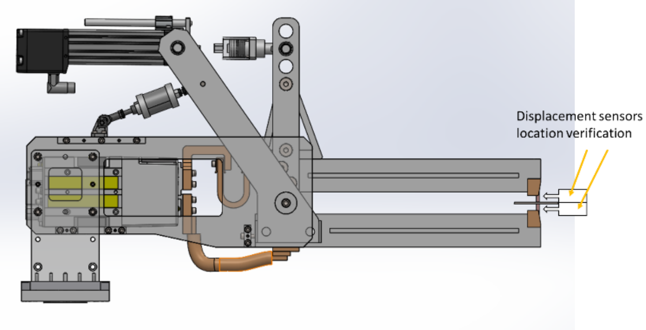

Figure 16.2: location of the Keyence laser sensor for experiment 2.

Experiment 3: Electrode rotation

The rotation of the electrodes is measured with a camera, depicted in figure 16.3. Again, the maximum electrode force is applied and the rotation of the electrodes is measured by calculating the amount of pixels the electrodes move. The camera will be set to the maximum quality (1920x1080p).

Two frames of the video will be analyzed, one just as the electrodes touch and almost no electrode force is applied, the second with maximum electrode force. The frames are put in Matlab where points on the edges of the electrode are selected by hand. The starting rotation and maximum force rotation are then compared to find the change in angle as a result of the applied electrode force. The equation used to find the rotation with respect to the vertical axis of each electrode in the frame is:

$$\theta = \operatorname{atan}\left(\frac{\Delta x}{\Delta \mathrm{y}}\right) \tag{16.2}$$

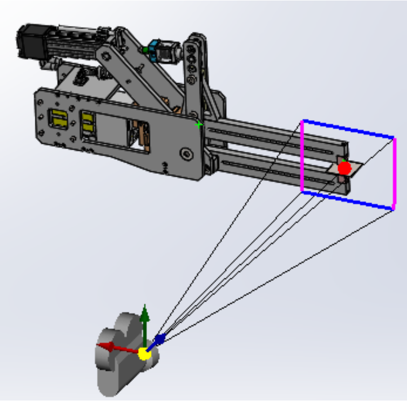

Figure 16.3: Camera placement during experiment 3.

Experiment 4: Vertical misalignment and follow-up

In this test the follow-up characteristics as well as welding stiffness and the vertical deflection are measured. Initially, the plan was to have two laser displacement sensors measuring at the same time, one for the upper arm and one for the lower arm. Sadly, after unpacking the sensors borrowed from the university, one essential cable was missing and therefore only one displacement sensor could be used during the experiments.

Because of the lack of one displacement sensor, the upper arm and lower arm vertical displacements were measured individually. The sensor locations are shown in figure 16.4. The same analysis as with the C-type is done for the calculation of the acceleration. The displacements of the upper and lower arm are summed for a total displacement of the arms. The velocity and acceleration are again numerically derived.

The contribution of each arm can also be calculated. It can be analyzed if the mass ratio of stiffness ratio is the main contributing factor.

The welding stiffness is calculated again with the drop force and displacement drop. Since the vertical displacements are calculated individually, an average displacement drop is used.

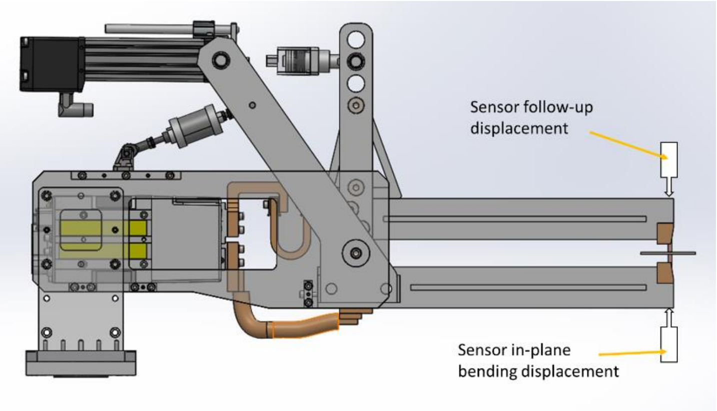
Sensor follow-up displacement
Sensor in-plane bending displacement

Figure 16.4: Locations of the Keyence displacement sensor for experiment 4.

16.1.3 Experiment setup

The complete setup is shown in figure 16.5. The PC has the weld controller program installed and is used to change the weld parameters and to start the welding sequence. The DAQ is also connected to the pc for the measurements of the Keyence laser sensors.

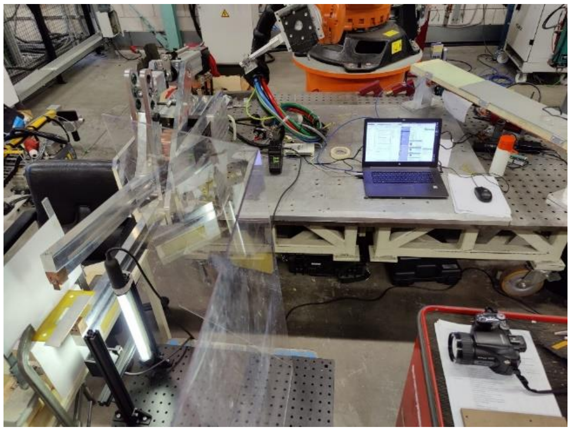

(a)

(b)

(c)

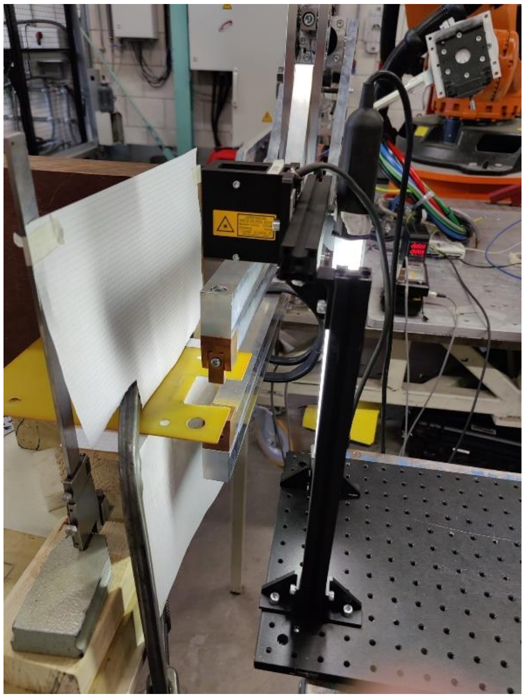

(d)

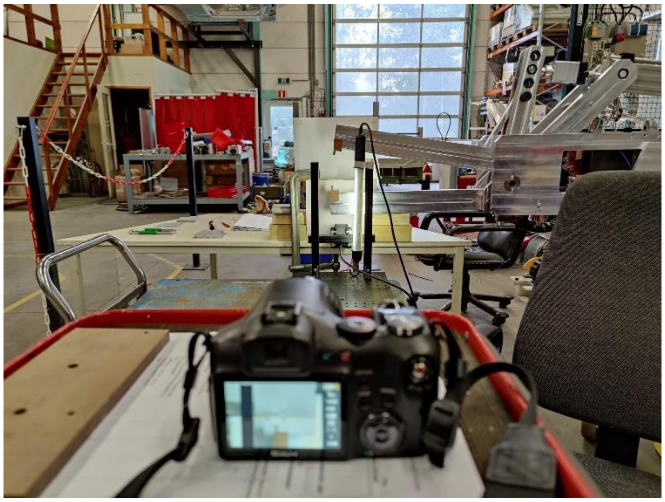

(e)

Figure 16.5: Photos of the experiment setup. a) Overview of the full setup, b) Placement of displacement sensor for experiment 2, c) and d) the setup for experiment 4, e) point of view from the camera with extra lighting for better slomotion videos.

16.2 Results

16.2.1 Experiment 1: Max force and total stiffness check

A total of 10 tests were made for the stiffness check, but when processing the data afterwardsI realized that the position data from the weld controller were not saved. This was probably due to some trouble shooting when connecting the X-type to the controller. Somewhere in the troubleshooting process the checkbox for saving the position data was unchecked. After these initial tests were done, the test location at the company was packed for moving to a new location. New tests could therefore not be performed again.

Old datasets with the position data was retrieved, but these datasets only contained measurements with an electrode force of 1000 N. An example of the graphs putputted by the weldcontroller is shown in figure 16.6. The resulting total suspension stiffness was calculated for each of the tests and can be found in table 16.3. The mean of the calculated stiffness is 200.76 N/mm.

The maximum force in the specifications for the servoactuator is said to be 5000N. For short times, the actuator force can actually be increased even more. A total of 3400N electrode force was applied and the machine had no trouble handling that force. The bolts and other heavy loaded parts are therefore strong enough to handle the maximum required force.

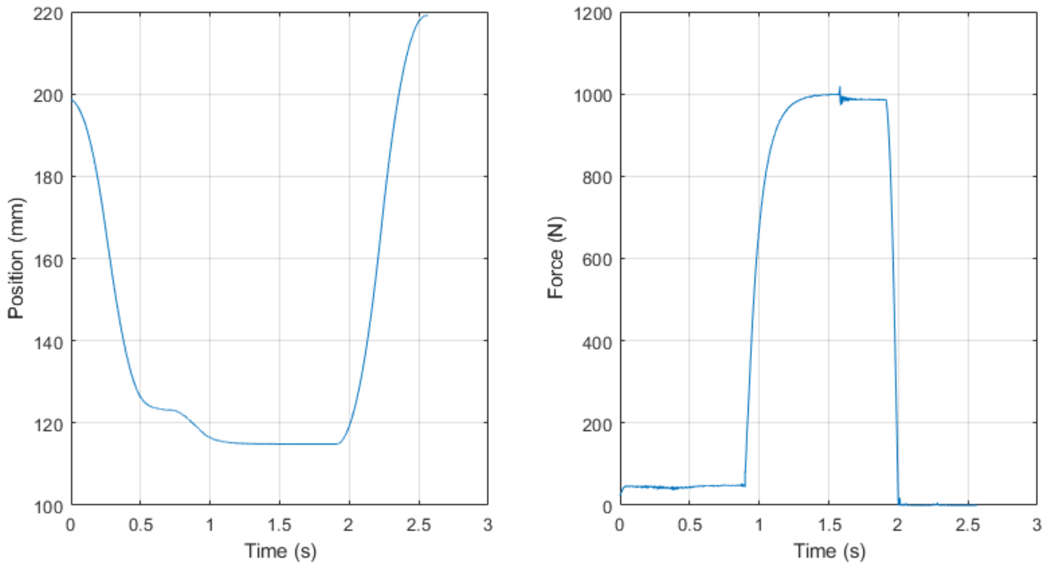

Figure 16.6: Position and applied force at the electrodes of a steel weld measured by the servo actuator.

Table 16.3: Measured total stiffness.

Measured total stiffness (N/mm)
197.65
205.34
204.60
205.20
203.66
200.14
196.15
201.23
206.69
188.61
206.86
206.63
195.98

16.2.2 Experiment 2: Horizontal bending

The laser sensor was positioned as close as possible to the ends of the electrodes. Figure 16.7 depicts the results from the experiment for the lower and upper electrode. Since the arm open and close, the electrodes are not always in front of the sensor. The displacement graph had to be analyzed to find the point where the electrodes touch and where the electrode force is applied.

The highest measured horizontal displacement is of the upper arm with a value of 0.194mm. The requirement was 0.5mm and the Solidworks simulation results were 0.416mm. The precision is therefore better than simulated, which is explained by the frictionless electrode contact in the simulation.

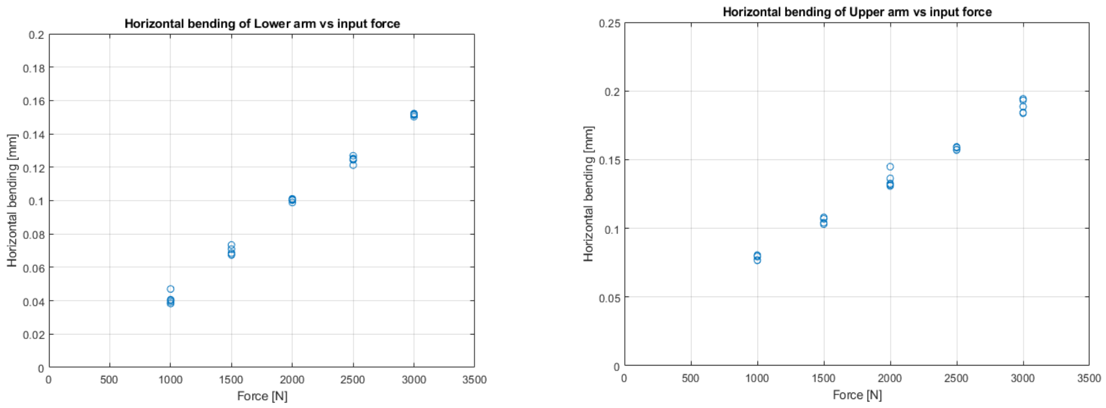

Figure 16.7: Horizontal deflection results with increasing electrode force. The lower arm deflections on the left and the upper arm deflections on the right.

16.2.3 Experiment 3: Electrode rotation

HD videos were recorded and an image before the electrode force is applied is compared with the image where full electrode force is applied. Figure 16.5 shows the two frames used for the calculation of the rotation. It can already be seen that there is almost no difference between the two pictures. Matlab confirms that. In appendix D.2 the full pictures and the selected data points can be found. Not all the points are perfectly on the edge of the electrode. But even with these measurements, the angle between electrodes stay well within the required precision.

It should be noted that the electrode tips move downwards slightly, explaining the reduction in angle for the upper arm. The total angle between the upper and lower electrodes are calculated for the loaded and unloaded positions, shown in table 16.4. It can be seen that the misalignment of the electrodes *reduce.* An explanation for this is that the electrodes seen to align themselves around the sample, and not rotate individually as was the assumption in Matlab.

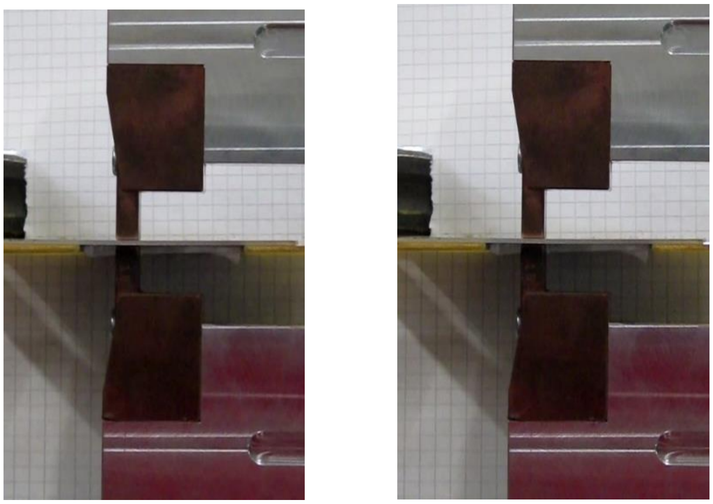

Figure 16.8: Frames taken from the high speed camera. Left is unloaded, in the right picture maximum electrode force is applied

Table 16.4: Measured electrode rotation and the difference in angle between the electrodes

	Unloaded angle (deg)	**Max electrode force angle (deg)**
Upper electrode	-0.922	-0.916
Lower electrode	-0.329	-0.661
Electrode angular misalignment	0.593	0.255

16.2.4 Experiment 4: Follow-up characteristics

The measured displacements did not result in valid results. Although the measured distance seem correct, the time frame does not. Comparing the timeframe with the camera results and the force measurements, it was clear the measured collapse time should have been a factor of 6 to 10 faster. For those still interested in the results, a graph can be found in Appendix D.3. There was no time left for yet another round of measurements.

Initially the average displacement drop of the lower arm, and the average of the upper arm, should have been calculated. Since these results are not available now, the results of the C-type displacement drops are used for the steel samples. The aluminum samples used in this test were not the same as in the C-type test so these results will not be used.

In table 16.5 these displacement drops and force drops are shown together with the resulting welding stiffness. It can be seen that the drop forces and therefore the welding stiffness is a lot higher than the results of the C-type and the expected results for this machine. As a matter of fact, it seems that the suspension spring is not being used during welding, since the total stiffness of the arms together do come close to the measured welding stiffness:

$$k_{arms} = \frac{1}{\frac{1}{k_U} + \frac{1}{k_L}} = 354.9\ N/mm \tag{16.3}$$

Table 16.5: Measured drop forces

Sample	**Drop force (N)**	**Average displacement drop (mm)**	**Welding stiffness (N/mm)**
Aluminum 1mm	83.4	-	
Aluminum 1mm	80.7	-	
Aluminum 1mm	82.9	-	

Aluminum 1mm	78.5	-	
Aluminum 1mm	82.4	-	
Steel 0.8mm	141.9	0.429	330.8
Steel 0.8mm	143.6	0.429	334.7
Steel 0.8mm	148.8	0.429	346.9
Steel 0.8mm	149.6	0.429	348.7
Steel 0.8mm	147.3	0.429	343.4

In the frames made by the slowmotion camera shown in figure 16.8, the follow-up of the electrodes can be seen. The zinc coating on the steel sheets causes the explosion. In the first four to five frames, follow-up takes place. The slowmotion was made with 300 frames per second, so the projection has collapsed in approximately 10 - 13.3 ms.

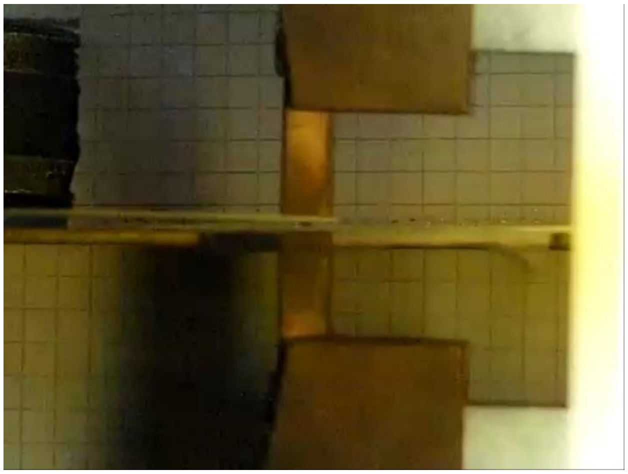

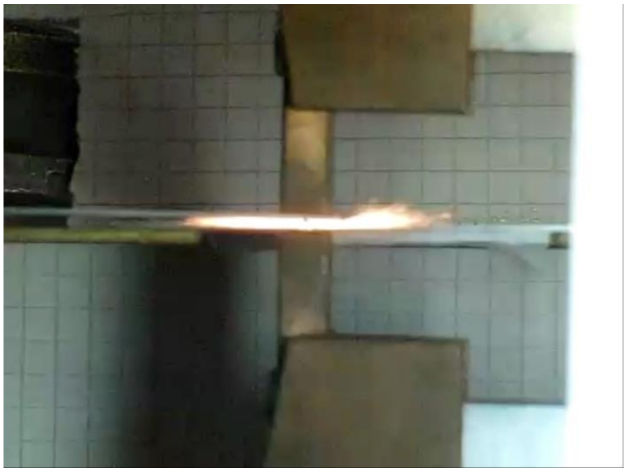

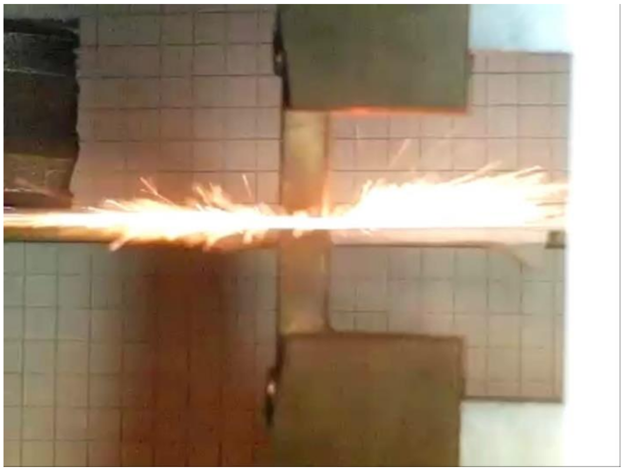

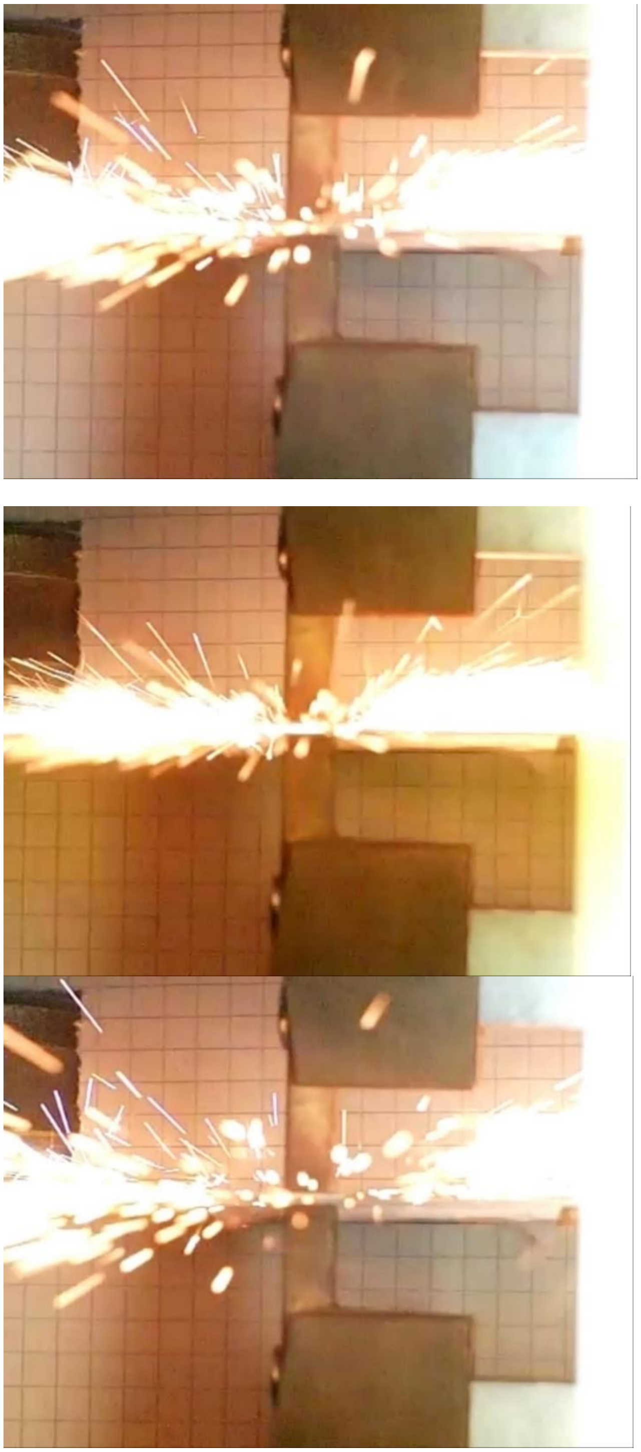

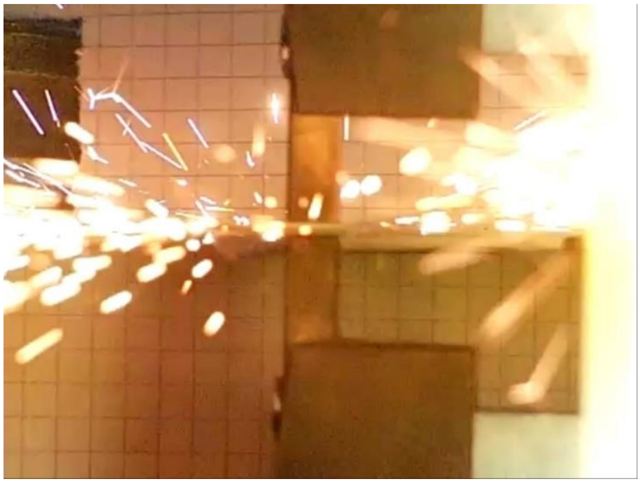

Figure 16.9: Frames captured by the slow-motion camera showing the welding and follow-up of a steel sample.

After all the follow-up tests have been performed it is time to analyze the welded samples. The results of the steel and aluminum welds can be seen in figure 16.10. For the steel samples it is clear which side contained the projection. The side without the dimple looks very good and is almost invisible, especially if the samples had been coated or painted afterwards. The aluminum welds look very similar on both sides, as it is always with aluminum sheets currently.

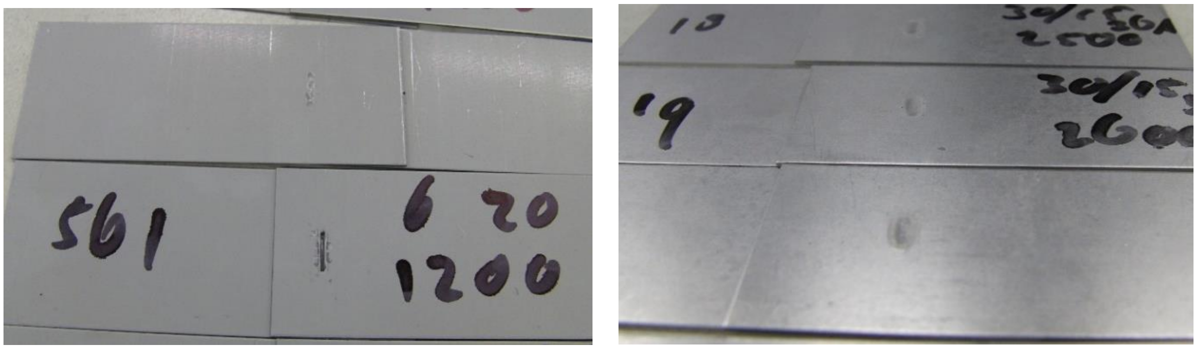

Steel samples

Aluminum samples

Figure 16.10: The results of the welded samples, both sides of the weld are depicted in the pictures.

Now that the welds have been inspected it is time for the peel and shear test to see if the weld nuggets are also similar as the samples made with the C-type. Figure 16.11 shows the results of the peel test. Both the steel and aluminum samples have made a strong bond and solid nuggets without cracks are seen.

Having inspected the weld with the peel test, it is time for the other samples to undergo the shear strength test. The test setup is shown in figure 16.12. The samples had to be clamped between two plates to make sure the samples break at the welds and not at the hole where the bolt is connected through. The results of the shear tests are found in table 16.6.

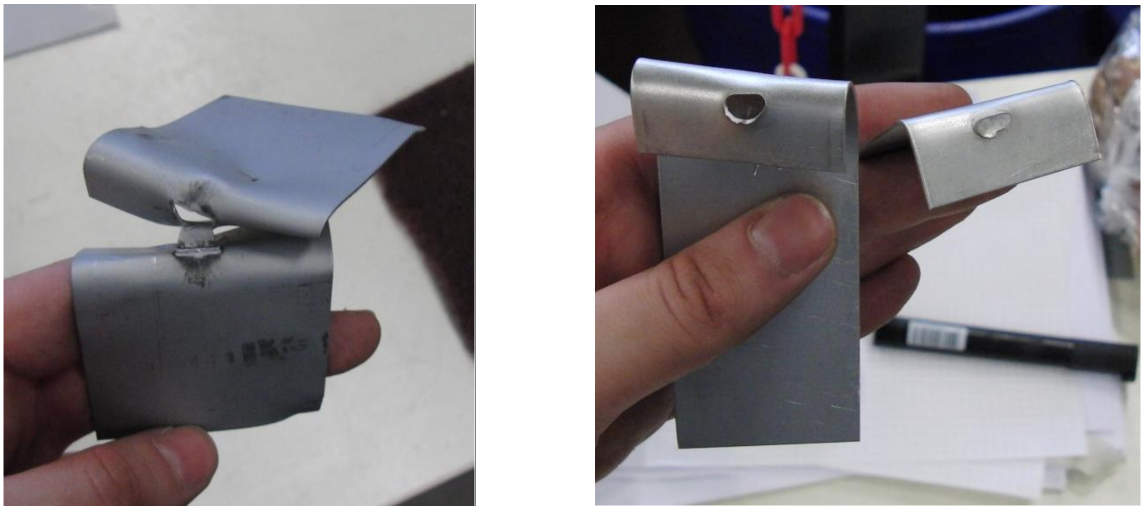

Figure 16.11: Peel test of the steel (left) and aluminum samples (right).

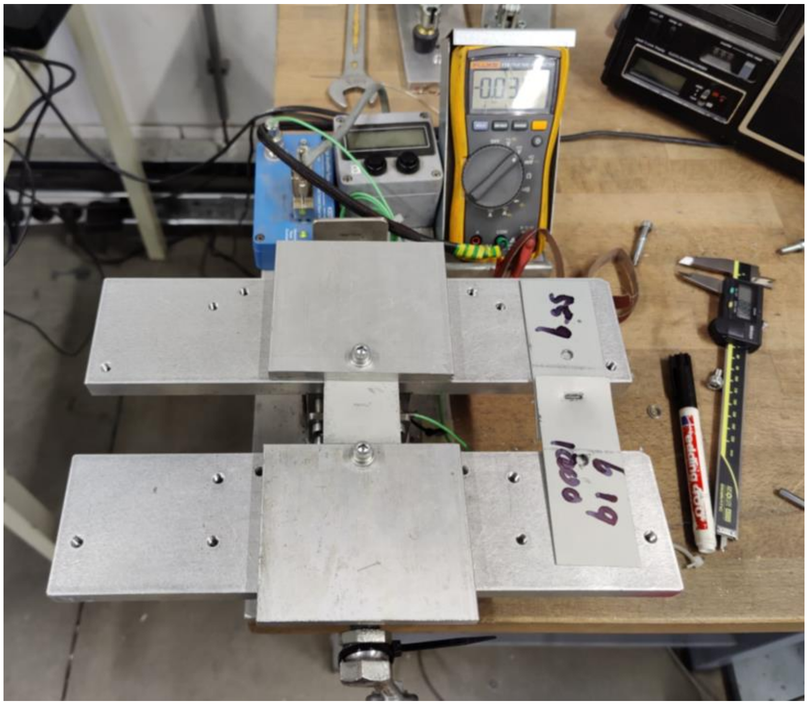

Table 16.6: Shear strength of the welded samples.

Sample	**Electrode force (N)**	**Current duration (ms)**	**Current amplitude (kA)**	**Shear strength (N)**
Steel 0.8mm	1200	6	20	4984
Steel 0.8mm	1200	6	20	5174
Steel 0.8mm	1000	6	19	4896

Steel 0.8mm	1200	6	19	4527
Steel 0.8mm	1200	6	20	5128
Steel 0.8mm	1000	6	18	4814
Steel 0.8mm	1300	6	18	4544
Aluminum 1mm	2200	25/15	28	1980
Aluminum 1mm	2500	25/15	38	1528
Aluminum 1mm	2500	25/15	38	2697
Aluminum 1mm	2500	25/15	38	2391
Aluminum 1mm	2500	30/15	40	2400
Aluminum 1mm	2500	30/15	36	2339
Aluminum 1mm	2500	30/15	36	2529
Aluminum 1.2mm	2500	30/15	40	3198

16.3 Discussion

In table 16.7, all the measured results are shown and are compared with the requirements and the theoretically calculated values. Some requirements could not be measured properly with only one displacement sensor. On top of that, the follow-up displacement results were not valid. Apart from that most measurement confirmed the theoretical models and design choices.

Table 16.7: Comparison of requirements with the theoretically determined values and the measured values.

Parameters	**Required**	**Calculated**	**Measured**
Electrode force	800-3000 N	0-3026N	0-3400N
Acceleration	>162 m/s^2	677 m/s^2	-
Suspension	ca. 200 N/mm	203.6 N/mm	200.76 N/mm
Electrode parallel misalignment	< 0.5mm	0.004 mm	-
Electrode angular misalignment	±1.5°	Upper arm: 0.121° Lower arm: 0.103° Total: 0.214°	Tot before force: 0.593° Tot after force: 0.255°
Lateral displacement	< 0.5mm	Upper arm: 0.416 mm Lower arm: 0.420 mm	Upper arm: 0.189mm Lower arm: 0.151mm
Vertical deflection	< 0.5mm	0.181 mm	-
Nugget size	9 - 9.5mm (3.5-5.5)x(7-8.5)mm		Steel: ca. 9.7mm Al.: ca.4x8mm

Tensile force	3000 - 3500N ca. 2500N	Steel: ca. 4866 N Al.: 2266 N
Indentation Marks of welding	Similar to C-type	
Drop force	Similar to C-type	

In the first experiment the maximum force and the total stiffness of the machine was tested. The maximum force was applied and it did not break the machine or deform parts it should not deform. The total stiffness is 1.4% lower than calculated, but even closer to the desired result. The total stiffness calculation made in section 15.3.1 are therefore correct. It also shows that the SolidWorks simulation software is quite accurate in regard to the calculation of the arm stiffnesses.

The measured horizontal, or lateral, displacement for both arms was well within the required precision. The mean horizontal deflection values of the upper and lower arm, 0.189mm and 0.151mm, were for better than simulated. Better SolidWorks simulation could be used next time by adding the electrode contact friction. This also means that the arm designs can be made more slender, resulting in lower moving masses. The relative misalignment due to fabrication inaccuracies or play was not measured since only one displacement sensor was available and changing the position of the one sensor would not result in accurate measurements.

The rotation of the electrodes was also measured. Although the analyzing method used, selecting points by hand, is not the most accurate method, it can be concluded that the electrode angular misalignment is within the required maximum rotation of 1.5 degrees. The measured total angular misalignment before the force buidup was 0.593° and after maximum electrode force was applied, the angular misalignment *reduced* to 0.255°. The electrodes even seem to become better aligned when electrode force is applied. The explanation is that the electrodes prefer to align with the sample instead of rotating individually.

The experiment with welding current was performed last. Both steel and aluminum samples were successfully welded. The resulting welds have a similar or even better weld strength as the welds made with the current C-type machine. The appearance of the welds was definitely good, but not yet exactly the same as the C-type welds. However, if more time is spent on finding the correct welding parameters, better looking welds could be made.

The measured drop force was not as expected. The total stiffness of the system is similar to the total stiffness of the C-type machine; hence, similar force drops were expected. However, the drop force was almost 50% higher than the drop forces measured with the C-type. It definitely seems if the suspension spring is not being used during welding. The total stiffness of just the arms is calculated and compared to the measured welding stiffness: a measured average of 340.9 N/mm compared to the calculated total arms stiffness of 354.9 N/mm.

This cannot be a coincidence. The bearings used in the design are all plain bearings, which were thought to be quite frictionless still, but when installing them they were not rotating as smoothly as hoped. The starting friction keeps the suspension spring from participating during welding. This should be solved immediately in a next version.

The results of the vertical displacement measurements did not correspond to the measurements made with the force sensor and slowmotion camera and were therefore left out of the thesis. A possible explanation is that the laser sensor was measuring a reflective surface changing in angle.

17Design conclusion

The theoretical design meets all the requirements set for the X-type. Not all the required requirements could be tested due to the lack of equipment and/or time. Of all the requirements tested, most were close or even better than simulated.

The main requirement not met is the welding stiffness. Due to the high friction in the bearings, the suspension spring is not participating during welding, causing the high drop forces measured. Luckily though, the total stiffness of the arms still make sure contact is kept between the electrodes and the metal sheets.

The welded samples were good looking welds and were similar or even stronger in the shear test, especially the steel samples. The welding parameters could still be better fine-tuned for even better results.

The X-type was also mounted on a robot and was able to make consecutive welds without losing its initial position while changing weld spots.

Recommended design changes, prioritized from high priority to low, are:

- Lower friction bearings, primarily the rotational bearings. The linear bearings seemed to work well enough
- A solid connection of the two main axis componenets
- Remove the Tox misalignment coupling which has some unwanted play
- Smaller beams for the upper and lower arms as horizontal displacement was far better than required, which was the decisive requirement for the beam design
- Add cooling system
- Better arm balance with the center of gravity at the main axis to deduce the necessary preload in the positioning spring
- Redesign position spring system with a better tested spring and a closed housing
- Motor connection balanced in the middle instead of at the head
- More space for tightening screws at the laminated shunt

18Overall conclusion and recommendations

Going back to the start of this thesis, the research question was:

> *"The design of a robot mounted far-reaching projection welding machine, using the technology of Arplas Systems, with at least similar mechanical characteristics as the current welding machine."*

The main focus was on the mechanical aspect of the welding machine with being able to weld as secondary goal. A design of a robot mounted far-reaching, or X-type, welding gun was successfully made. The mechanical characteristics of the current machine have been investigated and implemented in the design. The prototype was able to weld both steel and aluminum with similar weld strength and appearance, showing that the correct choices were made during this thesis.

Throughout the thesis all sub-questions have been answered. A literature survey resulted in a paper clearly distinguishing the different resisting welding techniques and their corresponding machines. The factors influencing weld quality were inverstigated and for the optimal machine characteristics, it was found that fast follow-up and accurate electrode alignment are most crucial for machine design.

Models were made of the current C-type machine and the machine was tested to find the machine characteristics. These results, combined with the results from the literature, were then used as requirements for the X-type.

The concept with the placement of the motor above the pivot point, the follow-up spring at the base and no misalignment tool was determined to be the best concept using multiple multi-criteria analyses. The final design of the X-type uses two dynamic arms and a positioning system to meet the electrode alignment requirements. The follow-up characteristics were calculated by making static and dynamic models of the X-type.

Theoretically, all requirements for the X-type have been met and the welding machine should therefore perform the same way as the current welding machine.

Experimentally, some requirements performed better than expected, such as the electrode alignment and total machine stiffness. The welding stiffness did not meet the requirement due to too high friction in the bearings. Even so, the machine was able to make strong welds for both steel and aluminum samples. The appearance was good and can be fine-tuned by taking time to find the best welding parameters. Follow-up acceleration was also not validated since the displacement measurement did not correspond with the measurements of force sensor and slowmotion camera.

The welding machine has also been mounted on a robot and was able to make consecutive welds without problems. High robot accelerations of the robot did not result in a contact loss of the positioning system. All in all, is the X-type welding machine quite different in design as the C-type machine, but has essentially the same mechanical characteristics.

Further research should include the influence of lower friction bearings and other small design flaws. A misalignment reduction tool could be investigated to reduce the dimensions of the arms, lowering the moving mass at the same time. To better manipulate the drop force, a spring with increasing stiffness could be investigated. The drop force could then be made equal for both steel and aluminum, making validating the weld easier. Further research of the models is also recommended to predict the machine behavior and optimize the machine characteristics. As a final recommendation, using the Fourier transform on the touching and welding response could be used to find the machine characteristics. A start was already made in this thesis but time did not allow me to finish it.

19 References

[1] E. Gauthier *et al.*, “Numerical modeling of electrode degradation during resistance spot welding using CuCrZr electrodes,” in *Journal of Materials Engineering and Performance*, 2014.

[2] Amada, “Resistance welding fundamentals.”

[3] D. Löveborn, “3D FE Simulations of Resistance Spot Welding,” KTH ROYAL INSTITUTE OF TECHNOLOGY, 2016.

[4] “Portable spot welding gun.” .

[5] “Nimak MultiframeGUN.” .

[6] W. Lucas and S. Westgate, “10 - Welding and Soldering,” in *Electrical Engineer’s Reference Book (Sixteenth Edition)*, Sixteenth., M. A. Laughton and D. J. Warne, Eds. Oxford: Newnes, 2003, pp. 10–51.

[7] P. N. Rao, *Manufacturing Technology*, no. v. 1. McGraw Hill Education, 2013.

[8] A.Goens, “Spot Welding vs. Projection Welding.” 2019.

[9] R. W. M. Association and J. F. Deffenbaugh, *Resistance Welding Manual*. Resistance Welder Manufactures assn, 2003.

[10] M. Priyanka, M. A. Kaushik, and M. Deepanjali, “Study of Projection Welding with degreasing Process on material AISI-1018,” 2016.

[11] K. Pieterman, “Method and system for real-time non-destructive testing of projection welds utilizing force sensor.” Google Patents, 2012.

[12] T. J. Bramervaer, “Method and device for manufacturing a projection weld connection for plate material.” Google Patents, 2002.

[13] H. J. Romer, M., Press, H. and Krause, “Mechanical properties of resistance spot welding machines and their mathematical determination,” *Weld. World/Soudage dans le Monde*, vol. 28, no. 9–10, pp. 190–196, 1990.

[14] Z. Chen, Y. Zhou, and N. Scotchmer, “Coatings on resistance welding electrodes to extend life,” in *SAE Technical Papers*, 2006.

[15] P. Van Rymenant, “Mechanical characterisation and modelling of resistance welding,” KU Leuven, 2010.

[16] P. Wu, “Testing and modeling of machine properties in resistance welding,” Technical University of Denmark, 2004.

[17] Y. Sakuma and H. Oikawa, “Factors to determine static strengths of spot-weld for high strength steel sheets and developments of high-strength steel sheets with strong and stable

welding characteristics," *Nippon Steel Tech. Rep.*, 2003.

[18] H. Zhang and J. Senkara, *Resistance welding: fundamentals and applications*. Boca Raton: Fla: CRC Press, 2006.

[19] N. T. Williams, "Factors influencing weldability and electrode life when welding coated steels in multi-welders and robotic cells," 1996.

[20] K. Fujimoto, S. Nakata, and M. Nishikawa, "Design and construction of loading system and its dynamic property -Optimization of loading system in high-current density spot welding (1st report)-," *Yosetsu Gakkai Ronbunshu/Quarterly J. Japan Weld. Soc.*, 1996.

[21] Titespot, "SPOT WELDING TECHNICAL INFORMATION." [Online]. Available: https://www.titespot.com/spot-welding-technical-information/ .

[22] M. Thornton, L. Han, and M. Shergold, "Progress in NDT of resistance spot welding of aluminium using ultrasonic C-scan," *NDT E Int.*, 2012.

[23] Z. Mikno, "Projection welding with pneumatic and servomechanical electrode operating force systems this research achieved an improvement in projection welding," *Weld. J.*, 2016.

[24] Z. Mikno, M. Stepien, and B. Grzesik, "Optimization of resistance welding by using electric servo actuator," *Weld. World*, 2017.

[25] O. Andersson, "Process planning of resistance spot welding," KTH Royal Institute of Technology, 2013.

[26] R. R. Patil, C. J. K. Anurag Tilak, V. Srivastava, and A. De, "Minimising electrode wear in resistance spot welding of aluminium alloys," *Sci. Technol. Weld. Join.*, 2011.

[27] M. Rashid, S. Fukumoto, J. B. Medley, J. Villafuerte, and Y. Zhou, "Influence of lubricants on electrode life in resistance spot welding of aluminum alloys," *Welding Journal (Miami, Fla)*. 2007.

[28] M. Mewborne, "AC, DC, CD or HF: Which Spot Welding Power Supply Should I Use?," 2012. [Online]. Available: http://info.amadamiyachi.com/blog/bid/164744/ac-dc-cd-or-hf-which-spot-welding-power-supply-should-i-use. [Accessed: 30-Sep-2019].

[29] H. Tang, W. Hou, S. J. Hu, H. Y. Zhang, Z. Feng, and M. Kimchi, "Influence of welding machine mechanical characteristics on the resistance spot welding process and weld quality," *Weld. J. (Miami, Fla)*, 2003.

[30] L. Dorn and P. Xu, "Influence of the mechanical properties of resistance welding machines on the quality of spot welding," *Weld. Res. Abroad*, 1994.

[31] T. Sato and J. Katayama, "Mechanical properties of spot welding machines and the effects on weld quality," *Weld. Int.*, 1988.

[32] O. Hahn, L. Budde, and D. Hanitzsch, "Investigations on the influence of the mechanical properties of spot welding tongs on the welding process," *Schweiss. und Schneiden/Welding Cut.*, 1990.

[33] H. J. Krause and B. Lehmkuhl, “Comparison of the Dynamic Mechanical Characteristics of Spot-Welding Machines.,” *Schweiss. und Schneiden/Welding Cut.*, vol. 37, no. 1, 1985.

[34] N. Ames, J. Gould, P. Denney, B. Yancey, and R. Gordon, “Advanced welding processes for the upstream oil and gas industry,” in *Proceedings of the International Offshore and Polar Engineering Conference*, 2004.

[35] “Heron.” [Online]. Available: http://heron-spotwelding.com/2-3-robotic-spot-welding-gun.html.

[36] Robot-welding, “No Title.”

[37] Tecna, “No Title.” [Online]. Available: https://tecnadirect.com/portable-welding-guns/tecna-3161/ .

[38] Prospot, “No Title.” [Online]. Available: http://www.prospot.eu/resistance-welding-machines/robot-welding-guns/screen-shot-2013-10-01-at-19-09-01/.

[39] H. Soemers, *Design principles for precision mechanisms*. 2017.

[40] “Fluid Power Actuators,” 2007. [Online]. Available: https://www.hydraulicspneumatics.com/technologies/other-technologies/article/21884185/chapter-15-fluid-power-actuators-part-1 .

[41] R. LeSar and R. LeSar, “Materials selection and design,” in *Introduction to Computational Materials Science*, 2013.

Appendix A.   Literature resistance welding

A.1 Physical aspects

Joule Heating

The first aspect is Joule heating. This is the generation of heat due to current flowing through an electrical resistance. As mentioned before, this is the physical phenomena \ac{erw} is based upon. The total heat delivered depends on the current and the resistance of the product and can be expressed with the formula:

$$Q(t) = \int_0^t I(t)R(t)dt$$

Where \$Q(t)\$ is the total heat energy delivered in \$[J]\$, \$I(t)\$ is the current sent through the electrodes in \$[A]\$, and \$R(t)\$ is the total resistance in \$[\Omega]\$. The amount of energy needed for a weld depends on the material properties, sheet thickness, and type of electrodes. Too much energy can result in a hole instead of a weld and too little energy won't produce enough heat to liquefy the metal.

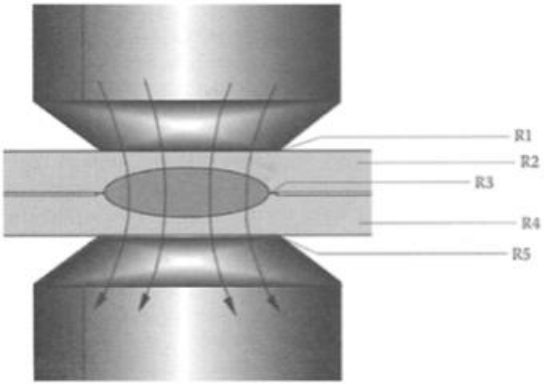

Fig 1.3: Different resistances when current flows through the electrodes by Love-born [2016]

The total resistance of a stack of sheets can be found by summing up five resistances as shown in \autoref{fig:Rtot}. \$R_1\$ and \$R_5\$ are the contact resistances between the electrode and the sheet, \$R_2\$ and \$R_4\$ are the bulk resistances of the sheets and \$R_3\$ is the contact resistance between the two metal sheets. Note that the bulk resistance of the electrode and base are neglected as they are small compared to the five before mentioned resistances. The total resistance can be calculated with:

$$R_{tot} = R_1 + R_2 + R_3 + R_4 + R_5$$

The bulk resistance of a material is determined by its electrical resistivity. This means that R_2 and R_4 depend on the resistivity with the following relation:

$$R = \frac{\rho L}{A}$$

With ρ the resistivity of the material in $[\Omega m]$, L is the thickness of a sheet in $[m]$ and A is the area the current goes through in $[m^2]$. High resistivity results in large bulk resistances.

For the contact resistances R_1, R_3 and R_5 even higher resistances will be found because of irregularities on the surfaces. These irregularities, or surface roughness, result in a smaller and discrete contact area. As current flows through a smaller area due to the discrete contact points, the resistance will increase which will generate more heat. To increase the contact area, a higher electrode force can be used although it lowers the contact resistance. This is shown in \autoref{fig:Force_roughness}.

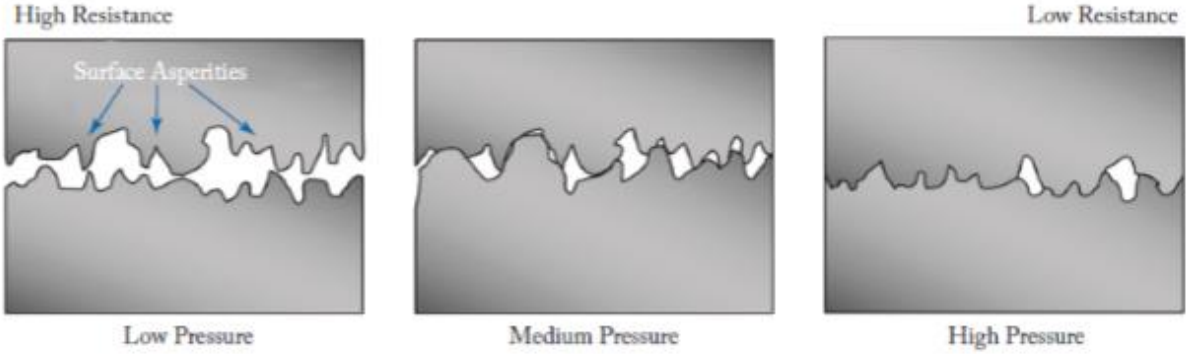

Fig1.5: The relation between electrode force and contact resistance. loveborn

The contact resistance is different for different materials contacting each other. Copper on steel has a much lower contact resistance than steel on steel, meaning that most of the heat will be generated at the contact between the steel sheets. \autoref{fig:RelativeResis} shows the relative resistances to each other. It can be seen that the contact resistances are higher than the bulk resistances and the contact resistance between the steel sheets is dominant.

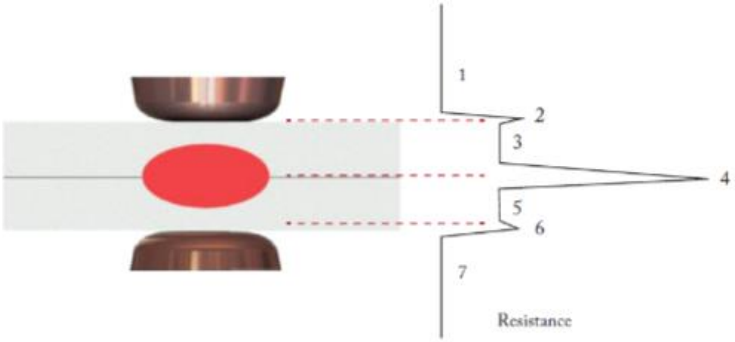

Fig 1.6: The relative resistances in resistance welding for a 2-sheet stack showing that the contact resistance between the metal sheets is relatively the highest and thus heat generation will focus there.

Dynamic resistance

\cite{Dickinson1980CHARACTERIZATIONMONITORING.} has combined all resistances and investigated the change of the total resistance throughout a welding process, or in other words the dynamic electrical resistance. He described five different phases (\autoref{fig:Dynamic_Resis}), phase \rom{01} being the surface breakdown. In this phase the surface films, oxide layers, or other contaminants will break down, causing a sharp drop in resistance.

Phase \rom{2} is where the last asperities will vanish, causing a small drop in resistance. But during this phase the contact between the metal sheets will generate heat, heating up the bulk material and the contact between them, and increasing the resistivity and resistance as was shown in \autoref{fig:ResistivityDia}.

In phase \rom{3} all all asperities are gone and the resistance increases with increasing temperature in the material. At the end of this phase the material will start to locally melt.

Multiple things are happening in phase \rom{4}, the heat is still slowly increasing and nugget formation has started. The increasing heat will still increase the resistance, but as the molten region grows, the contact area increases which decreases the resistance. Moreover, softening causes a mechanical collapse, shortening the distance the current has to travel as the electrodes come closer, also decreasing the resistance. At the β-peak the temperature is stabilizing and the nugget formation and mechanical collapse will start to dominate, decreasing the resistance.

In phase \rom{5} the resistance will drop further due to softening and nugget formation. As soon as the nugget has grown to a size that the surrounding material cannot contain it, the expulsion will occur.

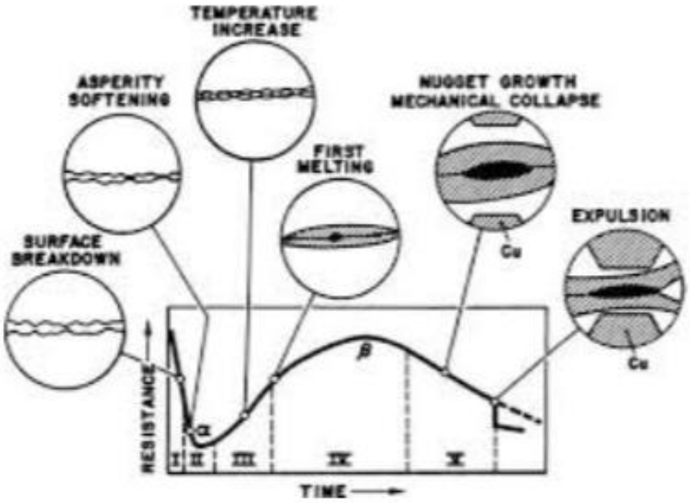
TEMPERATURE INCREASE
ASPERITY SOFTENING
NUGGET GROWTH MECHANICAL COLLAPSE
FIRST MELTING
EXPULSION
SURFACE BREAKDOWN
Cu
Cu
β
α
RESISTANCE
I
II
III
IV
V
TIME

Fig 1.7: The change in total resistance during a weld cycle.

The resistivity also changes during the welding process as can be seen in \autoref{fig:ResistivityDia}.

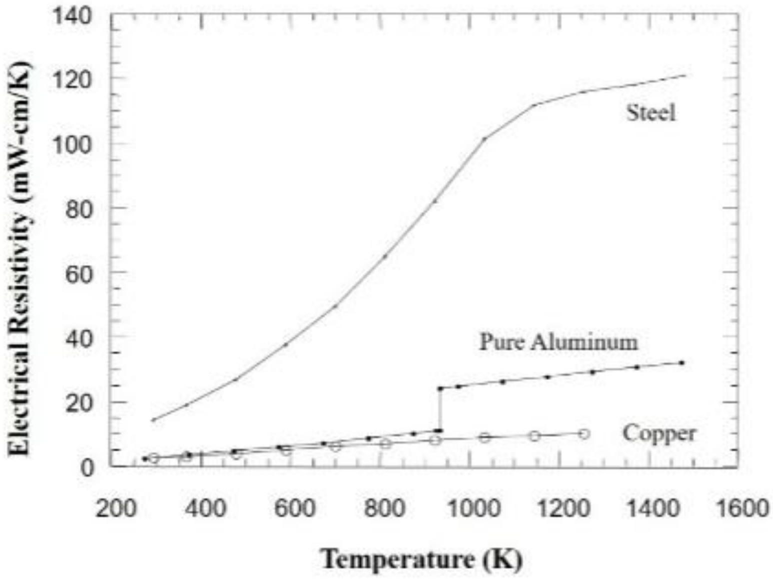

Fig 1.4: Diagram showing the electric resistivity changing with temperature for different materials. [sakuma en oikawa

Peltier effect

When welding two conductors with different materials, the Peltier effect can be observed. This thermoelectric effect is caused by a difference in Fermi levels, which makes the electrons change orbits. A current sent through the thermocouple will either generate or lose heat depending on the direction of the current (\cite{Li2015}). The equation for the generation or loss of heat energy is:

$$Q_p(t) = \int_0^t I(t)\,(\Pi_A - \Pi_B)\,dt$$

Where $Q_p(t)$ is the heat energy caused by the Peltier effect, $I(t)$ is the current, and Π_A and Π_B are the Fermi levels of the two materials.

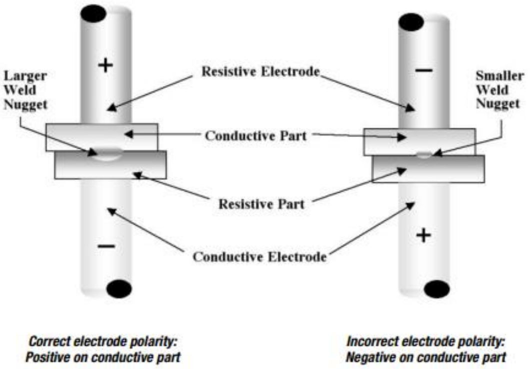
Larger Weld Nugget
+
Resistive Electrode
−
Smaller Weld Nugget
Conductive Part
Resistive Part
−
+
Conductive Electrode
Correct electrode polarity: Positive on conductive part
Incorrect electrode polarity: Negative on conductive part

Fig : Peltier effect either increasing or decreasing temperature.

A.2 Welding equipment

Welding gun

Table below shows the comparison between the automated and stationary welding guns (Uralath).

Table 2.1: Comparison between an automated and a stationary welding gun.

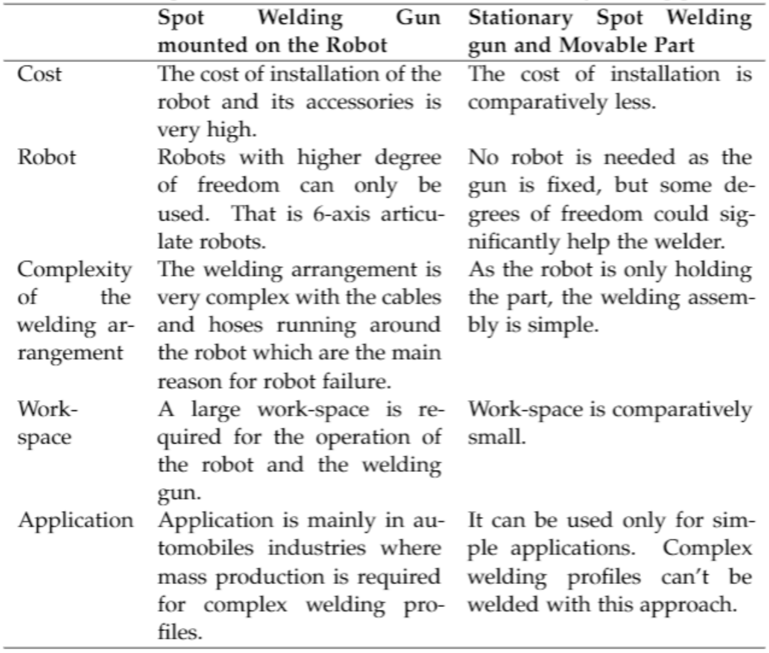

	Spot Welding Gun mounted on the Robot	**Stationary Spot Welding gun and Movable Part**
Cost	The cost of installation of the robot and its accessories is very high.	The cost of installation is comparatively less.
Robot	Robots with higher degree of freedom can only be used. That is 6-axis articulate robots.	No robot is needed as the gun is fixed, but some degrees of freedom could significantly help the welder.
Complexity of the welding arrangement	The welding arrangement is very complex with the cables and hoses running around the robot which are the main reason for robot failure.	As the robot is only holding the part, the welding assembly is simple.
Work-space	A large work-space is required for the operation of the robot and the welding gun.	Work-space is comparatively small.
Application	Application is mainly in automobiles industries where mass production is required for complex welding profiles.	It can be used only for simple applications. Complex welding profiles can't be welded with this approach.

Electrode

The electrodes are used to conduct the welding current to the workpiece, to be the focal point of the pressure applied to the weld joint, to conduct heat from the work surface, and to maintain their integrity of shape and characteristics of thermal and electrical conductivity under working conditions. Most electrodes are copper-based alloys, which are a great thermal and electrical conductor. Other types also exist like refractory metal electrodes having a mixture of copper and tungsten for high pressure and temperatures, but are generally not applicable in RSW.

The shape of the tip can also directly influence the shape and quality of the weld. Some common shapes can be seen in figure. The diameter of the electrodes should be chosen depending on the thickness of the workpiece with the rule of thumb d = 5t with t the thickness of one of the sheets \citep{Zhang2006}.

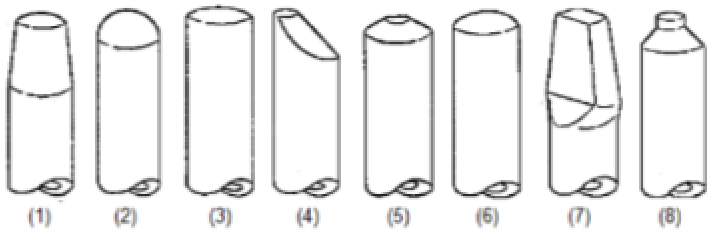

Fig: Different shapes of electrode tips.

Electrode degradation is also an important aspect of weld quality. With each welding cycle, the tip of the electrode is being affected by the heat and alloying with the workpiece. Softening, recrystallization, alloy formation, tip diameter growth and pitting are all types of degradation.

Softening happens when the electrode is heated multiple times in quick succession. The electrode will deform and increase in diameter because of the softening. In \autoref{fig:ElecWear} can be seen what a severely pitted electrode looks like \citep{Andersson2013}.

Fig : Example of electrode with heavy wear.

Recrystallization refers to the metallurgical process when the electrode reaches higher temperatures. Zinc in the workpiece can form an alloy with the copper at the tips of the electrode, creating a thin brass layer.

Due to the previous mentioned degradations the tip of the electrode can become uneven, resulting in pitting which increases the chance of expulsion \citep{Andersson2013}.

To reduce the degradation multiple solutions have been proposed. Electrode dressing is a maintenance method removing the top layer of the electrode containing the alloyed material. Electrode dressing can significantly increase the electrode life especially when welding aluminum sheets \cite{International2006}. Normally $10~\mu m$ to $0.1~mm$ is removed from the tip.

Adding a coating to the electrode can also significantly increase the lifetime, although specific coatings are needed for different materials. For example a $Ni - TiC_P/Ni - Ni$ coating significantly increased the electrode life for welding zinc coated steels \cite{Chen2006} and \cite{Patil2011} showed that a carbon black paste in fluidic form between the electrode-sheet interface could double the electrode life when welding aluminum.

Adding lubrication could also increase the lifetime as it reduces the thickness of the oxide layer on aluminum, decreasing the temperature between the electrode-sheet interface \citep{Rashid2007}.

A.3 Weld quality and inspection

\autoref{fig:NuggetSizevsTens} shows the relation between nugget size and its tensile strength \citep{Sakuma2003}. As can be seen in the figure increases the shear strength when the nugget size increases. Although most companies have a their own standard for nugget size, it is customary to have a nugget size of $3.5\sqrt{h}-5\sqrt{h}$ where h is the height of a sheet stack-up \citep{Zhang2006}.

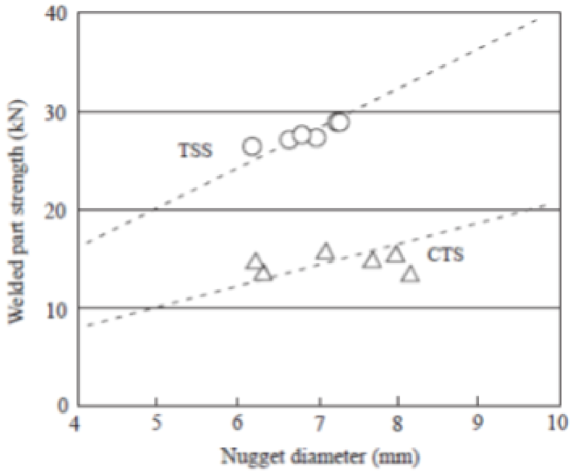

Fig 1.18: Relationship between nugget diameter and weld strength in two $1.8~mm$ thick $780~MPa$ cold-rolled steel sheets in both tensile shear strength (TSS) and cross tensile strength (CTS) \citep{Sakuma2003}.

All weld inspection techniques

Peel test

The peel test can be done with a roller or a pliers which removes one sheet to make the weld button visible. \autoref{fig:peeltest} shows how one sheet can be peeled loose to examine the weld button. The average of the maximum and minimum diameter is used for the quality control of the weld.

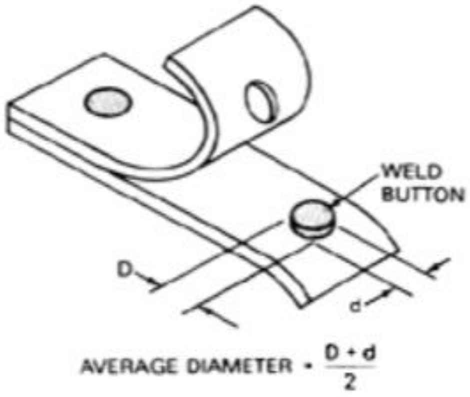

[titespot]

Chisel test

The chisel test is a simple test to measure the average diameter of a nugget. The chisel test is done with a chisel and is categorized as a destructive test. A chisel is driven between the sheets until fracture occurs. \autoref{fig:chiseltest} shows how a chisel test is performed. The goal is to remove one sheet of the sheet stack-up and examine the weld button as can be seen in \autoref{fig:peeltest}. From this diameter conclusions can be made about the quality of the weld.

A (partly) non-destructive method has also been used where the chisel is driven between the sheets until yielding or bending occurs. When no fractures are present in the sheets after driving the chisel between the sheets, the weld has been qualified as a good weld and the sheets are restored to their original shape.

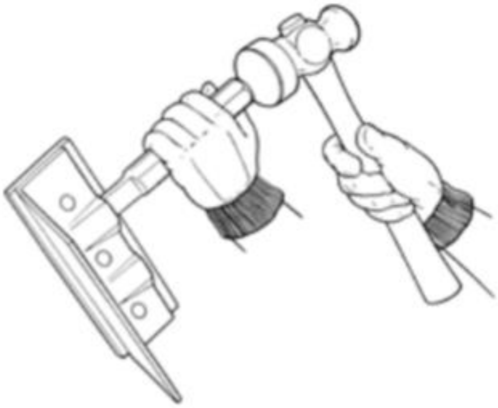

Fig 1.19: Chisel test [titespot]

Metallographic testing

A metallographic test is performed to inspect the weld for voids and cracks in the \ac{HAZ}. The welded part is cut exactly through the center of the weld and is polished. The weld can then be examined. \autoref{fig:NuggetwithCracks} shows a nugget cut through the center and some cracks and a void can be seen \citep{Tolf2015ChallengesIR}.

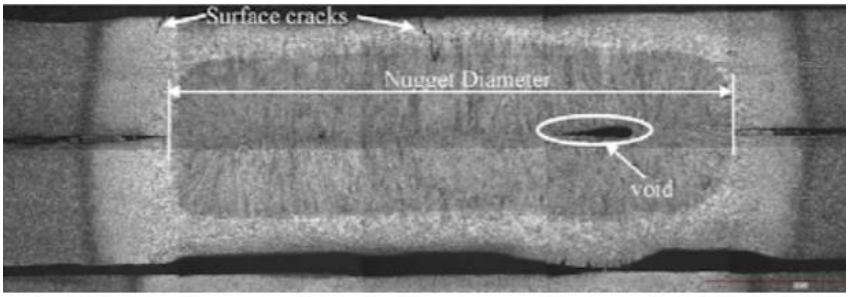

Non-destructive testing

There are multiple ways to inspect a weld with \ac{NDT}. Some of the more common examples are \ac{UT}, \ac{VT}, \ac{PT} and \ac{RT}. In the automotive industry \ac{UT} is generally used for \ac{NDT} \citep{Thornton2012}.

\ac{UT} is a method where ultrasonic sound waves are sent through a material and the timestamps that a wave returns is measured. The sound waves are reflected when the material properties of the medium suddenly changes. This way the nugget size, penetration, and the location of cracks or voids can be measured. \ac{UT} has the advantages of keeping the welded part intact and the process can be automated. The disadvantage is that complex geometries are hard to test with this method.

Weld control acoustic emission can be used to verify the completion of a weld by measuring the acoustic emission of the liquefying metal during welding \cite{Broomhead1990}. A metal emits sound waves when the internal stress changes. This can be measured to find the location of defects.

https://accendoreliability.com/non-destructive-testing-welds/

A.4 Factors influencing weld quality

Krause and Lehmkuhl [] studied the machine parts influencing the dynamic mechanical properties of a spot welding gun, shown in Table 2.1. Their purpose was to define and standardize the machine parts, making it possible to optimize the machine properties by assessing the individual components and their contribution. The results, from back in 1984, are still included in the ISO 669 standards.

They stated that a resistance welding machine is a vibrating system with masses, spring constants and damping effects. Forces that apply during electrode contacting and electrode follow up lead to deformations of several machine components.

Table 2.1 : Factors influencing dynamic machine properties []

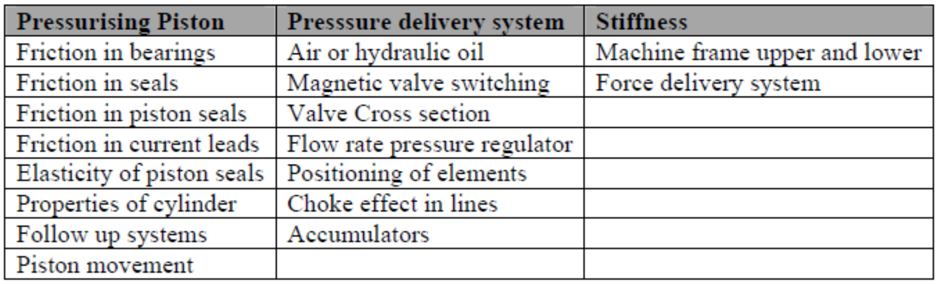

Pressurising Piston	Presssure delivery system	Stiffness
Friction in bearings	Air or hydraulic oil	Machine frame upper and lower
Friction in seals	Magnetic valve switching	Force delivery system
Friction in piston seals	Valve Cross section	
Friction in current leads	Flow rate pressure regulator	
Elasticity of piston seals	Positioning of elements	
Properties of cylinder	Choke effect in lines	
Follow up systems	Accumulators	
Piston movement		

Hahn et al [] developed an experimental spot welding gun to change the machine properties and studied the influence of changing the moving mass of the electrode arms, machine stiffness, friction and force system. Conclusions were based on the nugget diameter and tensile strength of the weld. Their main conclusions:

- Changes in the moving mass and stiffness of the electrode arms significantly influence the static mechanical properties and dynamic touching behavior
- With spot welding guns, the bending of the electrode arms primarily influences follow-up. Therefore, moving mass has a lower impact on follow-up behavior below the splash limit,

but it was found that lower moving mass and lower stiffness resulted in a reduction of scatter of the strength value.

- A hydraulic actuator stabilizes the force faster during touching and follow-up, and has a lower peak force, due to their lower mass and higher damping.

Satoh et al [sato] studied the difference in the four types of spot welding configurations shown in fig.. . The main conclusions were:

- In all cases, moving mass exerted little effect on the nugget diameter
- In type A, the influence of friction is considerable
- When the electrode arms have low rigidity (types B, C, and D), the influence of friction is small
- Electrode life is dependent on impact energy, which is influenced by the moving mass, friction and stiffness.
- It was noticed that when rigidity was low (types B, C, and D) moving mass and friction had less effect on the electrode life. This was explained as the low rigidity absorbing the other effects.
- In types C and D the nugget has a more elliptical shape.

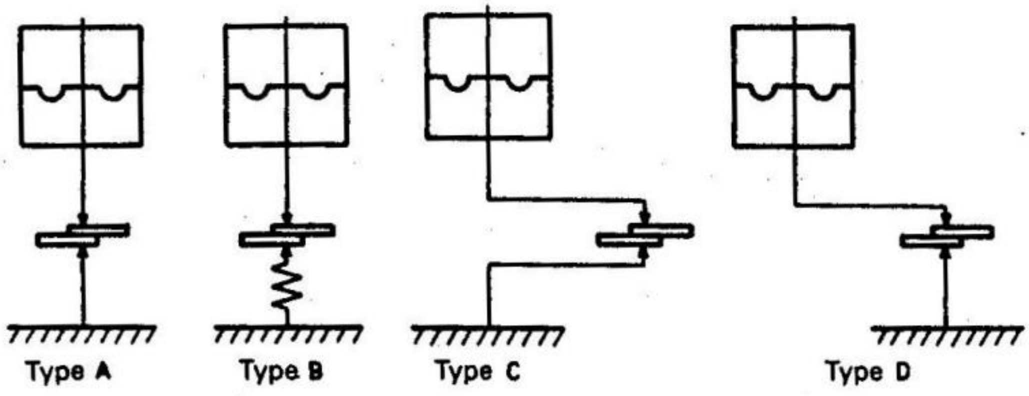

Fig: Four different weld gun configurations. Type A: Direct electrode force and high rigidity of lower electrode; Type B: Direct electrode and low rigidity of lower electrode; Type C: Indirect electrode force and low rigidity in both upper and lower electrode arms; Type D: Direct electrode force and different rigidity in upper and lower electrode arms; []

Dorn and Xu [] built a spot welding simulation device to study the individual influence of each machine property. Conclusions of this study were:

- The influence of machine properties is very complex. Trade-offs have to be made to optimize both touching and follow-up behavior.

- Lower stiffness of the lower electrode arm improves contact and follow-up behavior (short oscillations of electrode force), but increases bouncing effects
- Low friction worsens contacting, but improves follow-up.
- Low moving mass has no clear influence on weld quality or follow-up, but improves contacting.
- Stiffness and friction have the most significant influence on weld quality. This is due to the change in mean electrode force during follow-up.

Tang et al [] also studied the influence of the mechanical machine characteristics. They analyzed the influence of stiffness, friction and moving mass by adding springs, a friction element and additional masses. They also investigated the bending of the electrode arms and the resulting electrode misalignment. The weld quality was based on tensile strength of the weld. The main results of the study:

- High stiffness reduces electrode misalignment.
- The expulsion limit increases with an increasing stiffness.
- Higher stiffness also increases the forging effect after follow-up.
- Friction is generally unfavorable for the weld quality and should be minimized
- Moving mass has no significant influence on weld quality and to improve electrode life, should be minimized in order to reduce the impact at touching.

Williams et al [] noticed cyclic variations in the force while welding with AC current. Williams attributed these cyclic forces to electromagnetic attraction and repulsion. They estimated these forces with the Lorentz force equation:

$$F = \frac{\mu \ I_1 \ I_2 \ L}{2\pi \ a} \, [\mathrm{Nm}^{-1}]$$

With $\mu = 4\pi$ e-7, $I_1 = I_2$, L the throat length and a the distance between the electrode arms. Fujimoto et al confirmed the observations made by Williams []. Fujimoto et al mentioned that these variations in force adversely affect the welding process and depend on the machine characteristics.

Wu et al [wu not electric] investigated these Lorentz forces as well. He made a schematic overview of the secondary circuit path, shown in figure .. a and made a simplified model of this circuit (fig .. b). Wu used this model to calculate the Lorentz forces present in the system.

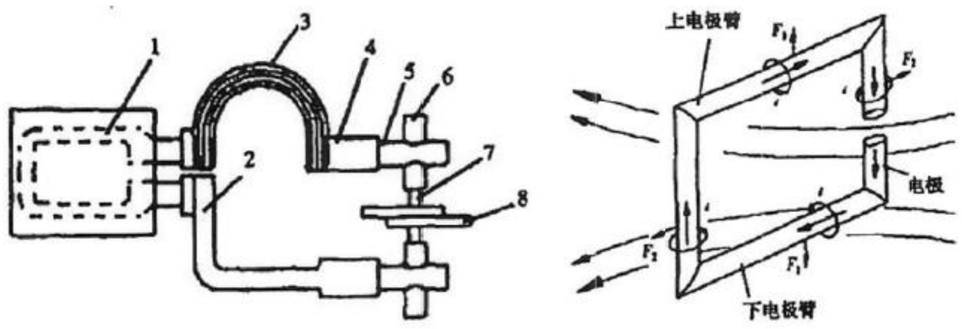
1
2
3
4
5
6
7
8
上电极臂
F_1
F_2
电极
下电极臂

Fig: Schematic representation of the Lorentz forces in a welding machine.

A.5 Modelling of welding machines

Römer, Press and Krause [] were the first to make a mathematical model of the welding process. They wanted to find the main influencing machine parameters before, during and after welding. A mass-spring-damper system was used to model the welding machine with a C-type frame.

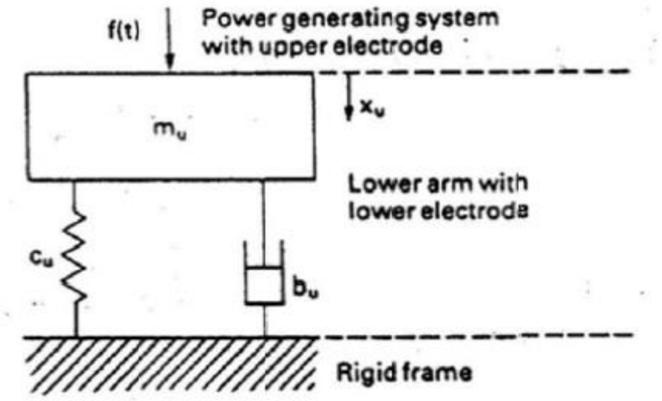
f(t)
Power generating system with upper electrode
x_u
m_u
Lower arm with lower electrode
c_u
b_u
Rigid frame

Fig: Mass-spring-damper model of a lower arm of a welding gun.

They assumed that when the electrodes touch, vibrations are induced as a shock function. The differential equation describing the response of the weld head becomes

$$m_u\ddot{x}_u + b_u\dot{x}_u + c_u x_u = f(t)$$

Giving the theoretical solution for touching behavior as

$$x_u = \frac{I}{m_o\omega} e^{-D_u t}.\sin\omega t \quad \text{and with } D_u = \frac{b_u}{2\,m_u}$$

Solving the differential equation for the welding/follow-up behavior gives:

$$x_o(t) = \frac{F_o}{4\, m_o\, D_o^2}\,[2D_o\, t - (1 - e^{-2D_o t})] \quad \text{with } D_o = \frac{b_o}{2m_o}$$

Using these solutions, theoretical optimal values can be determined for both touching and follow-up. Table 2.2 summarizes these optimal values and especially for the lower electrode, the results are sometimes contradictory meaning trade-offs have to be made.

Table 2.2: Theoretical best mass, damping and stiffnesses for upper and lower electrode.

Approach and contacting		Electrode follow-up	
Lower electrode	Upper electrode	Lower electrode	Upper electrode
Mass m_l low	Mass m_u low	Mass m_l low	Mass m_u low
Damping ζ_l low	Damping ζ_u high	Damping ζ_l high	Damping ζ_u high
Stiffness c_l low	Contact velocity v_a constant	Stiffness c_l high	

Chen et al [] made a Simulink model (fig ..) and used displacement and force measurements to calculate the machine characteristics. Although the machine had to be taken apart and all parts had to be weighted to find the lumped mass, the way of modeling and calculating the stiffness and damping factor is very interesting. Experiments also validated his approach.

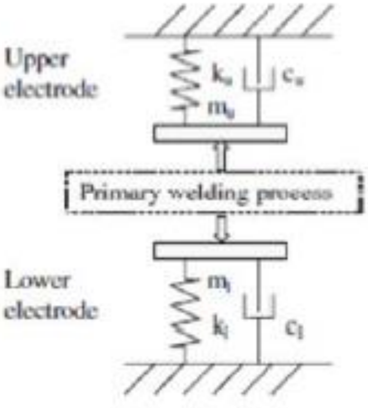

Rymenant et al [] modeled and tested multiple resistance welding guns, one of them a spot/projection welding gun with a spring coupling between the actuator piston and the moving mass. This spring reduces the mass needed to accelerate during follow-up, but introduces another spring constant in the model. The new model made by Rymenant is shown in figure.. .

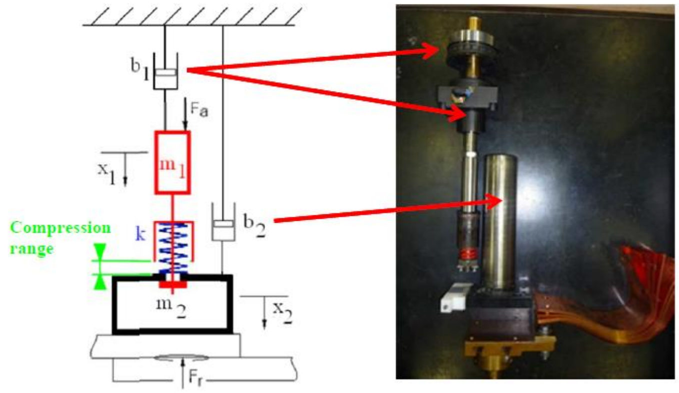

This kind of setup, with a coupling spring, is recommended in applications where follow-up is important, which is especially relevant for projection welding guns.

https://lirias.kuleuven.be/1925825?limo=0

A.6 Machine characteristic test methods

[Rymenant] and [Wu] developed two methods to measure the machine characteristics called the free fracture test and the explosion test. These tests are meant to find the in-situ machine characteristics without disassembling the whole machine and weighing/testing the individual parts. Both tests measure the force in the lower weld head and the relative displacement between the electrodes.

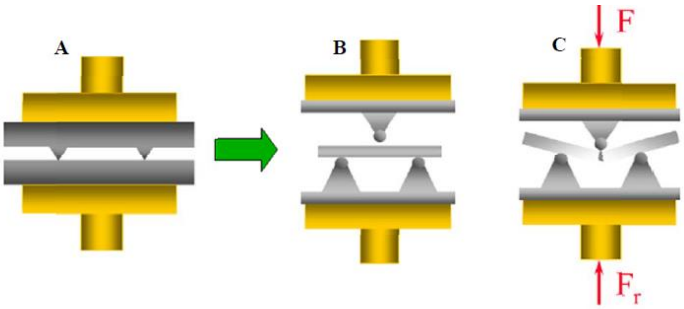

Fig: Free fracture test. A shows a regular projection weld. B and C show how a free fall is simulated by adding a rod made to break at a certain force.

In the free fracture test, shown in fig , a rod with the property of fracturing at a certain force is used to analyze the free fall of the upper weld head after fracturing. During a free fall, the reaction forces Fr become zero for a short time. Thus the machine characteristics can be calculated by solving eq. … .

$$m\frac{d^2x}{dt^2}+b\frac{dx}{dt}+kx=F-F_r$$

where m is the mass, b is the damping, k the stiffness, x is the relative displacement between the upper and lower electrode, and F the force. [Wu] studied the free breaking test and to find the machine characteristics, he used the time interval where the reaction force has dropped and solved the numeric matrix representation (eq …) in that time interval.

$$\begin{bmatrix} \ddot{x}_1\dot{x}_1x_1 \\ \ddot{x}_2\dot{x}_2x_2 \\ \cdots\ \cdots\ \cdots \\ \ddot{x}_n\dot{x}_nx_n \end{bmatrix} \begin{Bmatrix} m \\ b \\ k \end{Bmatrix} = \begin{Bmatrix} F \\ F \\ \cdots \\ F \end{Bmatrix},\ [A]\cdot\begin{Bmatrix} m \\ b \\ k \end{Bmatrix} = [F]$$

The explosion test, shown in fig \ref{} , is similar to the free fracture test but instead of a rod that fractures, a small ball or button is placed between the electrodes. The ball or button has similar height to the projection height and explodes after the current is applied. The explosion results in a free fall of the upper weld head, simulating a step response. Rymenant determined the mechanical characteristics by analyzing the step response with eq. \ref{} .

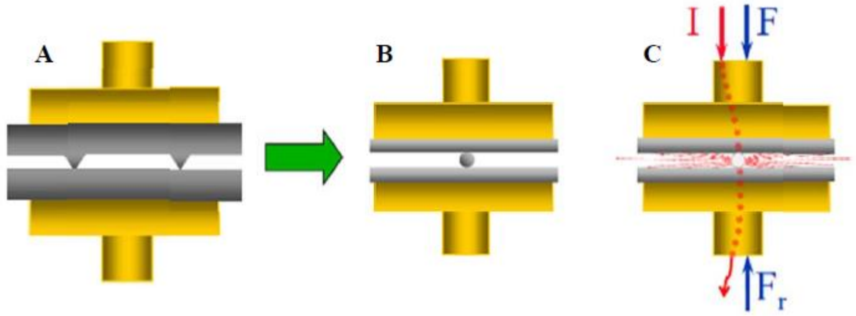

Figure 5-13 Operation principle of explosion test, A, B and C

Fig: Explosion test. A shows a regular projection weld. B and C show how a free fall is simulated by sending current through a small sphere or button. This sacrificial sphere "explodes" due to the high current and heat generation.

$$x(t)=\frac{F_a(t)\cdot m}{b^2}\cdot\left(e^{-\frac{b}{m}t}+\frac{b}{m}\cdot t-1\right)$$

$$v_{th}(t)=-\frac{F_{fracture}}{b}\cdot\left(e^{-\frac{b}{m}t}-1\right)$$

Appendix B. Concept phase

B.1 Concept generation

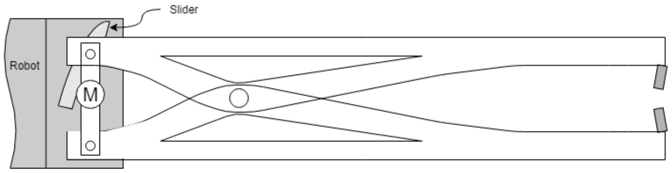
Slider
Robot
M

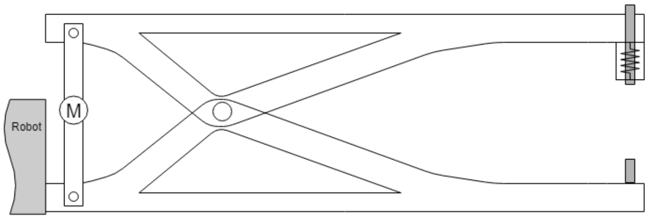

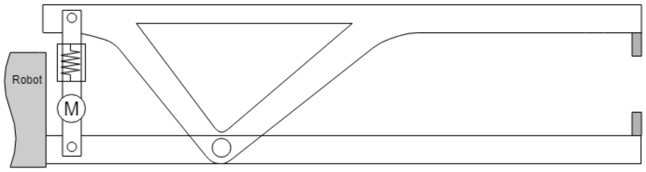

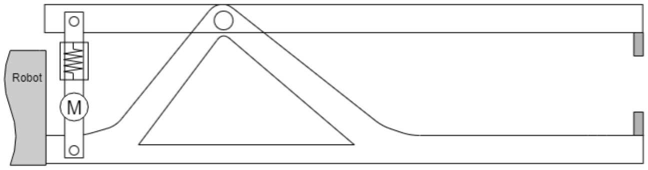

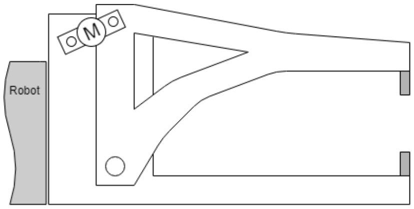

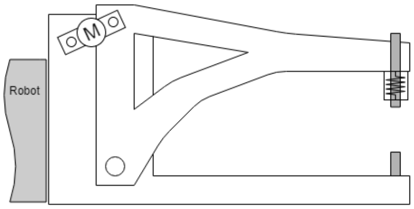

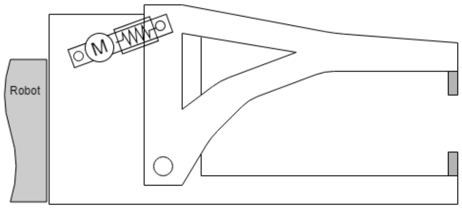

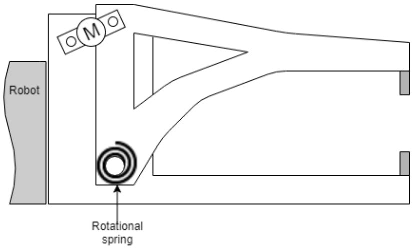
M
Robot
Rotational spring

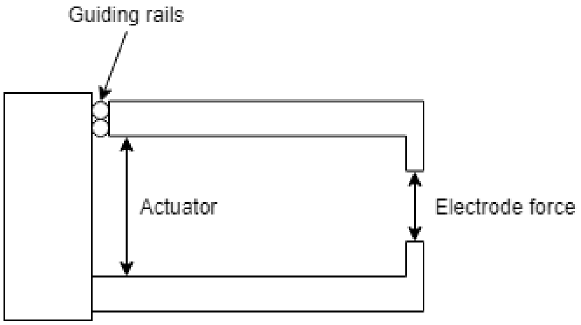
Guiding rails
Actuator
Electrode force

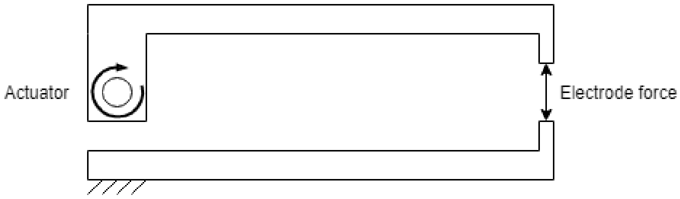
Actuator
Electrode force

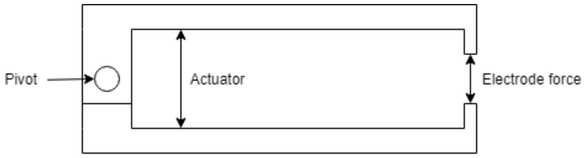
Pivot
Actuator
Electrode force

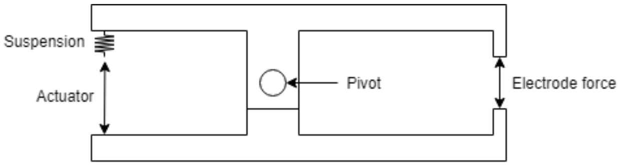
Suspension
Actuator
Pivot
Electrode force

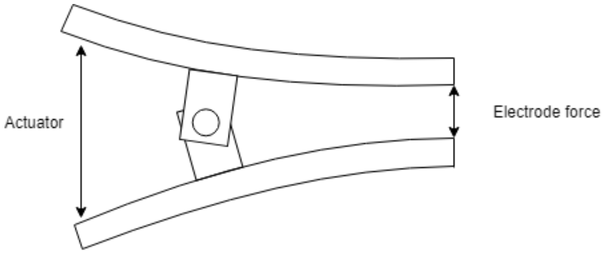
Actuator
Electrode force

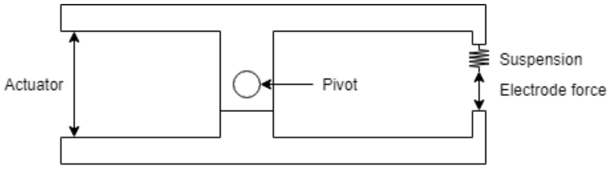
Actuator
Pivot
Suspension
Electrode force

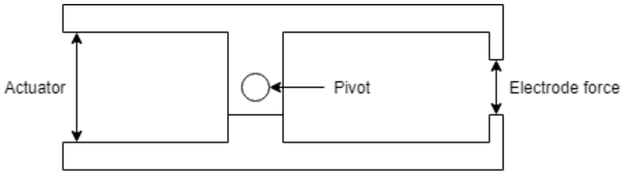
Actuator
Pivot
Electrode force

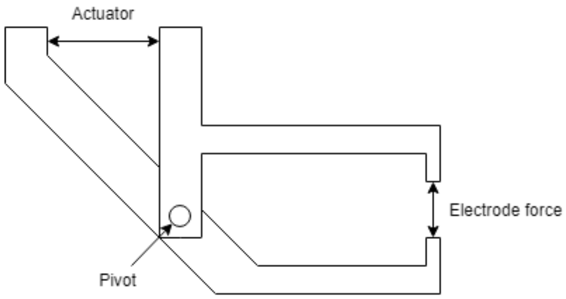
Actuator
Electrode force
Pivot

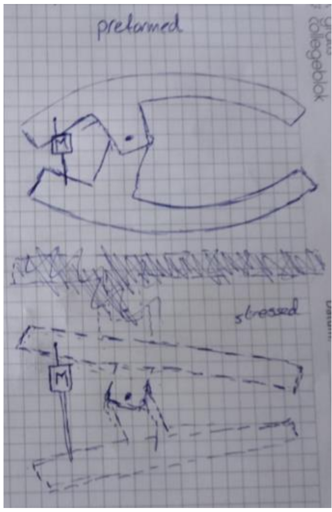
preformed
M
stressed
M

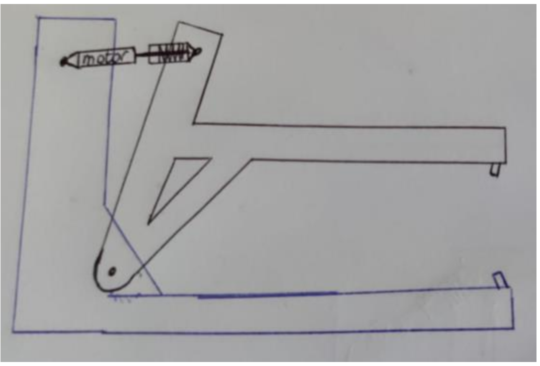

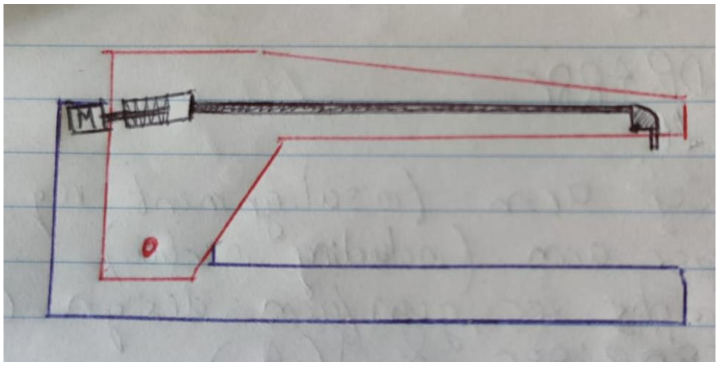

B.2 Concept selection

Strength potential calculations

Slider has high friction because of rails

Stiffness:

for a = b

Xtop and side th_L = P*a*b/(6EI)

at pivot Th_L = M*b/(6EI) = P*b^2/(6EI)

V: th_L = P*a*b*(L+a)/(6EI)

Slider: th_L = P*b^2/(2EI)

Appendix C. Detailed design

C.1 Motor selection

Mainly pneumatic and servo actuation is used as they provide high force in a short time. Pneumatic systems were popular back in the days, but servo actuation has become faster, more exact, produce less noise and has the ability to use force-control. The weld quality also increases significantly when using servo actuation, creating uniform nuggets more efficiently \citep{Mikno2016}, \citep{Mikno2017}.

Servo vs pneumatic:

Advantages resulting from the use of the electric servo system are (i) no need for a compressed air system, (ii) the reduction of noise and (iii) significantly faster travel of electrodes.

However, the use of the servo operating force system requires that the operating personnel perform additional preparatory activities before welding, i.e. (i) adjusting the geometrical zero of electrodes after each exchange and refurbishment of electrode terminals and (ii) creating the table of calibration, i.e. correlation between the servo actuator input current and the actual force of welding machine electrodes. [mikno]

Robots need linear motion control to close and open the weld tips at precise position with exact pressure. Pneumatic actuators have been popularly used. But due to the problems of consistency, weld quality and speed they have been replaced by electric servo actuators. A servomotor is attached to the servo actuator for adjusting the pressure applied to the work through movement of the movable welding electrode. It provides a better welding performance and quality, which is made possible by accurate control of position and torque. Control instruction send by the servo controller, which is part of the robot controller, drives the servo motor at a velocity and torque predefined by robotic programs

Electric:

- More consistent and accurate
- Fast response & cycle time
- Higher weld quality (due to better control?)
- Less noise
- Can generate extremely high forces
- More accurate force *and* position control
- Needs continuous recalibrating (?)
- Expensive investment but low operating cost

Pneumatic:

- Cheaper, but more maintenance
- Easier control, though only pressure/force control
- Higher power density
- Can achieve high speeds
- Dependent on availability of pressurized air or needs a compressor
- Air is compressible so less accurate and repeatable
- More prone to overshooting position and longer oscillation in open loop

	Dynamic response	Force/Torque cap.	Power density	Size	Complexity	Gear needed?	Control
Pneumatic	+	+	3	3	2	no	--
Hydraulic	-	++	5	5	1	no	+
PM DC	-		4	1	3	yes	+
Brushless DC/ Synchr AC				3	5	yes	-
induction AC				3	4	yes	/
Stepper				2	2	yes	++

C.2 Power source

The power source supplies the welding gun with the current needed for welding. \ac{AC} sources take energy directly from the power line and are commonly used for general-purpose welding machines. An \ac{AC} power supply can deliver high-energy output, but line voltage fluctuations can affect the weld quality. Also the control is less accurate (50Hz vs >1kHz for MFDC or HFDC).

\ac{DC} power sources have a capacitor bank, which is charged up, and the welding energy is released through a bank of transistors. The rise time can be extremely quick resulting in rise times up to \$0.01~ms\$. Moreover, a \ac{DC} power source is excellent in low energy control, making it especially useful for welding wires and thin foils \citep{Mewborne2012}.

\ac{MFDC} and \ac{HFDC} power sources use a pulse width modulator to convert the 3-phase direct line \ac{AC} to rectified \ac{DC}. This increases the rise time to almost the same as a \ac{DC} supply and is therefore highly used in the automated industry. \cite{Li2005} even suggests that \ac{MFDC} power sources are approximately 42\% more energy efficient than \ac{AC} power sources.

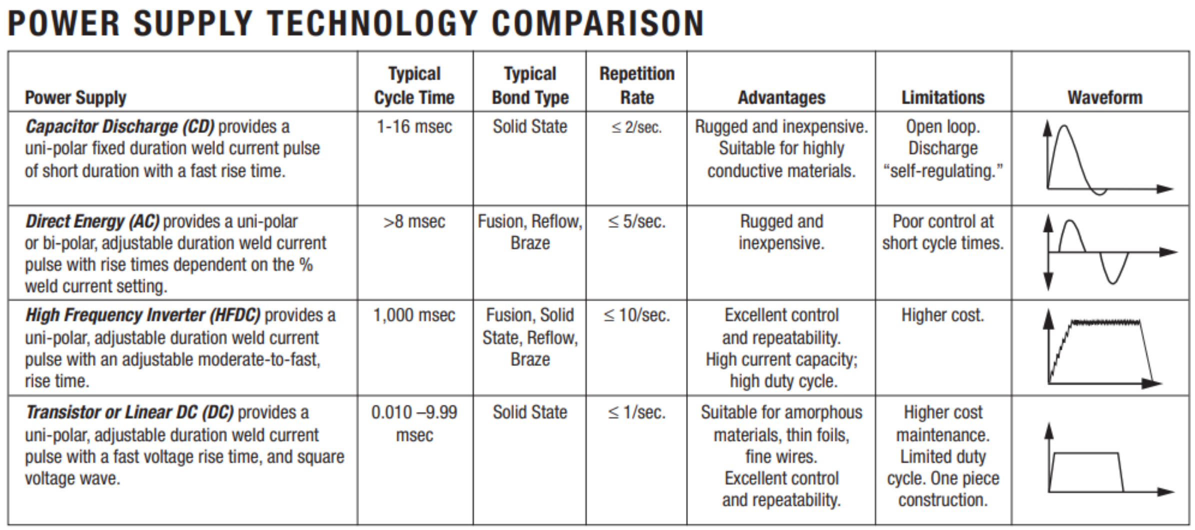

POWER SUPPLY TECHNOLOGY COMPARISON

Power Supply	Typical Cycle Time	Typical Bond Type	Repetition Rate	Advantages	Limitations	Waveform
Capacitor Discharge (CD) provides a uni-polar fixed duration weld current pulse of short duration with a fast rise time.	1-16 msec	Solid State	≤ 2/sec.	Rugged and inexpensive. Suitable for highly conductive materials.	Open loop. Discharge "self-regulating."	
Direct Energy (AC) provides a uni-polar or bi-polar, adjustable duration weld current pulse with rise times dependent on the % weld current setting.	>8 msec	Fusion, Reflow, Braze	≤ 5/sec.	Rugged and inexpensive.	Poor control at short cycle times.	
High Frequency Inverter (HFDC) provides a uni-polar, adjustable duration weld current pulse with an adjustable moderate-to-fast, rise time.	1,000 msec	Fusion, Solid State, Reflow, Braze	≤ 10/sec.	Excellent control and repeatability. High current capacity; high duty cycle.	Higher cost.	
Transistor or Linear DC (DC) provides a uni-polar, adjustable duration weld current pulse with a fast voltage rise time, and square voltage wave.	0.010 –9.99 msec	Solid State	≤ 1/sec.	Suitable for amorphous materials, thin foils, fine wires. Excellent control and repeatability.	Higher cost maintenance. Limited duty cycle. One piece construction.	

http://www.amadamiyachi.com/servlet/servlet.FileDownload?retURL=%2Fapex%2Feducationalresources_articles&file=01530000000Jybm

[amada]

C.3 Spring selection

Disc spring design ultimate handbook: http://www.industrialbearings.com.au/uploads/catalogs/schnorrhandbook_1343111178.pdf

[Schnorr

More linear behavior as h/t becomes closer to zero. As linear perforce is important for this application, careful selection of the disc spring should be taken into account.

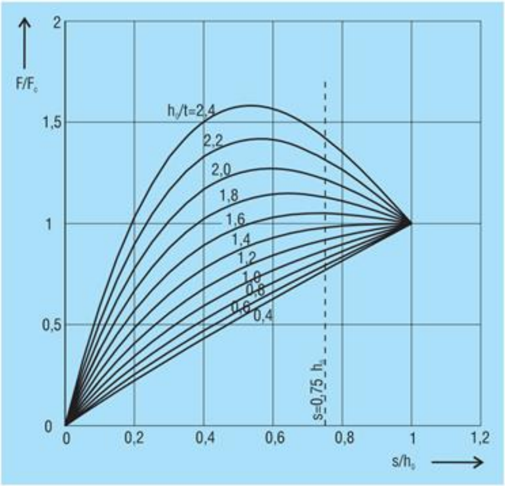

Guiding clearance is also necessary to keep the disc springs correctly stacked. Inner guidance is preferred. Table .. shows the guiding clearance for different sizes of disc springs.

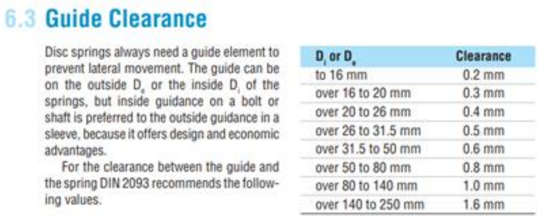

6.3 Guide Clearance

Disc springs always need a guide element to prevent lateral movement. The guide can be on the outside D_e or the inside D_i of the springs, but inside guidance on a bolt or shaft is preferred to the outside guidance in a sleeve, because it offers design and economic advantages.

For the clearance between the guide and the spring DIN 2093 recommends the following values.

D_i or D_e	Clearance
to 16 mm	0.2 mm
over 16 to 20 mm	0.3 mm
over 20 to 26 mm	0.4 mm
over 26 to 31.5 mm	0.5 mm
over 31.5 to 50 mm	0.6 mm
over 50 to 80 mm	0.8 mm
over 80 to 140 mm	1.0 mm
over 140 to 250 mm	1.6 mm

A total stiffness of 1259 N/mm is needed, resulting in heavy duty compression springs. An example of the dimensions of a compression spring with this stiffness is a spring from Lesjofors. This spring has a length of 102mm and an outer diameter of 63 mm. Springs that are more compact are available, but this gives a general idea of the length of a compression spring. https://catalog.lesjoforsab.com/product/61192-5-63102

Disc springs from Lesjofors, for example product 4336, can be stacked in series with five disc springs to achieve the same stiffness. However, the total size of this stack is a lot more compact as the compression spring. The length of one disc spring is 3.15mm, resulting in a total stack length of 15.75 mm. The length of the stack, compared to a compression spring, has decreased the total length of the spring by almost 85%. https://catalog.lesjoforsab.com/product/4336-ds-40x18-3x2

The outer diameter of the disc springs is 40mm, which is also smaller than the compression spring. The ratio of the height versus thickness, h0/t, for the disc spring is 0.575. The disc spring will therefore have an almost linear stiffness in the force range.

Loading the disc springs to more than 75% of their maximum deflection is discouraged [handbook]. Since the maximum load for the springs is 5000N, the disc spring will have a 10% safety factor.

C.4 Material selection

- Resistivity copper 1.7e-8
- Density copper: 8.96 g/cm3

https://www.tibtech.com/conductivite

- Resistivity fortal: Volume resistivity (ρ) 5.15e-8 Ohm*m
- Density fortal: 2.81 g/cm3

https://en.wikipedia.org/wiki/7075_aluminium_alloy

R = ρ*L/A

Cross section Fortal should be 3.03 larger for same electrical resistance.

M = L * A * density

Malu = L*3.03 A*dens/3.188

Malu = 3.03/3.188*mcopper = 0.95*mcopper

Since the total mass of aluminum is 5% lower than that of copper for the same electrical resistance, Aluminum is chosen instead of a copper beam.

C.5 Positioning system

Advantages and disadvantages of the 3 concepts:

2 mechanical stops:

- No spring interfering with lower arm during force buildup
- Simple system
- Movement of gun only possible in 1 orientation (only when against both stops)
- Needs check/sensor to check if gun is in open position before movement
- Passive system with active sensor

Position spring:

- Always active so no sensor needed
- Interferes with force buildup (minimal)
- Induces vertical bending displacement
- Fully passive system without sensors

Controlled locking pin:

- Needs sensor to check if open or closed
- Needs actuator to open and close
- No influence during force buildup
- Gun movement is allowed in any arm position (open/closed/half-open)
- Fully active system, controlled actuator with sensors

To calculate the required spring preload to keep the arms in place while accelerating with the robot, the model of an inverted pendulum on a cart can be used. With the equations of motion, the angular acceleration of the arms with motor assembly can be calculated. The required spring preload directly linked with the angular acceleration, assembly inertia and distance between spring and pivot.

Inverted pendulum model:

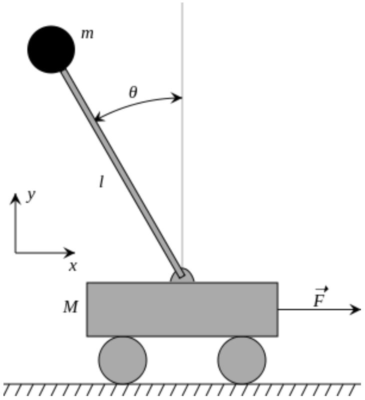

Equations of motion inverted pendulum:

$$(M+m)\,\ddot{x} - m\ell\ddot{\theta}\cos\theta + m\ell\dot{\theta}^2\sin\theta = F,$$
$$\ell\ddot{\theta} - g\sin\theta = \ddot{x}\cos\theta.$$

Fpreload = ang_acc * I / r_spring

With ang_acc calculated from the inverted pendulum model, I the moment of inertia around the main axis calculated by Solidworks, and r_spring the perpendicular distance from the spring to the axis.

C.6 Frequency analysis

Using Lagrange, the frequencies can be obtained. Recalculating the effective masses and placing them at the motor side resulted in the eigenfrequencies:

- 0 Hz (rigid body motion)
- 79.4 Hz
- 125.8 Hz
- 249.1 Hz

Appendix D. Testing the X-type

D.1 Horizontal displacement

Graph of horizontal displacement measurement:

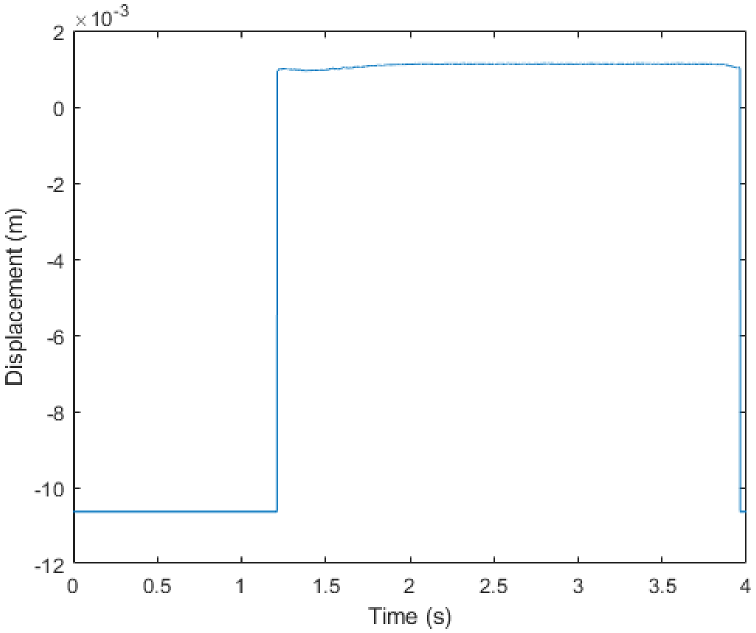

Table: The measured maximum horizontal displacement of each test

Electrode Force (N)	Upper arm horizontal displacement (mm)	Lower arm horizontal displacement (mm)
1000	0.077	0.039
1000	0.079	0.041
1000	0.080	0.040
1000	0.077	0.038
1000	0.080	0.047
1500	0.108	0.068
1500	0.108	0.067
1500	0.104	0.069
1500	0.103	0.071
1500	0.107	0.073
2000	0.131	0.099
2000	0.133	0.100
2000	0.145	0.100
2000	0.132	0.101
2000	0.136	0.101
2500	0.157	0.125
2500	0.159	0.125

2500	0.157	0.121
2500	0.159	0.127
2500	0.157	0.124
3000	0.184	0.150
3000	0.193	0.151
3000	0.189	0.152
3000	0.194	0.151
3000	0.184	0.152

D.2 Rotation measurements

Before applying electrode force:

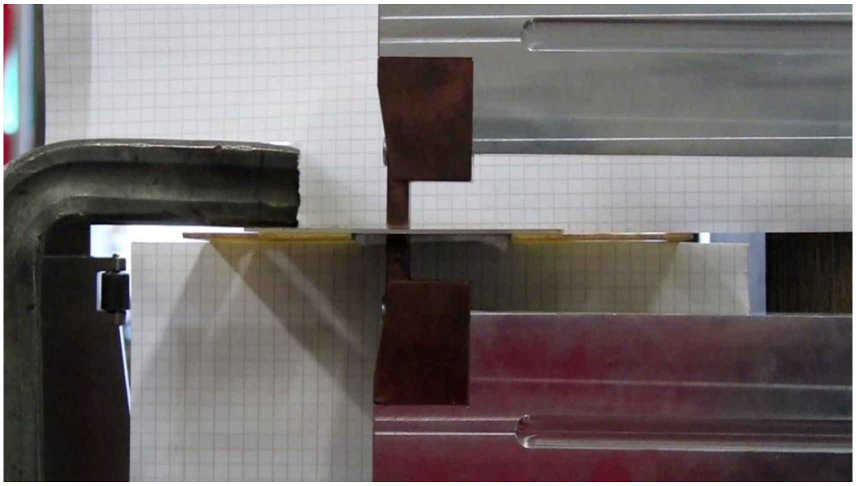

After applying electrode force:

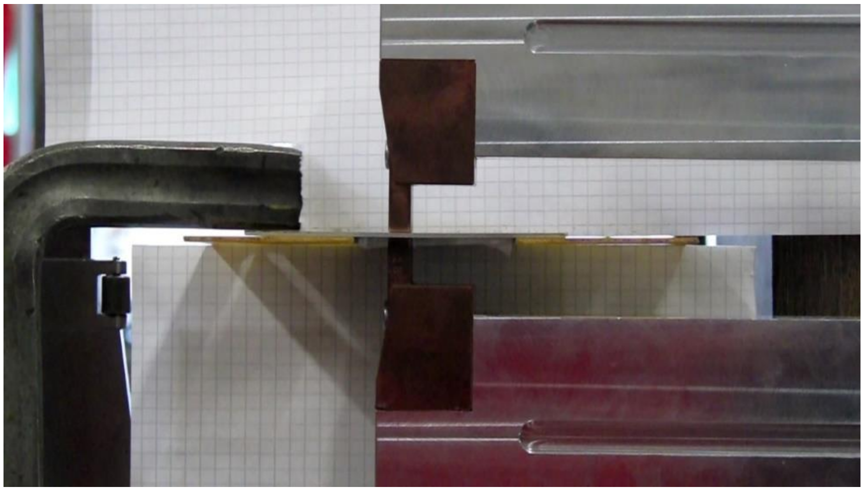

The Matlab datapoints used for the calculation of the rotation.

Upper electrode:

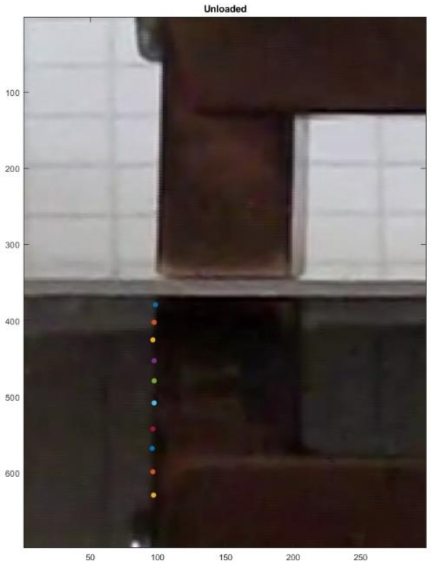
Unloaded
100
200
300
400
500
600
50
100
150
200
250

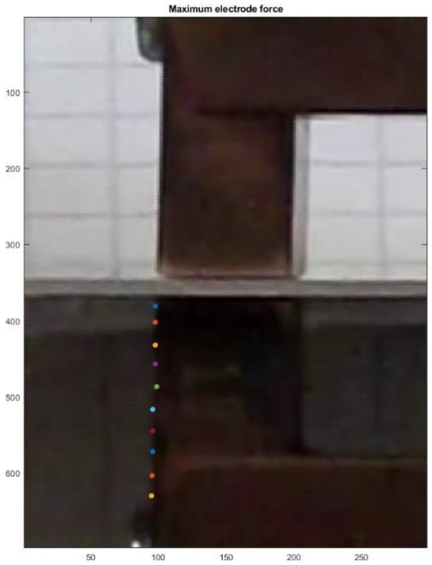
Maximum electrode force
100
200
300
400
500
600
50
100
150
200
250

Data points used	Unloaded angle (deg)	Max electrode force angle (deg)
1 (bottom) and 2	-2.07	-1.15
2 and 3	-1.89	-0.97
3 and 4	-1.19	-4.14
4 and 5	2.22	2.68
5 and 6	-0.97	-2.22
6 and 7	-2.01	-1.01
7 and 8	0.00	-1.11
8 and 9	-1.11	-1.04
9 and 10 (top)	-0.95	0.00
1 and 10	-0.922	-0.916

Lower electrode:

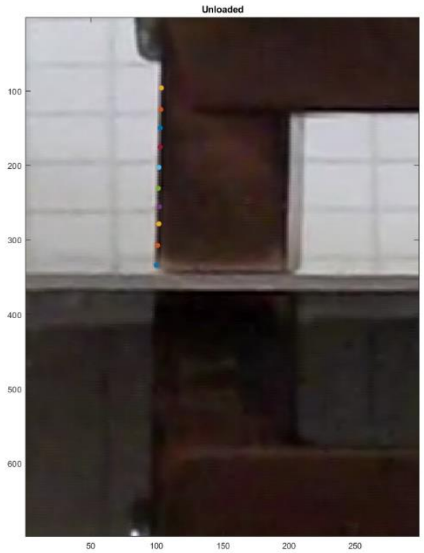
Unloaded
100
200
300
400
500
600
50
100
150
200
250

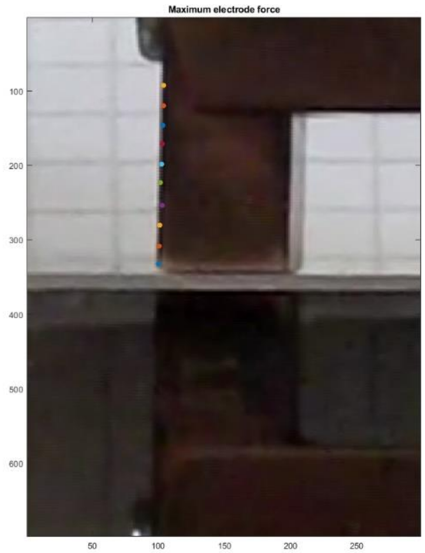
Maximum electrode force
100
200
300
400
500
600
50
100
150
200
250

Data points used	**Unloaded angle (deg)**	**Max electrode force angle (deg)**
1 (top) and 2	-2.38	0.00
2 and 3	-2.38	0.00
3 and 4	2.01	0.00
4 and 5	0.00	1.84
5 and 6	0.00	-5.50
6 and 7	-1.61	0.00
7 and 8	-1.07	0.00
8 and 9	0.89	-0.87
9 and 10 (bottom)	0.89	-1.04
1 and 10	-0.329	-0.661

D.3 Follow-up characteristics

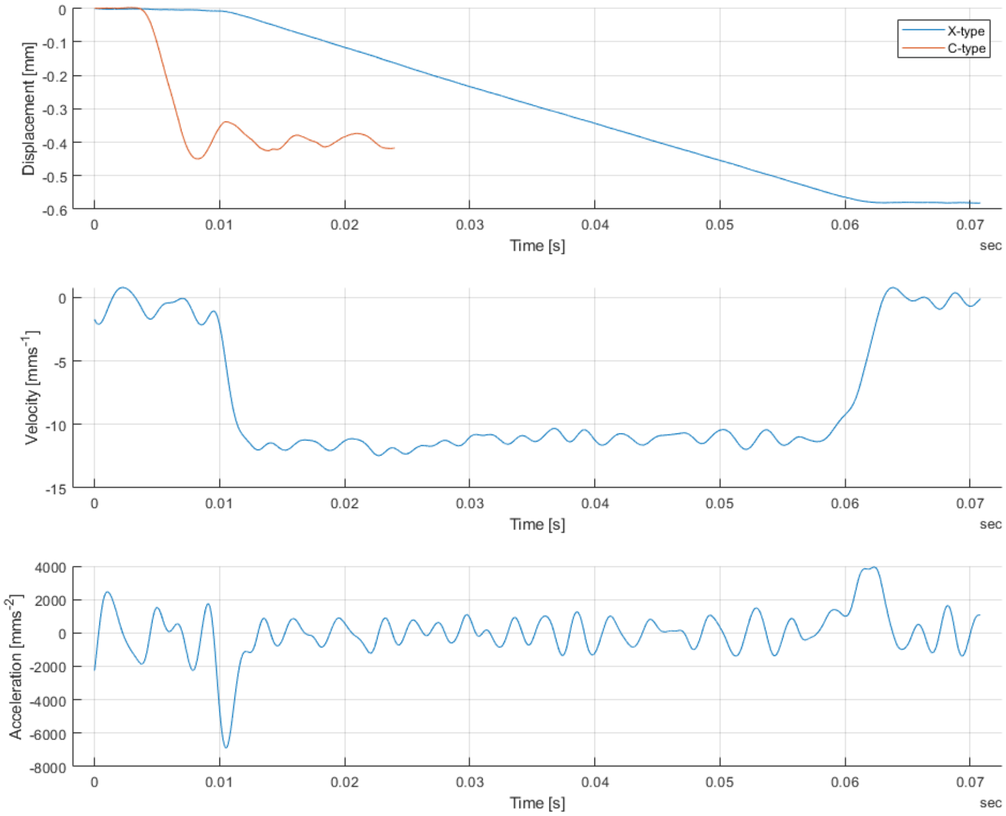

Appendix E. Full part list

1		4	ISO 4762 M6 x 16 - 16N		Socket Head Screw
2		4	ISO 4762 M8 x 20 - 20N		Socket Head Screw
3		11	ISO 4762 M8 x 25 - 25N		Socket Head Screw
4		18	DIN 6912 M8 x 25 - 25N		Socket Head Screw
5		2	ISO 4762 M8 x 50 - 50N		Socket Head Screw
6		8	ISO 4762 M10 x 25 - 25N		Socket Head Screw
7		2	ISO 4762 M12 x 30 - 30N		Socket Head Screw
8		1	ISO 4762 M12 x 50 - 50N		Socket Head Screw
9		1	ISO 4762 M12 x 200 - 200N		Socket Head Screw
10		4	ISO 7379 - 20 M16 x 55 --- N		Shoulder Bolt (pasbout)
11		12	Washer ISO 7089 - M8		Washer
12		10	ISO 8736 A 6 x 30		Dowel pin
13		2	ISO 8736 A 10 x 30		Dowel pin
14		1	GTX080		Servo Motor
15		1	9103A		QCS Force Sensor
16		6	1462303825		Insulation Bushing
17		6	GE 20 ESX-2LS		Plain bearing
18		2	GE 25 ESX-2LS		Plain bearing
19		1	PCM 101220 E		Linear bushing
20		1	PCM 252830 E		Linear bushing
21		5	4336		Disc spring
22		1	6780		Soft spring
23		1	ZWK.002.060.000		Radial misalignment compensator
24		1	31761 LBG-32		Clevis foot
25		2	9261 SGS-M10x1.25		Eye rod
26		3			Spacer disc 5mm
27		2			Spacer disc 2mm
28		0			Spacer disc 1mm
29		1			Spacer disc 0.5mm
30		0			Spacer disc 0.2mm
31		0			Spacer disc 0.1mm
32		1	PSG6180		Alu Transformer
33		1	A-300x200		A-cable L=200mm
34					
35		1	17.00703		Laminated Shunt
36		2	18.00510		Robot mounting side plate
37		1	18.00523		Robot mounting upper plate
38		2	18.00520		Square electrodes

39					
40		1	21.04101		Motor Flange
41		1	21.04102		Motor rod extension
42		1	21.04103		Spring rotation/Flange
43		1	21.04104		Main Axis Left
44		1	21.04105		Main Axis Right
45		1	21.04106		Transformer connection Upper arm
46		1	21.04107		Transformer connection Lower arm
47		1	21.04111		Main upper arm beam
48		1	21.04112		Upper side connector beam
49		1	21.04113		Upper side connector beam mirror
50		1	21.04114		Stiffener bracket
51		1	21.04115		Laminated shunt connection
52		2	21.04116		Electrode Holder
53		1	21.04121		Main lower arm beam
54		1	21.04122		Lower side connector beam
55		1	21.04123		Lower side connector beam mirror
56		2	21.04124		Lower arm spacer blocks
57		1	21.04125		Pos Spring attach rod
58		1	21.04126		Cable connector Lower arm
59		2	21.04127		Connection pin
60		1	21.04131		Spring housing Top cover
61		1	21.04132		Spring housing Enclosure
62		1	21.04133		Spring piston
63		1	21.04141		Spring holder M10
64		1	21.04142		Spring holder M20
65		1	21.04143		Inner shaft
66		1	21.04144		Outer shaft
67		1	21.04151		Side plate
68		1	21.04152		Side plate mirror
69		1	21.04153		pos spring mounting plate
70		2	21.04154		Transformer mounting
71		1	21.04155		Mech Stop Mounting